Biosynthese von Arabinan - ein komplexer Bestandteil der Zellwand in *Corynebacterianeae*

Inaugural-Dissertation

zur

Erlangung des Doktorgrades der

Mathematisch-Naturwissenschaftlichen Fakultät

der Heinrich-Heine Universität Düsseldorf

vorgelegt von

Diplom-Biologe

Mathias Seidel

aus Herne

April 2007

Auch die längste Reise beginnt
mit einem ersten Schritt.

Aus dem Institut für Biotechnologie I
der Forschungszentrums Jülich GmbH

Gedruckt mit der Genehmigung
der Mathematisch-Naturwissenschaftlichen Fakultät der
Heinrich-Heine Universität Düsseldorf

Referent: Prof. Dr. Hermann Sahm
Korreferent: Prof. Dr. Karl-Erich Jäger
Datum der Prüfung: 21.05.2007

Veröffentlichungen im Rahmen der Promotion:

Alderwick, L. J., Radmacher, E., Seidel, M., Gande, R., Hitchen, P. G., Morris, H. R., Dell, A., Sahm, H., Eggeling, L., Besra, G. S. (2005) Deletion of Cg-*emb* in Corynebacterianeae Leads to a Novel Truncated Cell Wall Arabinogalactan, whereas Inactivation of Cg-*ubiA* Results in an Arabinan-deficient Mutant with a Cell Wall Galactan Core. *J Biol Chem* **280:** 32362-32371

Alderwick, L. J., Seidel, M., Sahm, H., Besra, G. S., Eggeling, L. (2006) Identification of a Novel Arabinofuranosyltransferase (AftA) Involved in Cell Wall Arabinan Biosynthesis in *Mycobacterium tuberculosis*. *J Biol Chem* **281:** 15653-15661

Seidel, M., Alderwick, L. J., Sahm, H., Besra, G. S., Eggeling, L. (2007a) Topology and mutational analysis of the single Emb arabinofuranosyltransferase of *Corynebacterium glutamicum* as a model of Emb proteins of *Mycobacterium tuberculosis*. *Gycobiology* **17:** 210-219

Seidel, M., Alderwick, L. J., Birch, H. L., Sahm, H., Eggeling, L., Besra, G. S. (2007b) Identification of a novel arabinofuranosyltransferase AftB involved in a terminal step of cell wall arabinan biosynthesis in C*orynebacterianeae*, such as *Corynebacterium glutamicum* and *Mycobacterium tuberculosis*. *J Biol Chem in press*, March 26

Inhaltsverzeichnis

Abkürzungen

Im Folgenden sind die in dieser Arbeit verwendeten Abkürzungen aufgeführt. Ausgenommen sind die in der deutschen Sprache üblichen Abkürzungen und SI-Einheiten. Aminosäuren wurden in dem gebräuchlichen Ein-Buchstabencode abgekürzt.

Abb.	Abbildung
C-Terminus	Carboxyterminus
et al	*et alii* (und andere)
N-Terminus	Aminoterminus
Tab.	Tabelle
z.B.	zum Beispiel

A Einleitung

Die Unterordnung der *Corynebacterianeae* fasst eine heterogene Gruppe von Bakterien innerhalb der *Actinomycetales* zusammen (Stackebrandt *et al.*, 1997). Zu den *Corynebacterianeae* gehören unter anderem humanpathogene Spezies wie *Mycobacterium tuberculosis, Mycobacterium leprae, Corynebacterium diphteriae* und *Corynebacterium jekeium* (Brennan & Nikaido, 1995; Cole *et al*., 1998), aber auch apathogene und wichtige, großtechnisch genutzte Mikroorganismen. Darunter ist das Glutamat und andere Aminosäuren produzierende Bodenbakterium *Corynebacterium glutamicum* (Kinoshita *et al*., 1957) der momentan wirtschaftlich bedeutendste Vertreter (Eggeling *et al.*, 2001; Sahm *et al*., 2000). Trotz dieser gravierenden Unterschiede bezüglich ihrer Pathogenität besitzen nahezu alle Mitglieder der *Corynebacterianeae* strukturelle Gemeinsamkeiten, die in keiner anderen Bakteriengruppe zu finden sind.

1 Die Zellwand der *Corynebacterianeae*

Die Besonderheit der *Corynebacterianeae* liegt in ihrem einzigartigen Zellwandaufbau, wie er in Abbildung A-1 schematisch dargestellt ist (Dover *et al*., 2004; Puech *et al*., 2001).

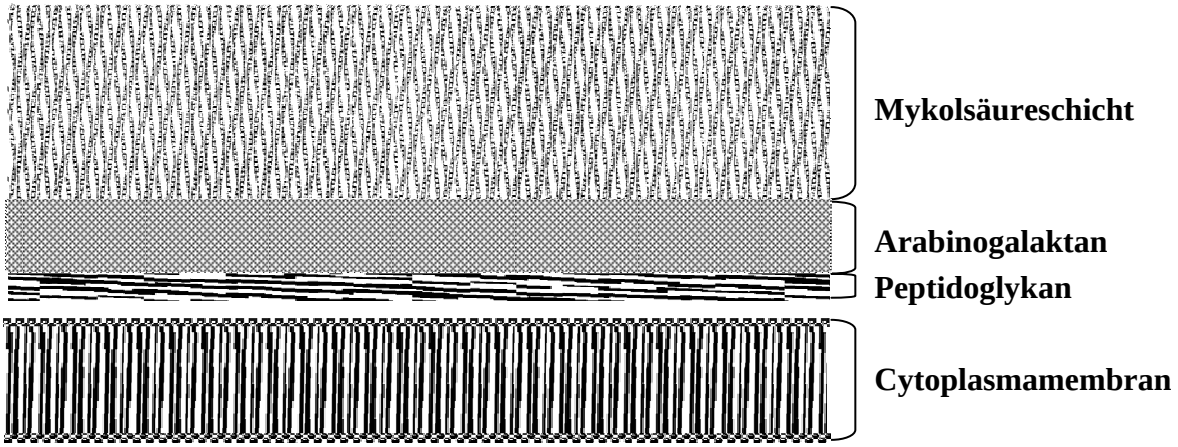

Abb. A-1: Schematische Darstellung der Zellwand von *Corynebacterianeae*. Der Cytoplasmamembran ist eine Peptidoglykanschicht aufgelagert. An diese schließt sich ein verzweigtes System aus Arabinose- und Galaktoseresten an, das Arabinogalaktan. Die terminalen Arabinosereste sind teilweise mit Mykolsäuren verestert, welche die äußere Lipidschicht bilden.

Aufgrund der Anwesenheit einer mehrschichtigen Peptidoglykanschicht, einem Netzwerk das sich aus alternierenden N-Acetyl-Glucosamin- und N-Acetyl-Muraminsäureresten zusammensetzt, die Peptidbrücken aus L-Alanyl-D-isoglutaminyl-*meso*-diaminopimyl-D-Alanin aufweist (Schleifer & Kandler, 1972), und der damit einhergehenden *Gram*-Färbbarkeit, werden die *Corynebacterianeae* zu der Gruppe der *Gram*-positiven Eubakterien gezählt (Stackebrandt *et al*., 1997).

Als zusätzliche Zellwandbestandteile besitzen die *Corynebacterianeae* ein verzweigtes System aus Arabinose- und Galaktoseresten, das Arabinogalaktan (McNeil *et al*., 1990), sowie Mykolsäuren (Brennan *et al.,* 1995). Das Arabinogalaktan ist über eine spezifische, Rhamnose enthaltende Verbindungseinheit (Abb. A-2) mit dem Peptidoglykan verbunden und stellt an der Außenseite einen Verankerungspunkt für die Mykolsäuren dar. Diesen verzweigten Fettsäurederivaten, die die Zellwand als eine zweite Lipidschicht umgeben, verdanken diese Bakterien auch die Bezeichnung *Mycolata* (Minnikin & Goodfellow, 1980). Unter anderem wird diese zweite Lipidschicht mit als Grund für die schlechte Therapierbarkeit von *M. tuberculosis* gesehen, aufgrund derer jährlich etwa 2 Millionen Menschen sterben (*World Health Organisation*, 2006). Diese äußere Membran ist als Permeabilitätsbarriere mit der zweiten Zellmembran *Gram*-negativer Bakterien vergleichbar, was sich z.B. darin zeigt, dass in beiden Organismen Porine in der äußeren Membran vorhanden sind (Schirmer, 1998; Niederweis, 2003). Wegen dieser zweiten Lipiddoppelschicht werden die *Corynebacterianeae* häufig phylogenetisch äquidistant zu *Gram*-positiven und *Gram*-negativen Bakterien eingeordnet.

Zusätzlich besitzen alle *Corynebacterianeae* als komplexes Glykolipid Lipomannan (Gibson *et al.,* 2003), und die Mycobakterien zusätzlich auch noch Lipoarabinomannan (Besra *et al.,* 1997), wohingegen *C. glutamicum* ein sehr spezielles Lipoarabinomannan mit einem nur sehr geringen Anteil an Arabinoseresten besitzt (Tatituri *et al*., 2007).

1.1 Aufbau des Arabinogalaktans

Bei den *Corynebacterianeae* ist, wie bereits erwähnt, das Peptidoglykan kovalent über eine spezielle Rhamnose enthaltende Verbindungseinheit (s. Abb. A-2) mit dem Zuckerpolymer Arabinogalaktan verbunden. Diese Verbindungseinheit besteht aus N-acetyl-Glucosaminphosphat und Rhamnopyranose, an welcher die Galaktosekette gebunden ist, die einen Teil der Arabinogalaktandomäne darstellt (McNeil, 1990). Die einzelnen Galaktosereste sind über (1→5) und (1→6) Bindungen verknüpft und weisen zusätzlich Arabinose-Seitenketten auf (Brennan & Nikaido, 1995).

Für *M. tuberculosis* ist bekannt, dass die Arabinankette aus verzweigten Arabinose-Einheiten besteht, die im Mittel aus 23 Arabinose-Einheiten gebildet wird (Besra *et al.*, 1995). Bei *C. glutamicum* liegen noch keine detailierten strukturellen Informationen zur Arabinandomäne vor. Aufgrund quantitativer Bestimmungen wird jedoch von kürzeren Arabinose-Seitenketten mit eventuell nur zwei Verzweigungen ausgegangen (Puech *et al.*, 2001).

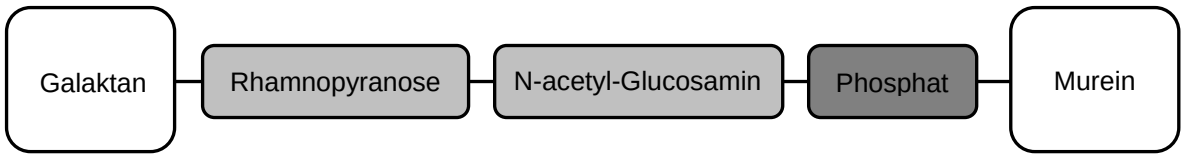

Abb. A-2: Schematischer Aufbau der Verbindungseinheit zwischen Murein und Galaktan im Arabinogalaktan der *Corynebacterianeae* (McNeil *et al.*, 1990).

Die Verbindungseinheit verknüpft die Arabinogalaktandomäne mit dem Peptidoglykan. Das Arabinogalaktan verbindet dadurch den Mureinsacculus kovalent mit der für *Corynebacterianeae* charakteristischen, allerdings für *Gram*-positive Organismen ungewöhnlichen, äußeren Lipidschicht. Daher ist das Arabinogalaktan als Bestandteil der Zellwand essentiell (Mills *et al.*, 2004; Pan *et al.*, 2001).

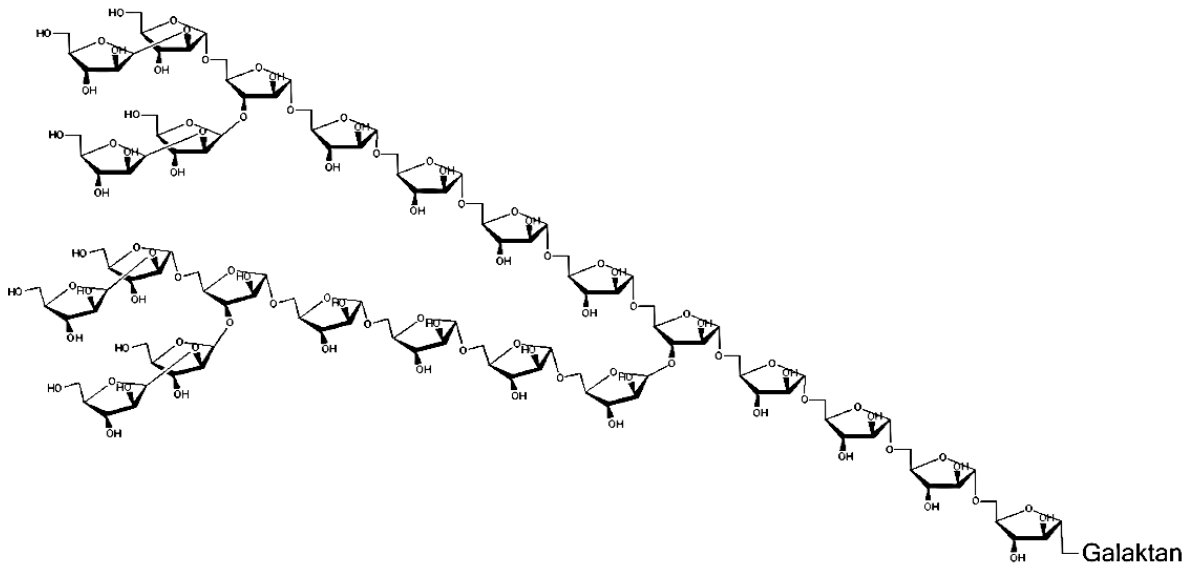

Abb. A-3: Mögliche Struktur von Arabinan im Arabinogalaktan der *Corynebacterianeae*. Dargestellt ist die lineare Verknüpfung von Arabinose durch die Verbindung von C1- und C5-Atomen α(1→5), die den größten Anteil am Arabinan ausmacht. Die Verzweigung der Arabinankette erfolgt an C3 Atomen und die endständigen Arabinosereste sind über C2 Atome verbunden (Daffe *et al.*, 1990; McNeil *et al.*, 1991; 1994).

Anders als für die lineare Galaktandomäne, wurde, wie in Abbildung A-3 dargestellt, für die Arabinandomäne auch verzweigt verknüpfte Arabinose mit α(1→3→5) glykosidischer Bindung nachgewiesen (Chatterjee *et al*., 1991; Puech *et al*., 2001). Ebenso ist auch gezeigt, dass der überwiegende Anteil im Arabinogalaktan aus linear verknüpfter α(1→5) Arabinose besteht und ein geringer Anteil von α(1→2) Arabinose dem terminalen Ende der Arabinandomäne zugesprochen werden kann (Chatterjee *et al*., 1991; Daffe *et al*., 1990; McNeil *et al*., 1994).

1.2 Biosynthese des Galaktans im Arabinogalaktan

Die Biosynthese des Galaktans beginnt an der Verbindungseinheit, so wie sie in Abbildung A-2 dargestellt ist. An der Synthese der Verbindungseinheit ist die Rhamnosyltransferase WbbL beteiligt, welche aus Rhamnose und Polyprenylpyrophosphat-N-acetyl-Glucosamin die Synthese des Glycolipids Polyprenylpyrophosphat-N-acetyl-Glucosamin-Rhamnose katalysiert (Mikusova *et al.*, 1996). Wie die enzymatische Katalyse der Phosphodiesterbindung zwischen der Verbindungseinheit und dem Mureinsacculus erfolgt, ist noch nicht bekannt. Allerdings gibt es Hinweise darauf, dass die Katalyse der Phophodiesterbindung erst nach abgeschlossener Synthese des Arabinogalaktans durch eine bislang unbekannte Transglykosylase erfolgt (Hancock *et al*., 2002; Yagi *et al*., 2003).

Der Rhamnoserest in der Verbindungseinheit wird am nicht reduzierenden Ende mit einer Uridylyl-diphosphat-Galaktose (UDP-Gal) verknüpft und stellt damit den Startpunkt der Galaktankette im Arabinogalaktan dar. Diese Reaktion wird durch die Galaktosyltransferase RfbE katalysiert (Mikusova *et al*., 2006), der auch die Verknüpfung der zweiten UDP-Gal mit dem C5-Atom der ersten Galaktose zugesprochen wird (Mikusova *et al*., 2006). Die anschließende Verlängerung der Galaktankette erfolgt, wie in Abbildung A-4 gezeigt, durch die Galaktosyltransferase GlfT, welche die Galaktose alternierend über die Atome C1 mit C5 (1→5) oder C1 mit C6, (1→6) als β-Glykoside verbindet (Daffe *et al*., 1990; Kremer *et al*., 2001; Mikusova *et al*., 2000). Die Aktivität des GlfT-Proteins führt zur Synthese von bis zu 30 Galaktose-Einheiten und damit zur Bildung der Galaktandomäne des Arabinogalaktans (Rose *et al*., 2006).

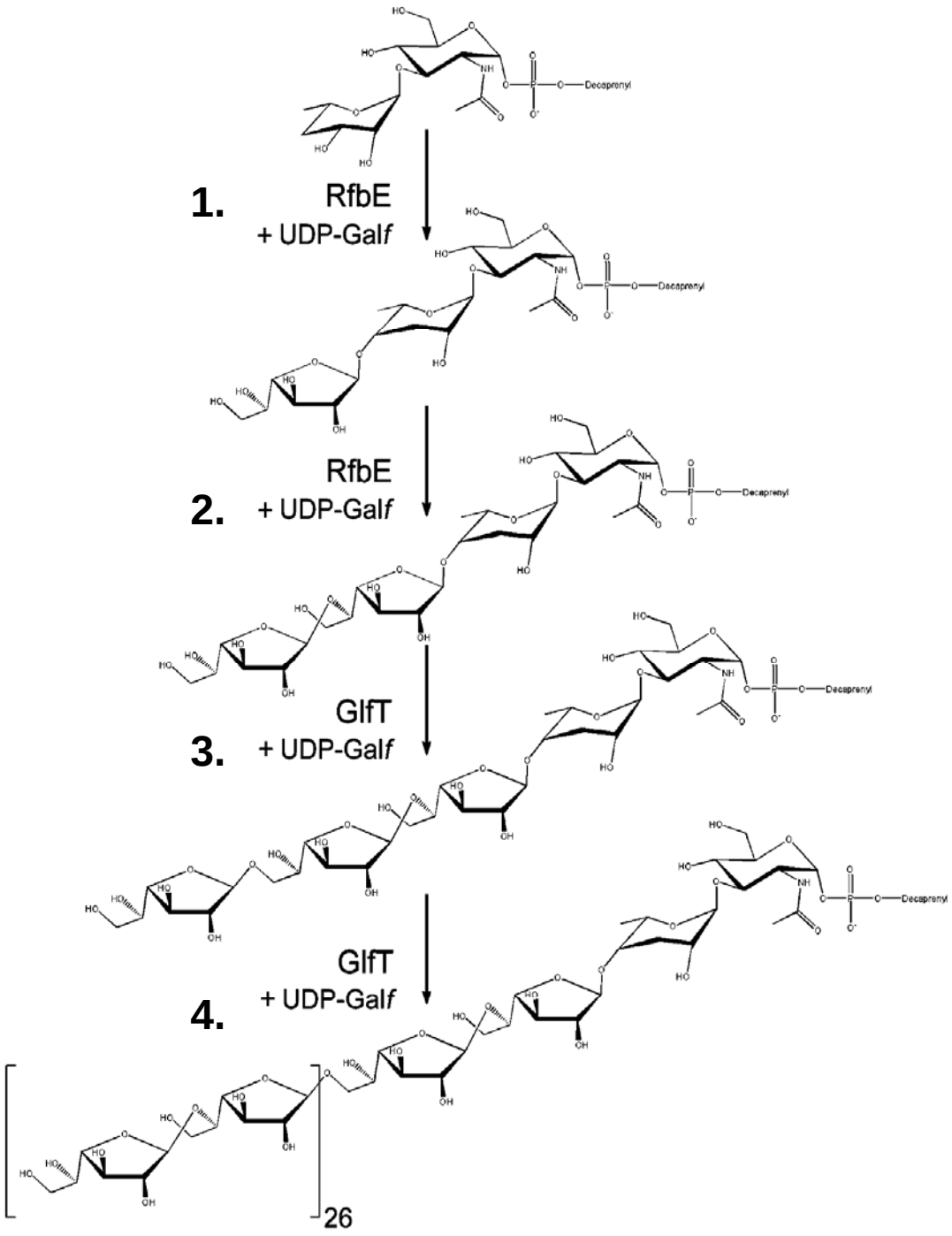

Abb. A-4: Die Galaktanbiosynthese der *Corynebacterianeae*. Dargestellt ist die Rhamnose-Verbindungseinheit sowie die daran anschließende Verknüpfung (1. und 2. Schritt) mit der ersten und zweiten Galaktose-Einheit. Im 3. und 4. Schritt wird gezeigt, dass die Galaktankette auf bis zu 30 Galaktose-Einheiten verlängert wird. Die beteiligten Enzyme RfbE und GlfT sind mit den Reaktionen gekennzeichnet. Weitere Erläuterungen hierzu befinden sich im Text (Kremer *et al*., 2001; Mikusova *et al*., 2000; Rose *et al*., 2006). Uridyly-diphosphat-Galaktofuranose, UDP-Gal*f;* Galaktofuranosyltransferase, GlfT und das referable-protein E, RfbE.

Da die Synthese der Galaktankette ein wesentlicher Teil der Arabinogalaktanbiosynthese ist, ist auch das Gen *glfT* in *M. tuberculosis* essentiell (Pan *et al*.,

2001). Daher wurden nach der Identifikation des GlfT-Proteins in *M. tuberculosis*, synthetische Inhibitormoleküle, auf der Basis von Iminozuckern synthetisiert, die spezifisch diese Enzym-Aktivität hemmen und damit die Grundlage für die Entwicklung neuer, synthetischer Antibiotika gegen *M. tuberculosis* bilden (Cren *et al*., 2004).

1.3 Biosynthese des Arabinans im Arabinogalaktan

Die Biosynthese der Arabinandomäne im Arabinogalaktan ist, aufgrund der Verzweigungen im Arabinan, wesentlich komplexer als die Biosynthese der Galaktandomäne. Es war bereits seit längerem bekannt, dass die in Arabinogalaktan eingebaute Arabinose aus Ribose isomerisiert wird (Scherman *et al*., 1995). Erst kürzlich konnte in *M. tuberculosis* gezeigt werden, dass die Synthese der Arabinose über Decaprenyl-Phosphoryl-Phosphoribofuranose (DPPR) erfolgt (s. Abb. A-5). Dabei entsteht DPPR durch die Übertragung eines Prenylrestes durch die Decaprenylphosphat-5-Phospho-Ribosyl-Transferase UbiA auf β-D-5-Phosphoribo-furanosyl-pyrophosphat (pRpp) (Huang *et al*., 2005).

Erste Experimente zeigen, dass sehr wahrscheinlich ein DPPR-Epimerasekomplex das DPPR zur Decaprenyl-Phosphoryl-Arabinofuranose (DPPA) isomerisiert. Abschließend katalysiert eine bislang unbekannte Phosphatase (Abb. A-5) die Dephosphorylierung von DPPA zu Decaprenylmonophospho-Arabinofuranose (DPA), welches als Substrat der Glykosyltransferasen der Arabinanbiosynthese gesehen wird (Mikusova *et al*., 2005).

Die an der Biosynthese der Arabinandomäne im Arabinogalaktan beteiligten Enzyme sind weitgehend unbekannt. In Anbetracht der strukturellen Komplexität des Arabinan im Arabinogalaktan wird vermutet, dass mehrere Arabinofuranosyltransferasen für die Katalyse der verschiedenen Verknüpfungstypen ($\alpha(1\rightarrow5)$, $\alpha(1\rightarrow3)$, $\beta(1\rightarrow2)$) in *Corynebacterianeae* vorhanden sind. Bislang konnten nur die Arabinosyltranferasen EmbA und EmbB in *M. smegmatis* und *M. tuberculosis*, welche in allen *Mycobacteria* Spezies hochkonserviert vorliegen, mit der Verknüpfung von Arabinan im Arabinogalaktan in Zusammenhang gebracht werden (Belanger *et al*., 1996; Escuyer *et al*., 2001). Zusätzlich besitzen *Mycobacteria* noch das EmbC-Protein. Demgegenüber haben *Corynebacterium* Spezies, wie *C. glutamicum* und *Corynebacterium diphteriae*, nur ein einziges Emb-Protein (Dover *et al*., 2004; Telenti *et al*., 1997; Puech *et al*., 2001). Die drei *mycobacteriellen emb*-Gene liegen als sogenanntes *embCAB*-Operon vor. Es sind sehr große Polypeptide mit einer Länge von 1100 Aminosäureresten, die sich mit einer Identität von 44% ausserordentlich ähnlich sind (Telenti *et al*., 1997). Weil *C. glutamicum* nur ein *emb*-Gen besitzt und auch bezüglich anderer paraloger Gene, wie z.B. den *accD* Genen (Gande *et al*., 2004), gegenüber *M. tuberculosis* und anderen *Corynebacterianeae* die geringere Zahl an Genen besitzt, wird *C. glutamicum*

auch als Archetyp der *Corynebacterianeae* mit wenigen Genduplikationen und evolutionär bedingten Veränderungen angesehen (Nakamura *et al*., 2003).

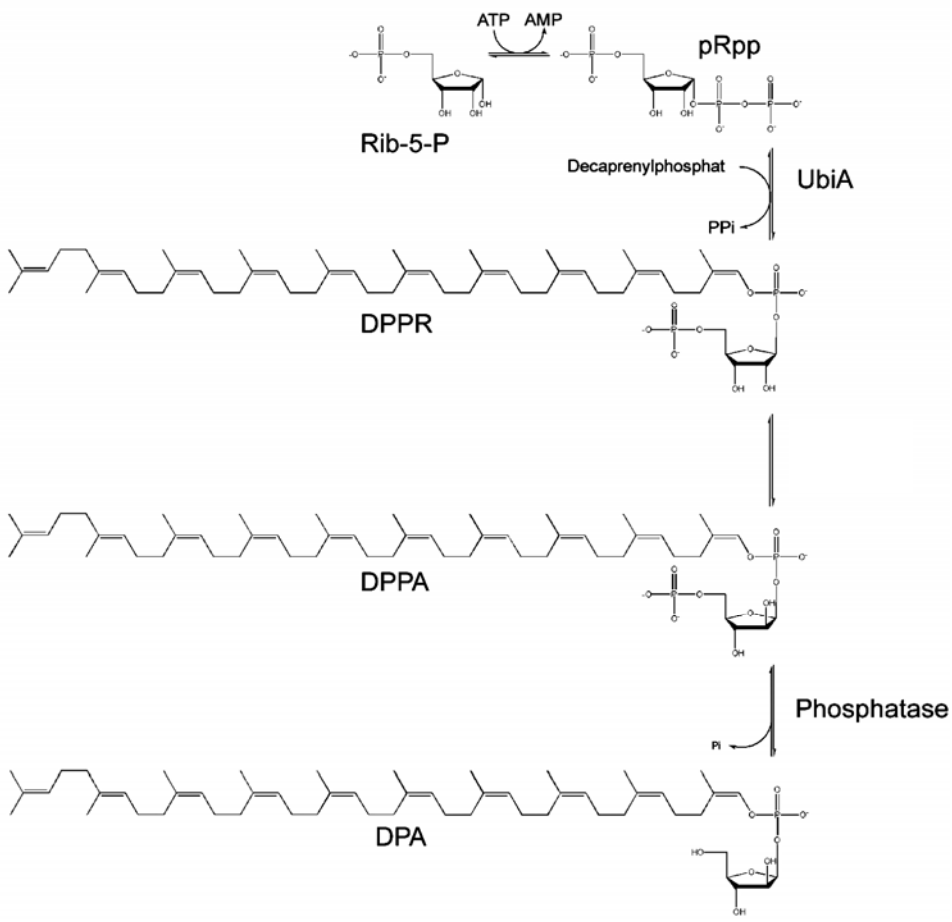

Abb. A-5: Die Bildung der Vorläuferprodukte des Arabinan im Arabinogalaktan von *M. tuberculosis*. Dargestellt sind die Moleküle Ribose-5-Phosphat (Rib-5-P), β-D-5-Phosphoribofuranosyl-Pyrophosphat (pRpp), Decaprenyl-Phosphoryl-Phosphoribofuranose (DPPR), Decaprenyl-Phosphoryl-Arabinofuranose (DPPA) und Decaprenylmonophospho-Arabinofuranose (DPA), sowie die an den Reaktionen beteiligten Enzyme (Huang *et al*., 2005; Mikusova *et al*., 2005). Die Abkürung UbiA steht für Decaprenylphosphat-5-Phospho-Ribosyl-Transferase. Weitere Erklärungen dazu befinden sich im Text.

Wie im Detail durch die Emb-Proteine Arabinosereste in die entstehende Arabinandomäne eingebaut wird, konnte noch nicht geklärt werden. Bislang ist nur bekannt, dass die Emb-Proteine in zwei Domänenhälften unterteilt sind (Ramaswamy *et al*., 2000; Telenti *et al*., 1997), die als N-terminaler, integraler Membranbereich, aus 12 bis 14 transmembranen Helices, und einem hydrophilen, globulären C-Terminus bestehen (Telenti *et al*., 1997). Untersuchungen zur Funktion der Emb-Proteindomänen und ihre Beteiligung an der Arabinanbiosynthese deuten darauf hin, dass dem N-terminalen Bereich der Emb-Proteine die spezifische Erkennung des Akzeptors und dem C-terminalen Bereich eher die katalytische Verknüpfungsreaktion zugesprochen werden kann (Zhang *et al*., 2003).

2 Zielsetzung dieser Arbeit

Die Untersuchung eines Organismus mit nur einem *emb*-Gen erlaubt die exakte Zuordnung von grundlegenden Funktionen des Emb Proteins im Rahmen der Arabinanbiosynthese. Daher eignet sich *C. glutamicum* als Modellorganismus, um die Funktionen des *emb*-Gens und anderer zum Teil noch unbekannter Gene der Arabinanbiosynthese zu untersuchen. Es sollten deshalb erstmals die Folgen einer *emb* Deletion auf den Aufbau des Arabinans untersucht werden. Weiterhin sollte versucht werden, Informationen zur Struktur des Emb-Proteins zu erhalten.

Aufgrund der chemischen Analysen von Deletionsmutanten und Genomvergleiche von *C. glutamicum* und *M. tuberculosis* sollte weiterhin versucht werden zusätzliche Proteine, z.B. Arabinosyltransferasen, zu identifizieren, die an der Synthese des Arabinan der *Corynebacterianeae* beteiligt sind.

B Ergebnisse & Diskussion

Das Ziel dieser Arbeit war es, die Biosynthese des Arabinans von *Corynebacterium glutamicum* ATCC13032 näher zu analysieren. Dabei sollte vor allem untersucht werden, welche Proteine beteiligt sind. Den Ausgangspunkt stellte dabei das Protein Emb dar, dessen Beteiligung am Aufbau der Arabinanschicht bereits bekannt war.

1 Das Arabinan aus *C. glutamicum* und *Mycobacterium tuberculosis*

Obwohl *C. glutamicum* und *M. tuberculosis* eng verwandt sind, stellte sich zu Beginn dieser Arbeit die Frage, ob der Stamm *C. glutamicum* ATCC13032 vergleichbare glykosidische Verbindungen im Arabinan beinhaltet, wie der pathogene Stamm *M. tuberculosis* H37Rv.

Zunächst wurde vermutet, dass *C. glutamicum* ATCC13032 über weniger komplex verknüpftes Arabinan verfügt, als *M. tuberculosis* H37Rv. Diese Annahme beruhte auf dem Befund, dass *M. tuberculosis* drei sehr eng verwandte Arabinosyltransferasen (EmbA, EmbB und EmbC-Protein) hat (Telenti *et al*., 1997), während *C. glutamicum* nur eine Arabinosyltransferase dieses Typs (Emb-Protein) besitzt.

Daher wurden in dieser Arbeit die glykosidischen Bindungen des Arabinans aus der Zellwand von *C. glutamicum* ATCC13032 bestimmt. Die Auftrennung der Zucker zeigt, dass die 5 C-Atome der Arabinosereste wahlweise an den C-Atomen 1,2,3 oder 5 verknüpft sind (s. Abb. B-1). Dabei setzt sich die Bindung z.B. einer 1,3,5-Arabinose aus den glykosidischen Bindungstypen 1→3 und 1→5 zusammen. Aus der Abbildung B-1 ist außerdem ersichtlich, dass den verschieden verknüpften C-Atomen der Arabinose nur die drei Bindungstypen 1→5, 1→3 und 1→2 zugrunde liegen, die entweder als einzelne Bindung vorkommen oder zusätzliche Bindungen aufzeigen, so dass Verzweigungen vorliegen. Als weitere Zucker der Zellwand zeigen sich Galaktose und Rhamnose (s. Abb. B-1). Interessanterweise zeigen diese Ergebnisse, wie in Tabelle B-1 aufgeführt, dass das Arabinogalaktan aus *C. glutamicum* im Wesentlichen die gleichen glykosidischen Bindungstypen aufweist, wie es auch für Arabinogalaktan aus *M. tuberculosis* bekannt ist (Besra *et al*., 1995). Der Unterschied in der Zusammensetzung des Arabinogalaktans beschränkt sich auf eine terminal-verknüpfte Rhamnose und einen 1,2,5-Arabinose Verzweigungstyp der noch nicht in *M. tuberculosis*

identifiziert wurde. Es ist jedoch nicht ausgeschlossen, dass diese Zucker auch in der Zellwand von *M. tuberculosis* nachgewiesen werden können.

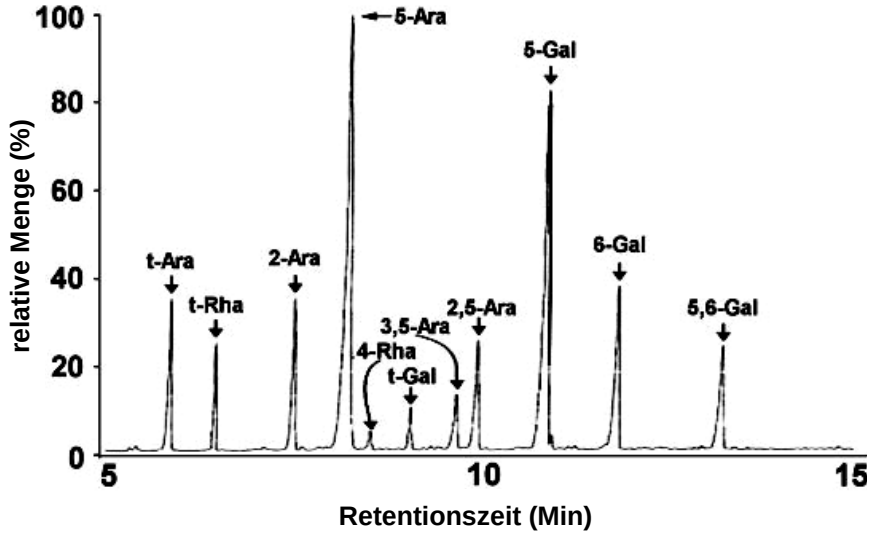

Abb. B-1: Die Zuckerverknüpfungen im Arabinogalaktan aus *C. glutamicum* ATCC13032. Die isolierten Zellwandzucker wurden mit Dimsylion methyliert und mittels GC/MS aufgetrennt, wie in Seidel *et al*. (2007b beschrieben. Alle Zucker sind am anomeren C-Atom (C1) und an der angegebenen Position (2, 5, 6, etc.) verknüpft. Ara, Arabinose; Gal, Galaktose; Rha, Rhamnose.

Tab. B-1: Bindungstypen von Zuckern im Arabinogalaktan der Zellwand aus *C. glutamicum* und *M. tuberculosis*. Die Daten für *C. glutamicum* stammen aus dieser Arbeit (Alderwick *et al*., 2006), die für *M. tuberculosis* aus Besra *et al*. (1995). Die angegebenen Positionen beziehen sich auf die C-Atome der einzelnen Zuckermoleküle.

	Verknüpfte Positionen am Zucker	***C. glutamicum* ATCC13032**	***M. tuberculosis* H37rv**
Arabinan	1	**X**	**X**
	1,2	**X**	**X**
	1,5	**X**	**X**
	1,2,5	**X**	
	1,3,5	**X**	**X**
Galaktan	1	**X**	**X**
	1,5	**X**	**X**
	1,6	**X**	**X**
Rhamnose	1	**X**	
	1,4	**X**	**X**

Diese Ergebnisse zeigen somit, dass die unterschiedliche Anzahl der Emb-Proteine in *C. glutamicum* und *M. tuberculosis* keinen Einfluss auf die Anzahl der Verknüpfungstypen von Arabinan in Arabinogalaktan hat. Untersuchungen mit *M. smegmatis* weisen darauf hin, dass nur zwei (EmbA und EmbB, Escuyer *et al.,* 2001) der drei Emb-Proteine in Mycobakterien an der Arabinansynthese im Arabinogalaktan beteiligt sind, während das dritte Emb-Protein (EmbC) bei der Arabinansynthese eines Lipoglykans, dem Lipoarabinomannan, involviert ist (Zhang *et al*., 2003). Dieses Lipoarabinomannan kommt in *C. glutamicum* nicht vor (Dover *et al*., 2004). Erst kürzlich konnten Khasnobis *et al.* (2006) zeigen, dass die Proteine EmbA und EmbB aus *M. smegmatis* nur eine Arabinansyntheseaktivität in einem heteromeren EmbA/EmbB Proteinkomplex haben. Daher kann postuliert werden, dass die Arabinansyntheseaktivität des Emb-Proteins aus *C. glutamicum* in einem homooligomeren Emb-Proteinkomplex erfolgt.

Um in *C. glutamicum* den Einfluss des Emb-Proteins auf den Arabinanaufbau zu untersuchen, wurde das *emb*-Gen in *C. glutamicum* deletiert. Dabei wurde gezeigt (Alderwick *et al*., 2005), dass in der Zellwand der Deletionsmutante von *C. glutamicum* nur noch terminale Arabinosereste vorliegen, die als Einzelmoleküle direkt mit dem Galaktan verknüpft sind. Im Einklang damit steht, dass mehr als 90% der Arabinose in der *C. glutamicum* Deletionsmutante fehlen. Ein identisches Bild ergab sich nach der Inkubation von *C. glutamicum* mit dem Antibiotikum Ethambutol, was bestätigt, dass Ethambutol die Aktivität des Emb-Proteins inhibiert (Alderwick *et al*., 2005; Radmacher *et al*., 2005).

Die Inaktivierung von jeweils einem der drei *emb*-Gene in *M. smegmatis* führte dagegen in keinem Fall zu einer derart drastischen Verringerung des Arabinangehalts in der Zellwand (Escuyer *et al*., 2001; Zhang *et al*., 2003). Hierbei muss berücksichtigt werden, dass durch die Inaktivierung eines einzelnen *emb*-Gens in *M. smegmatis* immer noch zwei *emb*-Gene vorliegen die zu 70% identisch sind und daher einander möglicherweise komplementieren können (Escuyer *et al*., 2001; Zhang *et al*., 2003).

Das Emb-Protein aus *C. glutamicum* katalysiert zumindest die Elongation des ersten Arabinoserestes, der am Galaktan verknüpft ist, um eine weitere Arabinose. Es kann zwar vermutet werden, dass die Arabinosekette durch das Emb-Protein weiter verlängert wird, der Beweis dazu ist aber nicht erbracht. Es kann auch nichts über die Beteiligung des Emb-Proteins an der Synthese mehrerer Verknüpfungen geschlossen werden. Es ist eher zu vermuten, dass spezielle Arabinosyltransferasen an den verschiedenen Bindungstypen beteiligt sind.

2 Der Start der Arabinansynthese in *Corynebacterianeae*

Da durch die Deletion des *emb*-Gens in *C. glutamicum* gezeigt werden konnte, dass es zusätzlich zu dem Emb-Protein noch mindestens eine weitere Arabinosyltransferase in *C. glutamicum* geben muss, welche die Verknüpfung der ersten Arabinose am Galaktan katalysiert, war es nun das Ziel, das entsprechende Gen zu finden.

In dieser Arbeit wurde gezeigt, dass der stromaufwärts vom *emb*-Gen lokalisierte offene Leserahmen für ein Arabinofuranosyltransferase A (AftA) genanntes Protein kodiert, welches für den Transfer der ersten Arabinose an das Galaktan im Arabinogalaktan von *C. glutamicum* und *M. tuberculosis* verantwortlich ist (Alderwick *et al*., 2006). Durch die Deletion des *aftA*-Gens, durch die Komplementation des Phänotyps mit *aftA* aus *C. glutamicum* und aus *M. tuberculosis*, sowie durch *in vitro* Analysen an synthetischen Akzeptormolekülen, konnte dem AftA-Protein eindeutig die Funktion zugeordnet werden, den ersten Arabinoserest mit dem Galaktan zu verknüpfen. Die Verknüpfung von Arabinose durch das AftA-Protein erfolgt dabei sehr spezifisch an die achte, zehnte und zwölfte Galaktaneinheit. Damit stellt das AftA-Protein eine bis zu diesem Zeitpunkt noch vollkommen unbekannte Arabinosyltransferase dar. In allen *Corynebacterianeae* wurden in dieser Arbeit AftA-homologe Proteinsequenzen identifiziert (Alderwick *et al*., 2006). Daher kann postuliert werden, dass der Mechanismus der Arabinaninitiation durch die AftA-Proteine, die Startreaktion bei der Arabinansynthese durch die Emb-Proteine in allen Vertretern der *Corynebacterianeae* darstellt.

Die offensichtlich hohe Spezifität der Arabinosyltransferasen AftA und Emb, die beide 5-Pospho-β-D-Arabinosemonophopho-decaprenol als Substrat verwenden (Alderwick *et al*., 2005; 2006), gegenüber dem Akzeptormolekül ist eine typische Eigenschaft von Glykosyltransferasen und ist als *one enzyme one linkage* Regel bekannt (Breton *et al*., 2002). Mit dieser Regel wird beschrieben, dass alle bekannten Glykosyltransferasen nur einen einzigen, sehr spezifischen Akzeptorzucker binden können (Breton *et al* 2002), wodurch sich die Glykosyltransferasen sehr deutlich von den Zucker-spaltenden Glykosylasen unterscheiden, die ein sehr breites Substratspektrum aufweisen (Breton *et al*., 2002). Dies erklärt auch, dass das Emb-Protein keine Arabinanverknüpfung mit dem Galaktan katalysieren kann, so wie es die experimentellen Befunde dieser Arbeit bestätigen.

Das AftA-Protein verknüpft demnach, wie in Abbildung B-2 dargestellt, ausschließlich die erste Arabinoseeinheit mit dem Galaktan und ist dadurch als initiale Glykosyltransferase charakterisiert, wie es beispielsweise auch für spezielle Glykosyltransferasen für die Initiation der Exopolysaccharid-Synthese durch das BceB-Protein in *Burkholderia cenocepacia* oder auch in *Lactococcus lacti* sowie *Streptomyces*

beschrieben wurden (Luzhetskyy *et al*., 2005; Dabour & LaPointe, 2005; Videira *et al*., 2005; Wang *et al*., 2003).

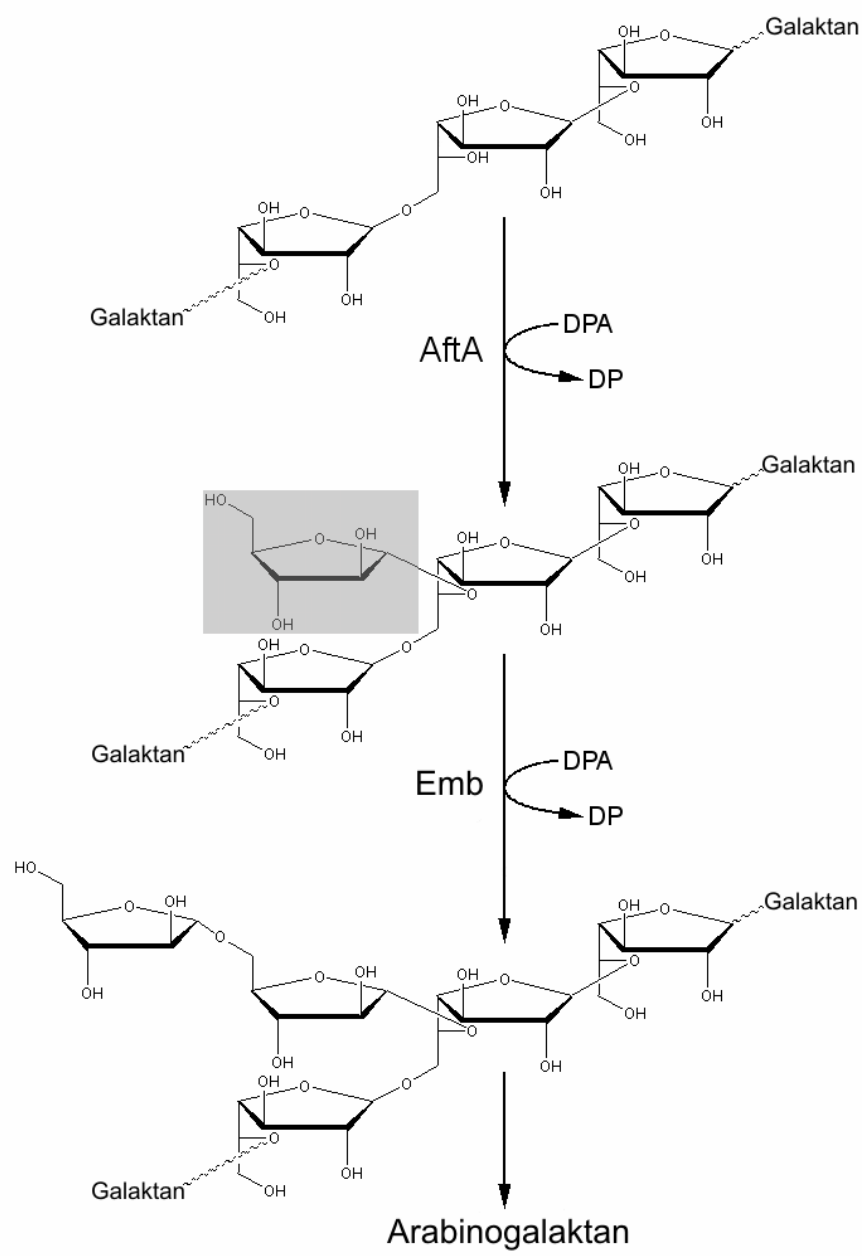

Abb. B-2: Der Start der Arabinansynthese am Galaktan. Die Bindung der ersten Arabinose (grau hinterlegt) erfolgt mit dem C5-Atom einer Galaktose. Die Bindung der zweiten Arabinose-Einheit erfolgt mit dem C5-Atom der ersten Arabinose-Einheit. AftA, Arabinofuranosyltransferase A; DPA, Decaprenol-Arabinose. DP, Decaprenolrest. Weitere Erläuterungen folgen im Text.

Auch für die Inititation der Galaktansynthese im Arabinogalaktan wurde vor kurzem eine spezifische Glykosyltransferase, das RfbE-Protein, identifiziert (Mikusova *et al*., 2006). In den Untersuchungen zum RfbE-Protein wurde wahrscheinlich gemacht, dass nicht nur die erste, sondern auch die zweite Galaktoseeinheit im Galaktan vom RfbE-Protein verknüpft

wird, was im Widerspruch zum *one enzyme one linkage*-Konzept steht (Breton *et al*., 2002). Bei diesen Untersuchungen konnte jedoch nicht unterschieden werden, ob die zweite Galaktose durch das RfbE-Protein oder eine weitere Galaktosyltransferase, das GlfT-Protein, katalysiert wird (Mikusova *et al*., 2006), da auf Gendeletionen verzichtet wurde und die Analysen mit Rohextrakt durchgeführt wurden, in dem alle Enzyme der Galaktanbiosynthese vorhanden waren (Mikusova *et al*., 2006).

3 Der Abschluss der Arabinansynthese in *Corynebacterianeae*

Aus Untersuchungen von McNeil *et al*. (1991) war bekannt, dass β(1→2) Verknüpfungen im Arabinan dem terminalen Ende der Arabinandomäne zuzuordnen sind, welche in *M. tuberculosis* und *C. glutamicum* einen Teil der kovalent mit den Mykolsäuren verbundenen Zucker im Arabinogalaktan darstellen (Puech *et al*., 2001).

Der Einbau der β(1→2) Arabinose konnte bislang noch keinem Enzym zugewiesen werden. Daher wurde nach Genen für Arabinosyltransferasen gesucht, die in *Corynebacterianeae* in syntenischer Anordnung mit bekannten Genen für Mykolyltransferasen vorliegen. Auf diese Weise wurde schließlich in dieser Arbeit (Alderwick *et al*., 2006) bereits die Arabinosyltransferase AftA identifiziert. Stromaufwärts des Gens der Mykolyltransferase FbpA konnte ein offener Leserahmen identifiziert werden, der für eine Arabinofuranosyltransferase B (AftB) kodiert (Seidel *et al*., 2007b). Sowohl für das AftB-Protein aus *C. glutamicum*, als auch aus *M. tuberculosis* konnte in dieser Arbeit eine Arabinosyltransferaseaktivität nachgewiesen werden (Seidel *et al*., 2007b). Es konnte gezeigt werden, dass das AftB-Protein den Transfer der letzten Arabinose an das Arabinan im Arabinogalaktan katalysiert. Das Protein AftB stellt damit, ebenso wie das AftA-Protein, eine bislang unbekannte Glykosyltransferase der Arabinanbiosynthese in *Corynebacterianeae* dar, wie sie in Abbildung B-3 gezeigt wird. Im Gegensatz zu den Arabinosyltransferasen Emb und AftA ist AftB in *C. glutamicum* nicht essentiell.

Die Analyse der Mykolsäuren in der *C. glutamicum* Deletionsmutante ergab, dass der Verlust von β(1→2) gebundener Arabinose zusätzlich zu einer Reduzierung der mit dem Arabinogalaktan verbundenen Mykolsäuren führt. Nur etwa 50% der gebundenen Mykolsäuren waren noch nachweisbar. Daher ist anzunehmen, dass die β(1→2) verknüpfte Arabinose in *C. glutamicum* etwa 50% der Verknüpfungspunkte zu den Mykolsäuren darstellt, wohingegen die anderen 50% der gebundenen Mykolsäuren mit α(1→5) Arabinose-Einheiten verbunden sind, wie es auch bereits für die Arabinan-Mykolsäure Verbindung in

M. tuberculosis beschrieben wurde (McNeil *et al*., 1991). Da aber erheblich mehr Mykolsäuren in *M. tuberculosis* an die β(1→2) und die α(1→5) Arabinose-Einheiten gebunden sind (Puech *et al*., 2001), ist das AftB-Protein für *M. tuberculosis* möglicherweise essentiell. Aus diesem Grunde könnte auch das AftB-Protein für die Synthese spezifischer Inhibitoren interessant sein. Generell scheinen membrangebundene Glykosyltransferasen interessante Ziele für die Entwicklung von synthetischen Hemmstoffen zu sein.

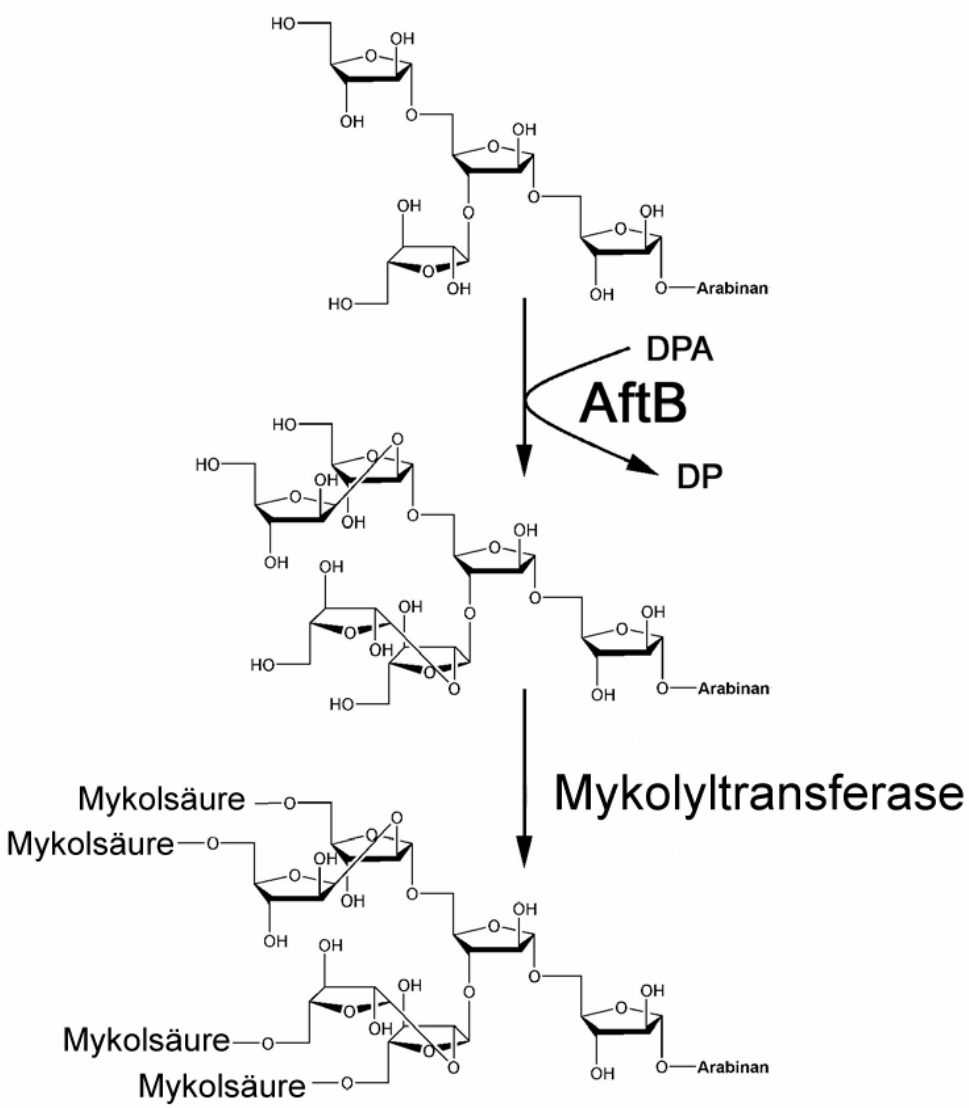

Abb. B-3: Die Synthese von Arabinan durch die Arabinofuranosyltransferase B (AftB) in *Corynebacterianeae*. Dargestellt ist die verzweigte Arabinankette und die Katalyse der β(1→2) Arabinose-Einheiten, die mit Mykolsäuren verestert werden. DPA steht für Decaprenolarabinose, DP steht für Decaprenolrest.

So konnten bereits für die neu identifizierte Galaktofuranosyltransferase GlfT (Kremer *et al*., 2001; Mikusova *et al*., 2000) Inhibitormoleküle auf Iminozuckerbasis synthetisiert werden, die spezifisch die Aktivität des GlfT-Proteins hemmen und damit die Grundlage für die Entwicklung neuer, synthetischer Antibiotika gegen *M. tuberculosis* darstellen (Cren *et al*., 2004). Dies könnte ein Ausweg sein, die mehrfachen Antibiotikaresistenzen in *M. tuberculosis* Stämmen zu umgehen (Ramaswamy *et al*., 2000; 2004; Sreevatsan *et al*., 1997).

4 Die Funktion und Struktur der Arabinofuranosyltransferase-Proteine

Die Emb-, AftA- und AftB-Proteine zeigen interessanterweise keine Gemeinsamkeiten in ihrer Primärsequenz auf. Das belegt auch die besondere Eigenschaft von Glykosyltransferasen, trotz großer Variationen in der Primärsequenz durchaus ähnliche Proteinstrukturen zu bilden, und dadurch ähnliche Funktionen erfüllen zu können (Breton *et al*., 2002; Coutinho *et al*., 2003).

Des Weiteren sind die Proteine Emb, AftA oder AftB in den verschiedenen Vertretern der *Corynebacterianeae* unterschiedlich stark konserviert. Während die Identität der orthologen AftA-Proteine in allen *Corynebacterianeae* etwa 37% zueinander beträgt, kann für die AftB-Proteine eine Identität von bis zu 75% ermittelt werden. Ein Grund für diese außergewöhnliche Konservierung der Aminosäuresequenzen könnte in einer Besonderheit der vom AftB-Protein katalysierten glykosidischen Bindung liegen. Denn anders als die α-glykosidischen Bindungen, die vom Emb-Protein und vom AftA-Protein katalysiert werden, vermittelt das AftB-Protein eine β-glykosidische Bindung. Das charakterisiert das AftB-Protein als konfigurationserhaltende Glykosyltransferase, da die β-Konfiguration der Arabinofuranose im Substrat 5-Pospho-β-D-Arabinosemonophopho-decaprenol (DPA) erhalten bleibt. Der Begriff „konfigurationserhaltend“ bezieht sich dabei auf die sterische Konfiguration am anomeren C-Atom des Substrats (Kapitonov & Yu, 1999; Thorson *et al*., 2001). Einerseits ist die β-glykosidische Bindung dafür bekannt, dass sie thermodynamisch stabiler als die α-glykosidische Bindung ist, andererseits müssen die konfigurationserhaltenden Glykosyltransferasen für die Katalyse einen intermediären Zustand mit dem Substrat einnehmen, um die Konfiguration des Zuckers erhalten zu können (Breton *et al*., 2006; Lairson *et al*., 2004). In diesem intermediären Zustand soll über sehr spezifische Bindemotive im Enzym eine starke Bindung zum Substrat bestehen (Lairson *et al*., 2004).

Das könnte ein Grund dafür sein, dass die homologen AftB-Proteine der *Corynebacterianeae* Übereinstimmungen von bis zu 75% aufweisen.

Die Gemeinsamkeiten aller Arabinosyltransferasen in *Corynebacterianeae* liegen eher in der Proteinstruktur begründet, wie es die in dieser Arbeit durchgeführten Vorhersagen zur Proteinsekundärstruktur für die Emb-, AftA und AftB-Proteine zeigen (Alderwick *et al*., 2006; Seidel *et al*., 2007a; 2007b. Allen drei Proteingruppen ist eine Domänenorganisation mit einem N-terminal transmembranen Bereich und einem C-terminal globulären Bereich gemeinsam, wie in Abbildung B-4 dargestellt. Dabei ist das Emb-Protein mit 1146 Aminosäureresten mehr als doppelt so groß als das AftA- oder AftB-Protein mit 643 bzw. 627 Aminosäureresten.

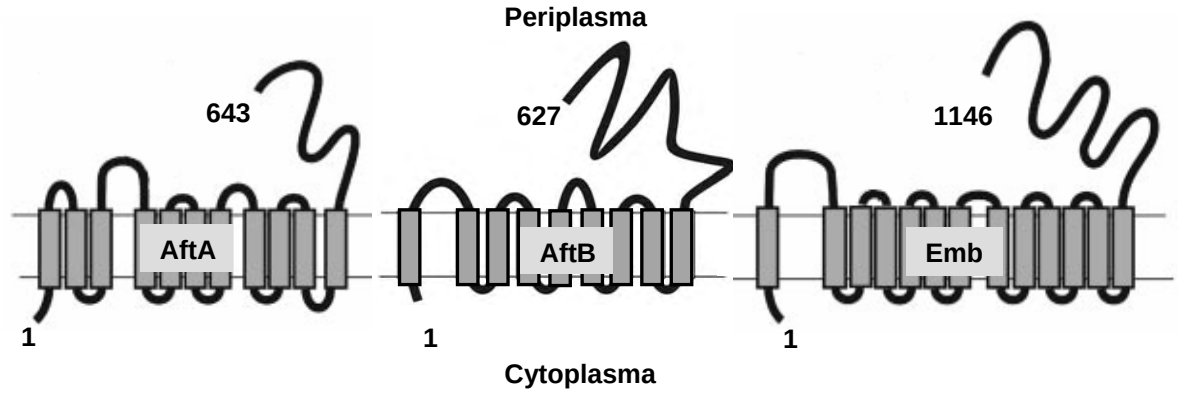

Abb. B-4: Schematische Organisation von Proteindomänen in der Cytoplasmamembran von den Arabinosyltransferasen AftA und AftB aus *M. tuberculosis* und Emb aus *C. glutamicum*. Dargestellt sind die hydrophoben Bereiche (grau) sowie die hydrophilen Bereiche (schwarz) der Arabinosyltransferasen. In Zahlen sind die ersten und letzten Aminosäurereste angegeben. Die Modelle wurden mit der *Density Alignment Surface Method* berechnet (Alderwick *et al*., 2006; Seidel *et al*., 2007a; 2007b.

Diese Domänenorganisation und die Verwendung von prenylierten-Substratzuckern machen die identifizierten Arabinosyltransferasen damit zu Mitgliedern der Glykosyltransferase Familie C (GT-C), die alle über die erwähnte Domänenorganisation verfügen, sowie prenylierte Zucker als Substrat verwenden, wie es von Liu & Mushegian (2003) für diese Proteingruppe beschrieben worden ist. Glykosyltransferasen der GT-C Familie lassen sich auch in eukaryotischen Organismen wie z.B. *Saccharomyces cerevisiae* oder *Homo sapiens* identifizieren. In prokaryotischen Organismen sind die Glykosyltransferasen der Zellwandbiosynthese aus den *Corynebacterianeae* hingegen die einzigen identifizierten GT-C Enzyme (Hitchcock *et al*., 2003; Imbach *et al*., 1999; Kojima *et al*., 2000; Körner *et al*., 1999). Da die Enzyme der GT-C Familie damit in Bakterien eine Besonderheit darstellen, scheint hier möglicherweise ein Schnittpunkt in der Biosynthese von prokaryotischen Exopolysacchariden und eukaryotischen Zelloberflächenglykosylierungen,

wie z.B. Glykosylphophatidylinositol (Maeda *et al*., 2001), zu bestehen.

Ein wesentliches Merkmal von vielen Glykosyltransferasen ist ein sogenanntes Glykosyltransferasemotiv. Dieses Motiv basiert auf Asparaginsäureresten (D), die in der Aminosäuresequenz in vielfältiger Kombination als D, DxD, D/E und, speziell für GT-C Enzyme, als DDx oder DEx identifiziert werden konnten (Liu & Mushegian, 2003). Ein DDx-Motiv findet sich, wie in Abbildung B-5 aufgeführt, auch in den Emb- und den AftB-Proteinen der *Corynebacterianeae*. In den AftA-Proteinen kann dagegen nur ein GT-C ähnliches Motiv identifiziert werden, welches von dem regulären Sequenzmotiv abweicht und mit einem Asparaginsäurerest, benachbart zu einem ebenfalls polaren Glutaminrest, vorliegt.

C. glutamicum Emb:	AS 291- LGANTS**DD**GFIMTMARVSQNADYMANYYRWFGVPESP
M. tuberculosis AftB:	AS 22- SQRRWIA**DD**GLIVLRTVRNLLAGNGPVFNQGERVEANTS
M. tuberculosis AftA:	AS 21- YLFGISV**DQ**QFRTEYLTRLTDTAALRDMTYIGLPPFYPPG

Abb. B-5: Lokalisation der GT-C Aminosäure Motive in den Aminosäuresequenzen der Arabinosyltransferasen Emb aus *C. glutamicum* und AftB aus *M. tuberculosis*, sowie ein unvollständiges GT-C Motiv in AftA aus *M. tuberculosis*. Die Asparaginsäurereste des GT-C Motivs sind unterstrichen, die Zahlen geben die Aminosäureposition (AS) an.

In dieser Arbeit wurden das GT-C Motiv im Emb-Protein aus *C. glutamicum* und dem AftB-Protein aus *M. tuberculosis* untersucht (Seidel *et al*., 2007a; 2007b). Die Arabinosyltransferasen wurde für Untersuchungen zur ortsgerichteten Mutagenese (D297A, D298A im Emb-Protein und D29A, D30A im AftB-Protein) verwendet und die Enzymaktivität zur Zuckerverknüpfung untersucht. Dabei wurde gezeigt, dass beide Asparaginsäurereste des GT-C Motivs im AftB-Protein aus *M. tuberculosis*, und mindestens einer der Asparaginsäurereste im Emb-Protein aus *C. glutamicum*, essentiell für die Arabinansynthese im Arabinogalaktan sind, da die entsprechenden Zuckerverknüpfungen von den mutierten Proteinen nicht katalysiert wurden. Auch die Analysen von Berg *et al.* (2005) weisen darauf hin, dass Variationen des GT-C Motivs durch ortsgerichtete Mutagenese im EmbC-Protein aus *M. smegmatis* zumindest zu einer Verringerung der Arabinansynthese im Lipoarabinomannan führen. Die Funktion der GT-C Motive in der Arabinansynthese im Arabinogalaktan der *Mycobacteria* wurde aber noch nicht untersucht. Aufgrund der in dieser Arbeit mit dem Emb-Protein aus *C. glutamicum* erhaltenen Ergebnisse zur Arabinogalaktansynthese (Seidel *et al*., 2007a) kann nun postuliert werden, dass auch die Asparaginsäurereste der GT-C Motive in den mycobacteriellen Arabinosyltransferasen EmbA

und EmbB essentiell für die Arabinansynthese im Arabinogalaktan der *Mycobacteria* sind.

Des Weiteren wurden diese Asparaginsäurereste in Enzymen der GT-C und der GT-A Familie, wie z.B. die Mannosyltransferasen PIG-M aus *H. sapiens* und MNN aus *S. cerevisiae*, untersucht und waren dort essentiell für die Enzymaktivität (Maeda *et al*., 2001; Wiggins & Munro, 1998). Strukturelle Untersuchungen dieses Motivs lassen vermuten, dass die Aminosäuren an der Bindung eines divalenten Kations (z.B. Ca^{2+}, Mg^{2+}, Mn^{2+}) beteiligt sind, welches für die Bindung der Phosphatgruppe des aktivierten Substratzuckers am aktiven Zentrum der Glykosyltransferase unbedingt notwendig ist (Gastinel *et al*., 1999; Lairson *et al*., 2004). Diese Theorie wird durch den Befund gestützt, dass Glykosyltransferasen der GT-B Familie für die Enzymaktivität keine divalenten Kationen benötigen und dementsprechend auch keine Asparaginsäuremotive aufweisen (Hu & Walker, 2002). Im Bereich der Aminosäuresequenz des GT-C Motivs könnte damit möglicherweise eine Substratzuckerbindende Domäne in den Arabinosyltransferasen Emb und AftB identifiziert worden sein.

Ein weiteres funktionelles Motiv in Glykosyltransferasen ist das sogenannte Prolin-Motiv. Im Rahmen dieser Arbeit wurden Mutationsstudien zum Prolin-Motiv im Emb-Protein aus *C. glutamicum* durchgeführt, in denen einfach (W659L oder P667L oder Q674E) und dreifach mutierte Varianten des Emb-Proteins näher betrachtet wurden (Seidel *et al*., 2007a). In allen Fällen konnte beobachtet werden, dass weniger Arabinofuranose im Arabinan der Zellwand eingebaut wird. Allerdings gibt es keinen generellen Verlust eines Verknüpfungstyps der Zucker im Arabinan. Die deutlichste Reduzierung des Arabinangehalts wurde dabei mit einer Dreifachmutation im Emb-Protein aus *C. glutamicum* erreicht, was auch mit den Beobachtungen von Berg *et al.* (2005) für die Arabinansynthese im mycobacteriellen Lipoarabinomannan übereinstimmt.

Das Prolin-Motiv wird mit der Bestimmung der Kettenlänge eines Polysaccharides durch prozessive Glykosyltransferasen in Verbindung gebracht. Dies wurde erstmals in der Glykosyltransferase ExoP aus *Rhizobium meliloti* untersucht (Becker & Pühler, 1998). Ein solches Motiv kann innerhalb der Enzyme für die Arabinansynthese in *Corynebacterianeae* nur in den Emb-Proteinen identifiziert werden, die auch mit der Katalyse von Arabinanpolysaccharidketten in Verbindung stehen (Belanger *et al*., 1996; Khasnobis 2006). Wahrscheinlich fehlt dieses Motiv in den AftA- und AftB-Proteinen, weil dadurch, wie in dieser Arbeit gezeigt wurde, nur monoglykosidische Verbindungen katalysiert werden (Alderwick *et al*., 2005; 2006). Im Gegensatz dazu wird dem Protein Emb auch die Katalyse von polyglykosidischen Verbindungen zugesprochen (Khasnobis *et al*., 2006).

Das Prolin-Motiv wurde auch in der Glykosyltransferase Wzz identifiziert, die an der

Lipopolysaccharid (LPS) Biosynthese in *Shigella flexneri* beteiligt ist (Daniels & Morona, 1999). Durch die Untersuchung dieses Motivs im Wzz-Protein aus *S. flexneri* konnte ein Zusammenhang mit der Länge des synthetisierten Polysaccharids demonstriert werden. Der Mechanismus der Kettenlängenbestimmung, in Abhängigkeit von den Aminosäureresten des Prolin-Motivs, konnte jedoch noch nicht aufgeklärt werden (Daniels & Morona, 1999). Die Glykosyltransferase Wzz wurde auch in *Salmonella typhimurium*, *Escherichia coli* und *Pseudomonas aeruginosa* mit der Bestimmung der LPS Kettenlänge in Zusammenhang gebracht (Daniels *et al*., 2002; Morona *et al*., 2000; Murray *et al*., 2003). Allerdings konnte für diese Organismen gezeigt werden, dass die Bestimmung der Polysaccharidkettenlänge über den oligomeren Zustand des Wzz-Proteins vom Dimer bis zum Hexamer reguliert wird (Daniels *et al*., 2002). Diese Befunde weisen darauf hin, dass die Variationen des Prolin-Motivs im Emb-Protein aus *C. glutamicum* möglicherweise an der Fähigkeit zur Oligomerisierung des Proteins und damit zu unterschiedlichen Arabinankettenlänge beitragen können.

Um die Ergebnisse der Mutationsstudien in ein topologisches Modell des Proteins einzuordnen, wurde die Topologie des Emb-Proteins aus *C. glutamicum* untersucht. Das sehr große Emb-Protein aus *C. glutamicum* (1146 Aminosäurereste) besitzt demnach einen transmembranen sowie einen globulären Bereich, der durch verschiedenste Topologievorhersagen nicht eindeutig dem periplasmatischen oder cytoplasmatischen Raum zugeordnet werden kann.

In dieser Arbeit konnte nun mittels LacZα/PhoA-Reporterprotein-Fusionen gezeigt werden, dass der globuläre Bereich des Emb-Proteins im periplasmatischen Raum lokalisiert ist (Seidel *et al*., 2007a). Darüber hinaus erlaubten die 62 Emb-Proteinfusionen eine Aussage über die peri- oder cytoplasmatische Orientierung von einzelnen Bereichen des Emb-Proteins. Zusammen mit den Informationen über die 15 hydrophoben und damit putativ membranständigen Segmente der Aminosäuresequenz ist ein Topologie-Modell des Emb-Proteins für den Bereich in der Cytoplasmamembran erstellt worden (siehe Abb. B-6).

Die Befunde der in dieser Arbeit (Seidel *et al*., 2007a) erstellten Topologieanalyse des Emb-Proteins aus *C. glutamicum* zeigen, dass die Asparaginsäurereste des GT-C Motivs im Emb-Protein dem periplasmatischen Raum zugewandt sind. In der Umgebung des GT-C Motivs im Emb-Protein aus *C. glutamicum* befinden sich auch Aminosäuresequenzen, die homolog zu Ethambutolresistenz vermittelnden Regionen der Emb-Proteine aus *M. tuberculosis* sind (Ramaswamy *et al*., 2000; Telenti *et al*., 1997). Die unmittelbare Nachbarschaft von katalytisch essentiellen und Inhibitor-sensitiven Aminosäuren zeigt die besondere Bedeutung dieses Bereiches der Emb-Proteine zwischen den hydrophoben

Segmenten III und IV. Die GT-C Sequenzmotive im AftB- und AftA-Protein lassen sich, abgeleitet von den Vorhersagen der Proteintopologien, ebenfalls im N-terminalen Bereich der Proteine zwischen den jeweiligen hydrophoben Segmenten III und IV bzw. I und II lokalisieren, was typisch für Enzyme der GT-C Familie ist (Liu & Mushegian, 2003).

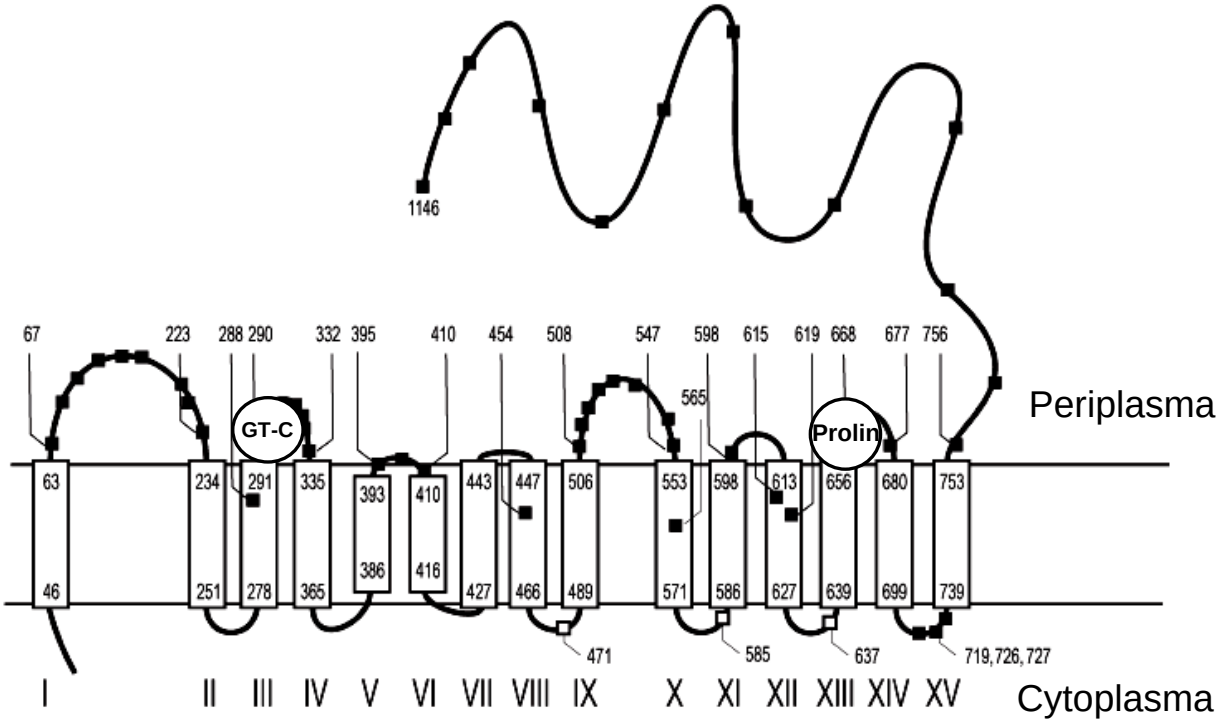

Abb. B-6: Topologiemodell der Arabinosyltransferase Emb aus *C. glutamicum*. Die ausgefüllten Quadrate stellen die Positionen dar, die als LacZα-PhoA Fusionsprotein PhoA Aktivität zeigten. Die nicht ausgefüllten Quadrate stellen Positionen dar, die als LacZα-PhoA Fusionsprotein β-Galaktosidase Aktivität aufwiesen. Die Nummern in den großen Rechtecken geben die Positionen der ersten und letzten Aminosäure der hydrophoben Segemente I bis XV wieder. Die Lokalisation der im Text näher beschriebenen, funktionellen Prolin und GT-C Motive, ist gekennzeichnet.

Die Aminosäuren des Prolin-Motivs befinden sich im Topologiemodell des Emb-Proteins alle zwischen den hydrophoben Segmenten XIII und XIV in einer Proteinschlaufe, die dem periplasmatischen Raum zugeordnet werden kann. Das erstellte Topologiemodell des Emb-Proteins lässt daher den Schluss zu, dass wenigstens zwei essentielle Schritte der Arabinofuranosyltransferaseaktivität, wie Substrat- oder Akzeptorbindung, sowie die Polysaccharid-Elongation im periplasmatischen Raum erfolgen. Dabei ist noch nicht klar, ob die Verlängerung des Arabinans direkt an der Zellwand gebunden oder an einem *carrier* erfolgt, und nachträglich mit der Zellwand verknüpft wird. Durch Untersuchungen aus *M. smegmatis* gibt es Hinweise darauf, dass das Arabinan vorsynthetisiert und erst abschließend mit der Zellwand verbunden wird (Hancock *et al*., 2002; Yagi *et al*., 2003).

Um das Arabinan synthetisieren zu können, müssen die Arabinosyltransferasen mit dem Substrat DPA in Kontakt kommen. Für die dekaprenylierte Arabinose kann angenommen werden, dass der Prenylrest mit der Cytoplasmamembran assoziiert ist. Zum Einbau in die Zellwand muss der lösliche Zuckeranteil im DPA von der cytoplasmatischen zur periplasmatischen Seite der Membran wechseln. Ob diese Reaktion durch eine bislang unidentifizierte Flippase oder z.B. durch das Emb-Protein selbst katalysiert wird, ist auch heute noch nicht geklärt. Es wird allerdings diskutiert, dass die Asymmetrie der Lipide in der Zellmembran keine enzymatisch katalysierte, sogenannte Flip-Flop Reaktion von Glykolipiden, wie z.B. DPA, erlaubt (Kol *et al*., 2002).

Auffällig war, dass die Topologievorhersage des Emb-Proteins aus *C. glutamicum* für den Bereich zwischen den hydrophoben Segmenten III und VII besonders variabel war, gleichzeitig aber die Aminosäuren in diesem Bereich in allen Emb-Proteinen den höchsten Konservierungsgrad aufwiesen (Subramanian *et al*., 2005). Die mathematische Vorhersage gab zwei hydrophobe Segmente für diesen Bereich der Aminosäuresequenz vor. Die experimentell ermittelten Informationen mit den periplasmatisch zugeordneten Enzymfusionen L395, P396 und G410 gaben Hinweise auf mindestens drei, z.T. sehr kurze, hydrophobe Segmente in diesem Bereich des Emb-Proteins. Es wäre möglich, dass diese sehr kurzen hydrophoben Segmente einen sehr spezifischen Bereich des Membranproteins darstellen, der nicht vollständig transmembran organisiert ist. Dadurch würde die periplasmatisch orientierte Schlaufe im Emb-Protein zwischen den hydrophoben Segmenten V und VI nur in die Cytoplasmamembran eintauchen und damit eine besondere funktionelle Bedeutung für den Substrattransport besitzen. Die dreidimensionalen Proteinstrukturen von z.B. Aquaporin oder dem Glutamattransporter aus *Pyrococcus horikoshii* zeigen, wie in ähnlicher Weise in die Membran eintauchende Proteinschleifen direkt an der Transportaktivität der Enzyme beteiligt sind (Yernool *et al*., 2004).

Die neu identifizierten Arabinofuranosyltransferasen AftA und AftB, sowie das Emb-Protein sind damit aufgrund ihrer Aktivität und Spezifität charakterisiert worden. Aus der Topologieanalyse des Emb-Proteins und den Topologievorhersagen für das AftA- und das AftB-Protein kann auch auf strukturelle Gemeinsamkeiten in den Arabinofuranosyl-transferasen geschlossen werden, die sich nicht allein aus der Aminosäuresequenz ableiten lassen. Damit wurde für die neu identifizierten Arabinofuranosyltransferasen die Grundlage für weitere Untersuchungen gelegt, die sich insbesondere auf die Proteinstrukturen und die daraus abzuleitenden Gemeinsamkeiten konzentrieren könnten.

C Publikationen

1 Deletion of Cg-*emb* in Corynebacterianeae Leads to a Novel Truncated Cell Wall Arabinogalactan, whereas Inactivation of Cg-*ubiA* Results in an Arabinan-deficient Mutant with a Cell Wall Galactan Core

published in *The Journal of Biological Chemistry* 2005; **280:** 32362-32371

by Luke J. Alderwick[1], Eva Radmacher[2],**Mathias Seidel**[2], Roland Gande[2], Paul G. Hitchen[3,4], Howard R. Morris[3,4], Anne Dell[3], Hermann Sahm[2], Lothar Eggeling[2], and Gurdyal S. Besra[1]

From the [1]School of Biosciences, University of Birmingham, Edgbaston, Birmingham B15 2TT, United Kingdom, the [2]Institute for Biotechnologie 1, Research Centre Juelich, D-52425 Juelich, Germany, the [3]Division of Molecular Biosciences, Faculty of Life Sciences, Imperial College, London SW7 2AZ, United Kingdom, and [4]M-SCAN Mass Spectrometry Research and Training Centre, Silwood Park, Ascot SL5 7PZ, United Kingdom

Summary

The cell wall of *Mycobacterium tuberculosis* has a very complex ultrastructure which consists of long chain mycolic acids connected to peptidoglycan *via* arabinogalactan (AG) with the entire structure abbreviated as the mAGP complex. The mAGP is crucial for the growth, survival and pathogenicity of *M. tuberculosis* and is the target of several anti-tubercular agents. Apart from sharing a similar cell wall, mAGP and the availability of the complete genome sequence, *Corynebacterium glutamicum* has proven useful in the study of orthologous *M. tuberculosis* genes essential for viability. In this study we examined the effects of particular genes involved in AG polymerization by gene deletion in *C. glutamicum*. The anti-tuberculosis drug ethambutol is thought to target a set of arabinofuranosyltransferase enzymes (Emb) which are involved in arabinan polymerization. We have shown that deletion of the *emb* gene in *C. glutamicum* results in a viable, yet slow growing mutant with profound morphological changes. Furthermore, chemical analysis has revealed a dramatic reduction of arabinose resulting in a novel truncated AG structure possessing only singular terminal arabinofuranoside (t-Ara*f*) residues with a corresponding loss of cell wall bound mycolic acids. Treatment of wild type *C. glutamicum* with ethambutol and subsequent cell wall analyses resulted in an identical phenotype comparable to the *C. glutamicum emb* deletion mutant. Additionally, disruption of the *ubiA* gene of *C. glutamicum*, the first enzyme involved in the biosynthesis of the sugar donor decaprenol phosphoarabinose (DPA) biosynthesis resulted in a complete loss of cell wall arabinan. Herein, we establish for the first time, (i) that

in contrast to *M. tuberculosis embA* and *embB* mutants, deletion of *C. glutamicum emb* leads to a highly truncated AG possessing singular *t*-Ara*f* residues, (ii) the exact site of attachment of arabinan chains in AG, (iii) and that DPA is the only Ara*f* sugar donor in AG biosynthesis suggesting the presence of a novel *emb*-related gene responsible for "priming" the galactan domain for further elaboration by Emb, resulting in the final maturation of the native AG polysaccharide.

Introduction

The Corynebacterianeae represent a distinct and unusual group within Gram-positive bacteria, with the most prominent members being the human pathogens *Mycobacterium tuberculosis* and *Mycobacterium leprae* (1). In addition, the human pathogen *Corynebacterium diphtheriae* is the causal agent of diphtheria, and serious economic losses occur from the infection of animals by corynebacterial strains, such as *Corynebacterium pseudotuberculosis* and *Corynebacterium matruchotii* (2, 3). Furthermore, non-pathogenic bacteria belong to this taxon, such as *Corynebacterium glutamicum*, which is used in the industrial production of amino acids (4). A common feature to all these bacteria is that they possess an unusual cell wall matrix composed of mycolic acids, arabinogalactan, and peptidoglycan and is often referred to as the mycolyl-arabinogalactan-peptidoglycan $(mAGP)^6$ complex (5–9).

Arabinogalactan (AG) plays a crucial role in covalently anchoring the outer lipid layer to peptidoglycan. Synthesis of AG begins with the formation of the linker unit through the transfer of GlcNAc-1-P and Rha from their respective sugar nucleotides (UDP-GlcNAc and dTDP-Rha) to form polyprenol-P-P-GlcNAc and polyprenol-P-P-GlcNAc-Rha lipid intermediates (10, 11). The intermediates polyprenol-P-P-GlcNAc and polyprenol-P-P-GlcNAc-Rha then serve as acceptors for the sequential addition of galactofuranose (Gal*f*) residues from UDP-Gal*f* (generated from UDP-Gal*p* via Glf (12, 13)) to form polyprenol-P-PGlcNAc-Rha-Gal_{30} through a novel enzyme designated GlfT (Rv3808c). This latter enzyme expresses two glycosyltransferase activities, a UDPGal*f*: β-D-(1→5)-Gal*f* and a UDP-Gal*f*:β-D-(1→6)-Gal*f*, both activities being required for alternating β(1→5) and β(1→6) linkages during galactan polymerization (11, 14). Chemical analysis of the mature lipidlinked galactan, synthesized *in vitro* (11), suggests that this intermediate then serves as the acceptor for the subsequent addition of arabinofuranose (Ara*f*) residues from the arabinose sugar donor β-D-arabinofuranosyl-1-monophosphoryldecaprenol (DPA) in the formation of the Ara*f* portion

(α1→5, α1→3, and β1→2 linkages) of AG (15–18). The AG-lipid intermediate at some point is mycolylated and transglycosylated to peptidoglycan (19, 20).

Early studies demonstrated that administration of ethambutol (EMB) led to a rapid cessation of mycolic acid transfer to the cell wall and an accumulation of trehalose monomycolate and trehalose dimycolate (21). Subsequently, EMB was shown to inhibit specifically AG biosynthesis (22). The precise molecular target of EMB occupies the *emb* locus in *Mycobacterium avium* and *M. tuberculosis*. The locus consists of *embRAB* in *M. avium* (23) and *embCAB* in *M. tuberculosis* (24). To further define the role of EmbCAB proteins in arabinan biosynthesis, *embA*, *embB*, and *embC* genes were inactivated individually in *Mycobacterium smegmatis* (25, 26). Although all three mutants were viable, only the crucial terminal Ara6 motif, which is the template for mycolylation in AG, was altered in both *embA* and *embB* mutants with the remainingAGstructure intact (25). This suggested that both EmbA and EmbB are involved in the formation of the terminal Ara_6 motif in AG, and EmbC in the formation of arabinan in lipoarabinomannan (26). Our preliminary attempts to obtain deletion mutants of *embA* and *embB* in *M. tuberculosis* or *embAB* in *M. smegmatis* have proved unsuccessful,[7] presumably due to the essentiality of cell wall mAGP (27–29).

In the present study we have established through comparative genomic analyses the first biochemical and molecular description of compete ablation of cell wall arabinan biosynthesis in a non-mycobacterial spp., and we highlight the inherent usefulness of examining related spp. to probe complex biosynthetic pathways.

Material and Methods

Strains and Culture Conditions—C. glutamicum ATCC 13032 (the wild-type strain, and referred for the remainder of the text as *C. glutamicum*) and *Escherichia coli* DH5αmcr were grown in Luria-Bertani (LB) broth (Difco) at 30 °C and 37 °C, respectively. The mutants generated in this study were grown on BHIS (5 g of Tryptone, 5 g of NaCl, 2.5 g of yeast extract, 18.5 g of brain heart infusion (Difco), and 90.1 g of sorbitol per liter). Kanamycin and ampicillin were used at a concentration of 50 μg/ml. The minimal medium CGXII was used for *C. glutamicum* (30). Samples for lipid analyses were prepared by harvesting cells at an optical density (OD) of 10–15, followed by a saline wash and freeze drying. Cultivation of *C. glutamicum_emb* for lipid and cell wall analysis required two pre-cultures: Firstly, a 5-ml BHIS culture was grown for 8 h, which was then used to inoculate a 50-ml BHIS culture for 15 h. This was then used to inoculate a 100-ml BHIS culture to OD 1, which was harvested after reaching an OD 3.

Construction of Plasmids—The vectors used for deletion and inactivation were as follows: pK19mobsacBΔ*emb* (*NCgl0184*, *embC*), pCg::*ubiA* (*NCgl2781*, *Rv3806c*), with the gene numbers of the *C. glutamicum* and *M. tuberculosis* orthologs added in parentheses. The plasmid used for overexpression was pEKEx2*emb*. To enable deletion of gene cross-over PCR was applied to generate the fragments carrying fused sequences adjacent to the gene in question. The resulting fragments were ligated with pK19mobsacB, and the final plasmids were confirmed by sequencing. For *emb* deletion, the primers used were *emb*_start_in 5´-CCC ATC CAC TAA ACT TAA ACA CTC AAC TAC ATC TGA CAC GTT GAT C-3´, *emb*_start_out 5´-GCT TGG TGA GTT CGG AAA CAG GA-3´, *emb*_end_in 5 -TGT TTA AGT TTA GTG GAT GGG CTC TGG AAT CCA GGG CAT ATG AAG-3´, and *emb*_end_out 5´-TTC CAT GAG CAG CTG GCG ATA AC-3´. For the second PCR the primer pair *emb*_start_out and *emb*_end_out was used again. The resulting fragment was ligated with SmaI-cleaved pK19mobsacB to generate pK19mobsacBΔ*emb*. For inactivation of *ubiA* an internal fragment of 321 bp was amplified (p*ubiA*-for: ATC TTC AAC CAG CGC ACG ATC; p*ubiA*-rev: AAT ATC GAT CAC TGG CAT GTG C), which was made blunt and ligated into the SmaI site of the non-replicative vector pK18mob to yield pCg::*ubiA*.

Genomic Mutations—To enable chromosomal inactivation of *ubiA*, pCg::*ubiA* was introduced into *C. glutamicum* by electroporation. Selection for resistance to kanamycin yielded clones whose correct disruption of *ubiA* was confirmed with different primer pairs annealing in the vector and the bacterial chromosome.

Southern Blot Analysis—Genomic DNA was extracted from *C. glutamicum*Δ*emb* and the wild-type strain and cleaved with EcoRV. The resulting fragments were separated on a 1% agarose gel and blotted onto a Nytran NY13N nitrocellulose membrane, with subsequent washings according to standard protocols. Detection was carried out with a fragment generated by PCR with primers pEmbΔ1 (5´-GTG GTT TAG GGG GTC TGT TGG G-3´) and pEmbΔ2 (5´-GGC AGC GTG CCG ATC ATC GCC-3´) as probe that was labeled with digoxigenin (DIG labeling and detection kit, Roche Applied Science).

Extraction and Analysis of Cell Wall Bound Mycolic Acids from C. glutamicum Strains—Cells were grown as described above, harvested, washed, and freeze-dried. Cells (100 mg) were extracted by two consecutive extractions with 2ml of $CHCl_3/CH_3OH/H_2O$(10:10:3, v/v) for 3h at 50 °C. The bound lipids from the delipidated extracts or purified cell walls (see below) were released by the addition of 2 ml of 5% aqueous solution of tetrabutylammonium hydroxide, followed by overnight incubation at 100 °C. After cooling, water (2 ml), CH_2Cl_2 (4 ml), and CH_3I (500 µl) were added and mixed

thoroughly for 30 min. The lower organic phase was recovered following centrifugation and washed three times with water (4 ml), dried, and resuspended in diethyl ether (4 ml). After centrifugation the clear supernatant was again dried and resuspended inCH_2Cl_2 (100 µl). An aliquot (10 µl) from each strain was subjected to TLC using silica gel plates (5735 silica gel $60F_{254}$, Merck), and developed in petroleum ether/acetone (95:5, v/v) and charred using 5% molybdophosphoric acid in ethanol at 100 °C to reveal corynomycolic acid methyl esters (CMAMES) and compared with known standards (31).

Isolation of the mAGP Complex—The thawed bacterial cells were resuspended in phosphate-buffered saline containing 2% Triton X-100 (pH 7.2), disrupted by sonication and centrifuged at 27,000 *g* (6, 7). The pelleted material was extracted three times with 2% SDS in phosphate-buffered saline at 95 °C for 1 h to remove associated proteins, successively washed with water, 80% (v/v) acetone in water, and acetone, and finally lyophilized to yield a highly purified cell wall preparation (6, 7).

Glycosyl Composition of Cell Walls by Alditol Acetates—Cell wall preparations were hydrolyzed in 250 µl of 2 M trifluoroacetic acid at 120 °Cfor 2 h as described (6, 7). Sugar residues were reduced with 50 µl of NaB_2H_4 (10 mg/ml in ethanol:1 M NH_3 (1:1)), and the resultant alditols were per-*O*-acetylated and examined by gas chromatography (GC) as described previously (6, 7).

Glycosyl Linkage Analysis of Cell Walls—Cell wall preparations (10 mg) were suspended in 0.5 ml of Me_2SO (anhydrous) and 100 µl of 4.8M dimethyl sulfinyl carbanion (6, 7). The reaction mixture was stirred for 1 h, and then CH_3I was slowly added, and the suspension was stirred for a further 1 h; this process was repeated for a total of three times. The reaction mixture was then diluted with an equal volume of water, and the entire contents were dialyzed against water overnight. The resulting per-*O*-methylated cell wall samples were applied to a C_{18} Sep-Pak cartridge and purified as described previously (6, 7). The per-*O*-methylated cell walls were hydrolyzed using 250 µl of 2 M trifluoroacetic acid at 120 °C for 2 h. The resulting hydrolysate was reduced with NaB_2H_4, per-*O*-acetylated, and examined by gas chromatography/mass spectrometry (GC/MS) as described previously (6, 7).

Mass Spectrometry of Per-O-methylated Cell Walls—Per-*O*-methylated cell walls were prepared as described above. Methanolic-HCl was Prepared by bubbling HCl gas into ~2ml of methanol until hot to the touch (~1 molar). The reagent (100 µl) was added to the per-*O*-methylated cell wall sample, and aliquots were analyzed by matrix-assisted laser desorption/ionization-time of flight mass spectrometry (MALDITOFMS) to monitor hydrolysis. The reaction was terminated by drying under nitrogen. MALDI-MS was

performed using a PerSeptive Biosystems Voyager DE^{TM} STR mass spectrometer (Applied Biosystems, CA) in the reflectron mode with delayed extraction. Samples were dissolved in methanol, and 1-µl aliquots were loaded onto a metal plate with 1µl of the matrix 2,5-dihydrobenzoic acid. Sequazyme peptide mass standards were used as external calibrants (Applied Biosystems, CA).

GC and GC/MS of Sugar Composition and Sugar Linkage Analysis—Analysis of alditol acetate sugar derivatives was performed on a CE Instruments ThermoQuest Trace GC 2000. Samples were injected in the splitless mode. The column used was a DB225 (Supelco). The oven was programmed to hold at an isothermal temperature of 275 °C for a run time of 15min. GC/MS was carried out on a Finnigan Polaris/GCQ Plus^{TM}. The column used was a BPX5 (Supelco).

Results

Genome Comparison of the emb Locus—M. tuberculosis, M. bovis, M. leprae, and *M. avium* subsp. *paratuberculosis* have three *emb* genes (Fig. 1*A*), and at least one of these, *embB,* is suggested to be the target of EMB in mycobacteria (24, 32–34). However, *C. diphtheriae* and *C. glutamicum* have only one *emb* gene (35, 36). This is in accordance with the notion that the genome of *Corynebacterium* is considered to represent the archetype of Corynebacterianeae and has a low frequency of structural alterations and gene duplications (37). Interestingly, the single *emb* of *C. glutamicum*, *Cg-emb*, exhibits a higher identity to *embC* than to *embA* and *embB* of *Mycobacterium,* and increased expression of *Cg-emb* increases resistance of *C. glutamicum* toward EMB (38). In *M. leprae* and *M. avium* spp. *paratuberculosis* the paralogous *embAB* genes are separated by divergently transcribed genes that might indicate a more specific function and a separate regulation in these mycobacteria.

The above genomic comparison and the availability of the complete genome sequence of *C. glutamicum* has proven useful in the study of orthologous *M. tuberculosis* genes that are essential for viability. Therefore, in this study we examined the effects, in terms of arabinan biosynthesis and utilization of the sugar donor DPA, of firstly, Cg-*emb* by gene deletion in *C. glutamicum,* and secondly, disruption of *Cg-ubiA* (Fig.1*B*), an enzyme recently shown to be involved in the biosynthesis of the sugar donor DPA.

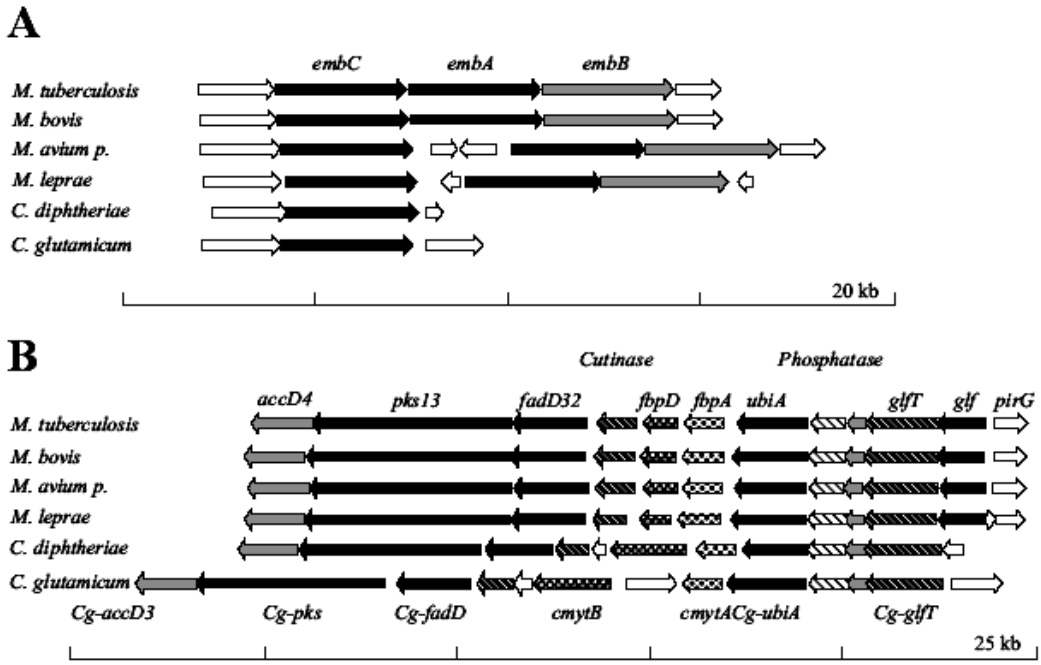

FIG. 1. Comparison of the mycolylarabinogalactan locus within the Corynebacterianeae. *A*, the locus consists of *embC* with its upstream gene. *B*, the ten genes delimited by *glfT* and *accD4*. The open reading frames of *M. tuberculosis* shown in *panel A* cover the genome sequence from nucleotide 4,235,265 to 4,251,005, and in *panel B* from nucleotide 4,254,380 to 4,274,593, they are separated by fadE35 and a transposase (not shown). *M. avium p.*, *M. avium* subp. *paratuberculosis.*

*Construction of C. glutamicum*Δ*emb*—In our recent studies on *emb* of *C. glutamicum* we placed the chromosomally encoded gene under the control of a tetracycline repressor (38) and observed a number of physiological consequences, including reduced growth in presence of repressor (38). These studies encouraged us to test whether it would be possible to obtain a deletion of *emb* in *C. glutamicum*. The non-replicative plasmid pk19mobsacBΔ*emb* was constructed carrying sequences adjacent to *emb*. The vector was introduced into *C. glutamicum* and in several electroporation assays 3 kanamycin resistance clones were obtained, indicating integration of pk19mobsacBΔ*emb* into the genome by homologous recombination (Fig. 2, *A* and *B*). The *sacB* gene enables for positive selection of a second homologous recombination event that can result either in the original wild-type situation or in clones deleted of *emb*. More than 200 clones were obtained after 2–4 days and analyzed by PCR, but in all of them the wild-type situation was restored, illustrating a strong disadvantage of *emb* deletion. Only 3 clones appearing after 10 days were shown by PCR to have *emb* deleted.A further confirmation of *emb* deletion in one of the clones chosen was obtained in a Southern blot analysis (Fig. 2*C*). The chromosomal EcoRV fragment of the wildtype is 7.82 kb in size, whereas that of the *emb* deletion mutant is reduced to 4.35 kb, which mirrors the

absence of *emb* of 3,438 bp. This confirms the integrity of the gene locus in the *emb* deletion mutant.

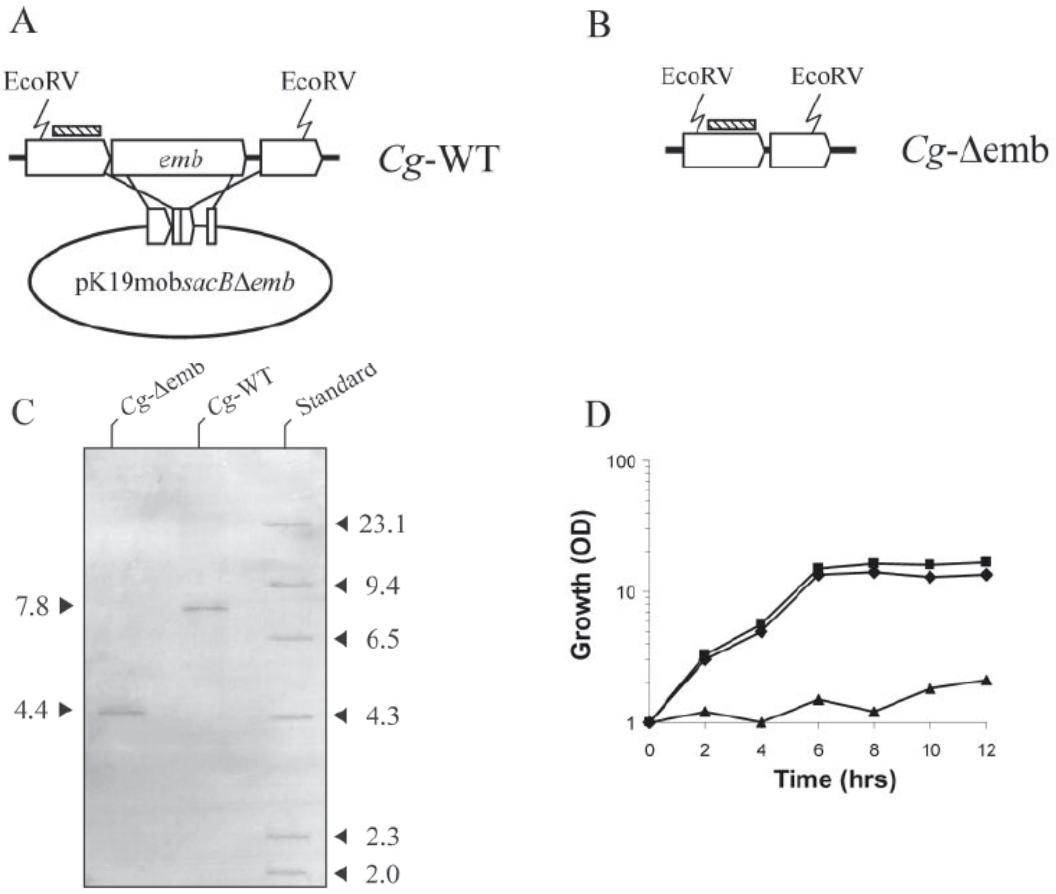

FIG. 2. Construction of *C. glutamicum_emb* mutant and growth analysis. ***A***, illustrated is *emb* with its adjacent genes of unknown function and the strategy to delete *emb* using the deletion vectorpK19mob*sacB*Δ*emb*. The deletion vector carries 12 nucleotides of the 5´-end of *emb* and 12 nucleotides of its 3´-end thereby enabling the in-frame deletion of almost the entire *emb* gene. The *hatched small box* locates the probe used for the Southern blot analysis to detect hybridizing sequences on the 7.82-kb EcoRV fragment of the wild-type containing *emb*. Distances are not drawn to scale. ***B***, situation of the original *emb* locus after deletion of *emb*, showing the intact organization of the originally adjacent genes in *C. glutamicum*Δ*emb* with the digoxigenin-labeled probe given as *hatched boxes* in *panelsA*and *B*. ***C***, final confirmation of the constructed strain via Southern blot analysis using chromosomal DNA from *C. glutamicum*Δ*emb* (*lane 1*), and Cg-WT (*C. glutamicum*) (*lane 2*). The *right lane* contains standards with their sizes given in kilobases. The *left lane* gives the sizes of the EcoRV fragments obtained from the wildtype, and the *emb* deletion mutant. The calculated sizes were 7.82 kb for the wild-type, and 4.35 kb for the deletion mutant. ***D***, consequences of *emb* deletion on growth of *C. glutamicum* (■), *C. glutamicum* deleted of *emb* (*C. glutamicum*Δ*emb*, (□)), as well as the same strain expressing plasmid encoded *emb* (*C. glutamicum_emb* pEKEx2*emb* (♦)).

*In Vitro Growth Analysis of C. glutamicum*Δ*emb*—The deletion mutant was transformed with pEKEx2*emb* (38), and growth was studied on brain-heart-infusion media supplemented with sorbitol for osmotic stabilization (30). Whereas growth of *C. glutamicum* was completed after 8 h at an OD of 16, *C. glutamicum*Δ*emb* hardly reached an OD of 2 (Fig.

2*D*). However, complementation of the deletion mutant with pEKEx2*emb* restored the wild-type growth phenotype. mRNA transcript quantifications using LightCycler technology confirmed a 5-fold overexpression of *emb* due to pEKEx2*emb* when comparing expression of *emb* with its chromosomal copy (data not shown). *M. tuberculosis embC*, *embA*, and *embB* were cloned into pEKE2, however, although expression and sequence integrity of each clone was confirmed, no complementation of *C. glutamicum_emb* was achieved (data not shown). Analysis by light microscopy and electron micrographs showed that when compared with *C. glutamicum*, *C. glutamicum_emb* exhibited profound morphological changes similar to that of *C. glutamicum* treated with 100 µg/ml EMB (38) (data not shown).

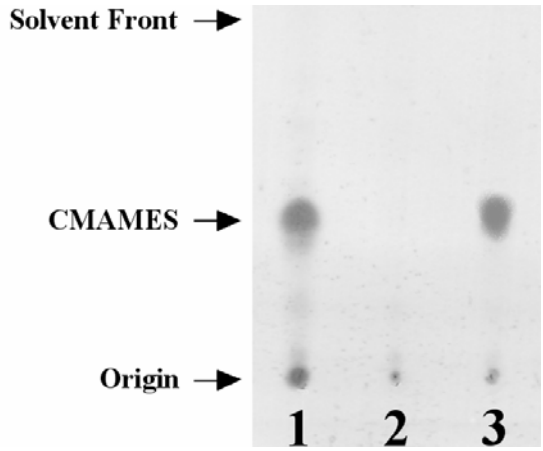

FIG. 3. Analysis of cell wall bound CMAMES from delipidated cells of *C. glutamicum*, *C. glutamicum*Δ*emb*, and *C. glutamicum*Δ*emb* pEKEx2*emb*. *Lane 1*, *C. glutamicum*; *lane 2*, *C. glutamicum*Δ*emb*; and *lane 3*, *C. glutamicum*Δ*emb*pEKEx2*emb*. The bound corynomycolic acids from the delipidated extracts or purified cell walls were released by the addition of tetrabutylammonium hydroxide at 100 °C overnight and methylated as described under "Materials and Methods." An aliquot from each strain was subjected to TLC using silica gel plates (5735 Silica Gel 60F254, Merck), and developed in petroleum ether/acetone (95:5, v/v) and charred using 5% molybdophosphoric acid in ethanol at 100 °C to reveal CMAMES and compared with known standards (31).

Lipid Characterization of Mutants—To relate the phenotypic changes of the *C. glutamicum_emb* mutant to its cellular composition, the *C. glutamicum*Δ*emb* and its *Cg-emb* complemented strain along with *C. glutamicum* were analyzed for arabinogalactan-esterified corynomycolic acids. Bound lipids were analyzed by hydrolysis and the preparation of corynomycolic acid methyl esters (CMAMES). The profile of the extracted CMAMES is shown in Fig. 3. In the *C. glutamicum*Δ*emb* mutant, cell wall-bound corynomycolic acids were completely absent. The complementation of this strain with Cg-*emb* led to a restoration

of cell wall-bound corynomycolic acids. These results suggest that Cg-*emb* is involved in arabinan biosynthesis of AG whereby deletion removes the sites of mycolylation (8).

Glycosyl Compositional Analysis of Cell Walls from C. glutamicum, C. glutamicum_emb, and Cg-emb-complemented C. glutamicum_emb—GC analysis of alditol acetates prepared from *C. glutamicum* cell walls (Fig. 4) reveals the presence of rhamnose (Rha), arabinose and galactose (Gal), respectively. Analysis of *M. tuberculosis* AG sugar composition shows that there are subtle differences when compared with *C. glutamicum*, with relatively reduced amounts of Rha (data not shown) (6, 7). Analysis of alditol acetates prepared from *C. glutamicum_emb* depicts a situation with a dramatically reduced (~90%), but not complete absence of arabinose content in the cell wall. It is also interesting to note that the relative amount of Rha is also reduced in this mutant. These results suggest that the presence of a high proportion of Rha in the cell walls of *C. glutamicum* is located or associated to the arabinan domains of the cell wall AG. Overall, these phenotypes are also observed upon treatment of *C. glutamicum* with 100 μg/ml of the anti-mycobacterial drug EMB (data not shown). Complementation of the embmutant with plasmid-encoded Cg-*emb* restored the glycosyl composition to that of *C. glutamicum* (Fig. 4).

Glycosyl Linkage Analysis of Cell Walls from C. glutamicum, C. glutamicumΔemb, and Cg-emb-complemented C. glutamicumΔemb— Per-*O*-methylated alditol acetate derivatives of *C. glutamicum*, *C. glutamicumΔemb*, and *C. glutamicumΔemb* complemented with plasmid-encoded *emb* are shown in Fig. 5. Glycosyl linkages present in *M. tuberculosis* (data not shown) and *C. glutamicum* include t-Ara*f*, 2-Ara*f*, 5-Ara*f*, 4-Rha*p*, t-Gal*f*, 3,5-Ara*f*, 5-Gal*f*, 6-Gal*f*, and 5,6-Gal*f*.

The major difference between *C. glutamicum* and *M. tuberculosis* AG includes the presence of 2,5-Ara*f* and t-Rha*p* residues in *C. glutamicum*. In *C. glutamicumΔemb* a loss of 5-Ara*f*, 3,5-Ara*f*, 2,5-Ara*f*, and t-Rha*p* is observed with only t-Ara*f* residues appearing alongside 5-Gal*f*, 6-Gal*f*, and 5,6-Gal*f* residues. These results suggest that Cg-Emb actually plays a much larger role in the arabinosylation of AG in comparison to the results previously obtained with *M. smegmatis* EmbA and EmbB mutants (25), possibly suggesting some partial complementation of EmbA and EmbB in the singular *M. smegmatis emb* disruption mutants (25). In addition, the AG of *C. glutamicum* is unusual in that it would appear that the arabinan domains are also capped by t-Rha*p* residues, because these are absent in the *C. glutamicumΔemb* mutant. Complementation of the *emb* mutant with plasmid-encoded Cg-*emb* restored the glycosyl linkage profile to that of *C. glutamicum.* Glycosyl linkage

analysis of *C. glutamicum* treated with 100 µg/ml of EMB yielded a CG/MS trace comparable to that of C. *glutamicumΔemb* (data not shown).

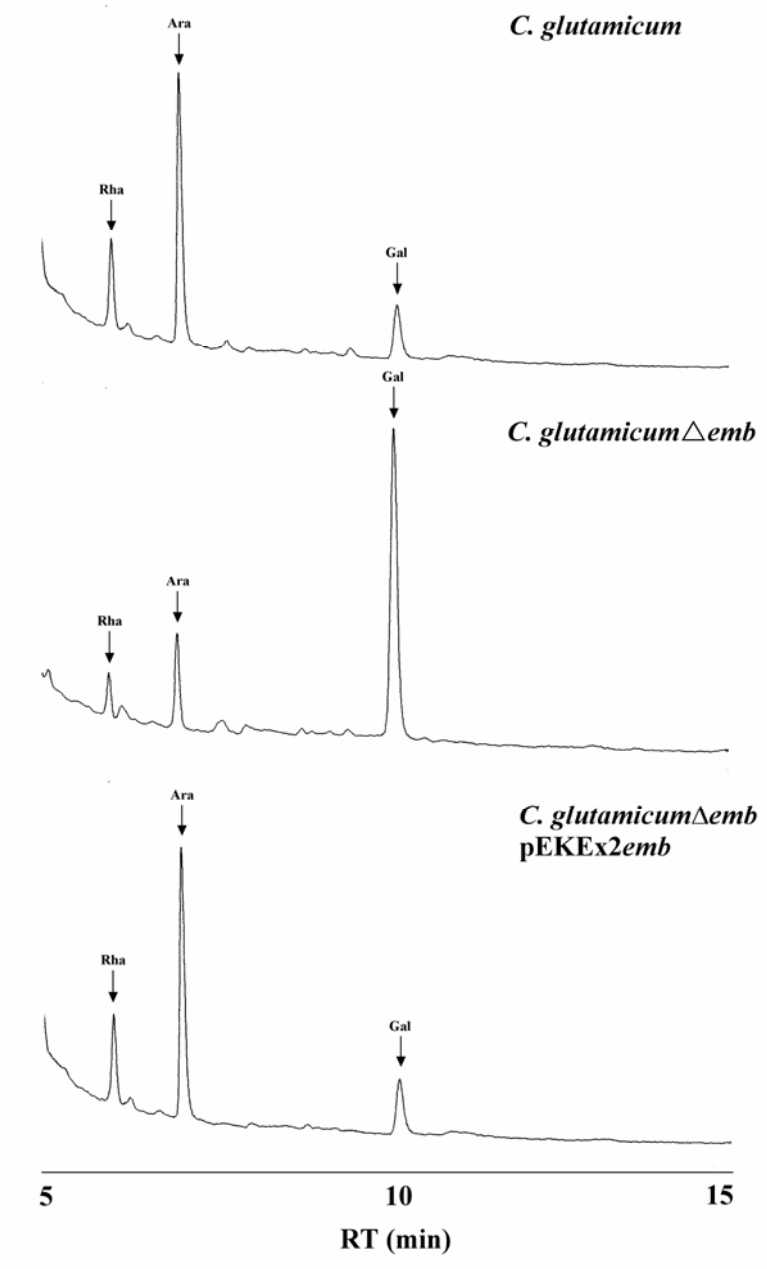

FIG. 4. Glycosyl compositional analysis of cell walls of *C. glutamicum*, *C. glutamicum_emb*, and *C. glutamicum_emb* pEKEx2*emb*. Samples of purified cell walls were hydrolyzed with 2 M trifluoroacetic acid, reduced, per-*O*-acetylated, and subjected to GC as described under "Materials and Methods." Alditol acetate standards (Supelco) of Rha, Ara, and Gal were analyzed with retention times of 6, 7, and 10.1 min, respectively.

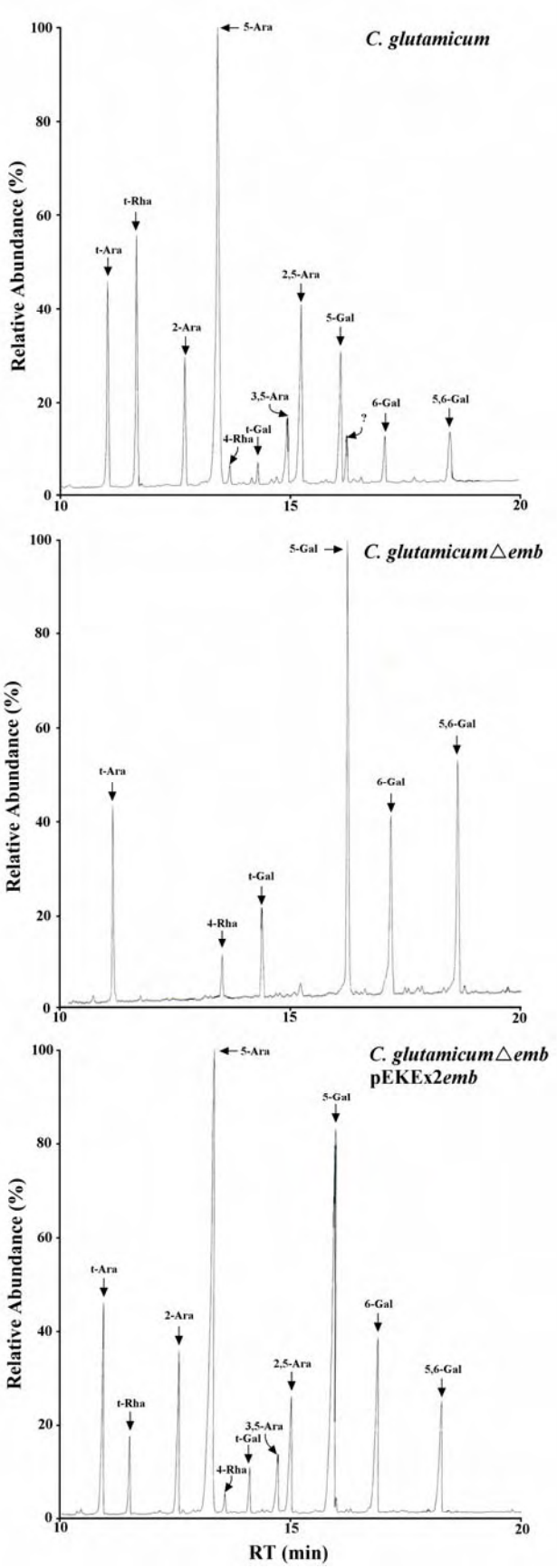

FIGURE 5. Glycosyl linkage analysis of per-*O*-methylated cell walls prepared from *C. glutamicum*, *C. glutamicum_emb*, and *C. glutamicum_emb*pEKEx2*emb*. Cell walls were prepared as described under "Materials and Methods" per-*O*-methylated, hydrolyzed, reduced, and per-*O*-acetylated. The resulting partially per-*O*-methylated, per-*O*acetylated glycosyl derivatives were analyzed by GC/MS as described (6, 7).

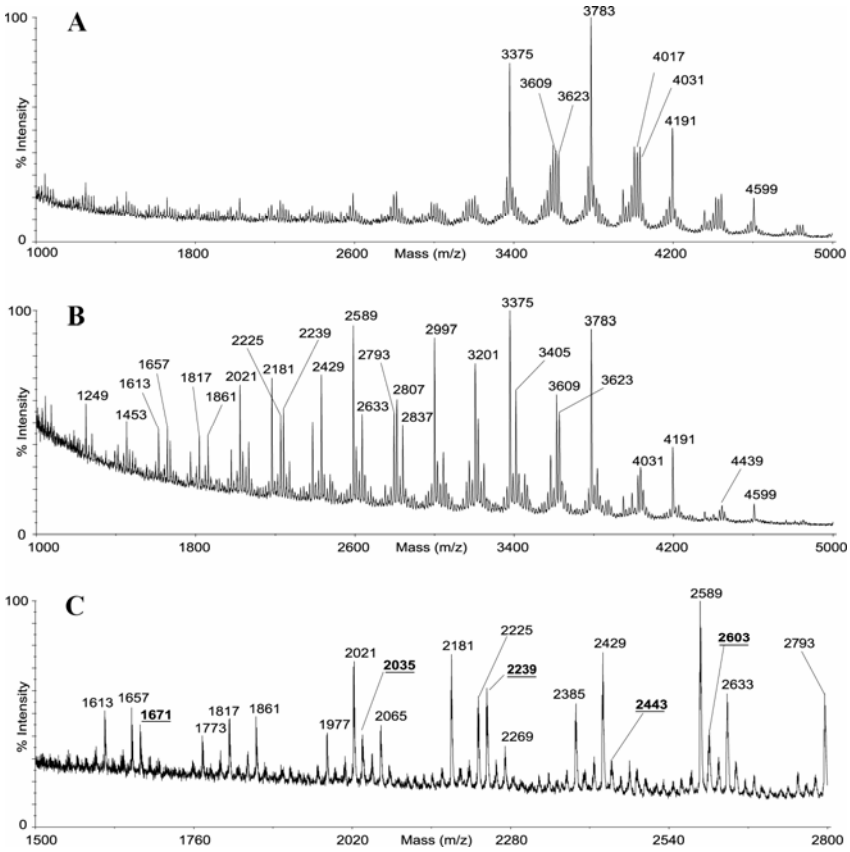

FIG. 6. MALDI-TOF MS of per-*O*-methylated cell walls derived from *C. glutamicum*Δ*emb*. *A*, intact per-*O*-methylated cell walls. *B*, Per-*O*-methylated cell walls after partial hydrolysis with methanolic HCl followed by re-methylation. *C*, the key region of spectrum B expanded with salient signals *underlined*. Signal compositions are assigned in the text. The 100% Sep-Pak fractions are shown. All labeled signals are $[M+Na]^+$.

MALDI MS Analysis of Per-O-methylated Cell Walls from C. glutamicumΔemb—Cell walls derived from *C. glutamicumΔemb* were per-*O*-methylated and analyzed by MALDI-TOF MS, and the data are shown in Fig. 6*A*. The cluster of signals around *m/z* 4000 can be attributed to an AG polymer with truncated arabinan branching. The signals at *m/z* 3375, 3783, 4191, and 4599 are consistent with an AG glycan containing increasing numbers of Gal residues, $Ara_3Gal_{13}Rha$, $Ara_3Gal_{15}Rha$, $Ara_3Gal_{17}Rha$, and $Ara_3Gal_{19}Rha$, respectively.

Tab. 1. Assignment of the partial hydrolytic products detected by MALDI-TOF MS resulting from per-*O*-methylated AG derived from *C. glutamicum*Δ*emb*.

m/z	Assignment*	m/z	Assignment*	m/z	Assignment*
1059	Gal_4Rha	2647	$AraGal_{11}Rha$	3375	$Ara_3Gal_{13}Rha$
1263	Gal_5Rha	2807	$Ara_2Gal_{11}Rha$	3419	$Ara_2Gal_{14}Rha$
1467	Gal_6Rha	2851	$AraGal_{12}Rha$	3463	$AraGal_{15}Rha$
1671	Gal_7Rha	3011	$Ara_2Gal_{12}Rha$	3579	$Ara_3Gal_{14}Rha$
2035	$AraGal_8Rha$	3055	$AraGal_{13}Rha$	3623	$Ara_2Gal_{15}Rha$
2239	$AraGal_9Rha$	3171	$Ara_3Gal_{12}Rha$	3783	$Ara_3Gal_{15}Rha$
2443	$AraGal_{10}Rha$	3215	$Ara_2Gal_{13}Rha$		
2603	$Ara_2Gal_{10}Rha$	3259	$AraGal_{14}Rha$		

The additional signals observed can be assigned to AG glycans lacking an Ara or Rha residue, possibly resulting from the derivatization process. To define the Ara branching pattern on the galactan polymer, the per-*O*-methylated sample was subjected to time course methanolysis followed by re-methylation. The data generated (Fig. 6*B*) show numerous partial hydrolytic products affording informative ion series. A key region of the spectrum is shown expanded in Fig. 6*C*, and the assignment of significant products containing Rha are presented in Table 1. Collectively, the data indicate that a linear galactan polymer extends from the reducing Rha and that the first Ara branch appears on the eighth Gal residue with further Ara branches appearing on the tenth and twelfth Gal residues. These results are supported by data generated from partial hydrolysis followed by per-*O*-deuteromethylation of the resulting hydrolytic products. The mass shifts observed resulting from per-*O*-deuteromethylation (data not shown) support the proposed Ara branching pattern. MALDI MS analysis of per-*O*-methylated cell walls derived from *C. glutamicum* treated with 100 μg/ml EMB revealed a similar profile to that observed for cell walls derived from *C. glutamicum*Δ*emb*. In addition, partial hydrolysis confirmed that *C. glutamicum* treated with EMB produced an AG, which had the same Ara branching pattern as described above in *C. glutamicum*Δ*emb* (data not shown) illustrating the effects of EMB and *emb* deletion are super imposable.

Disruption of Cg-ubiA—Wewere intrigued by UbiA, a putative 4-hydroxybenzoate polyprenyltransferase and the possibility that UbiA was perhaps involved in DPA formation from 5-phosphoribofuranose pyrophosphate and decaprenol phosphate. The *ubiA* gene is

present in Corynebacterianeae in synteny within the locus of other cell wall-related genes (Fig. 1*B*). The orthologue of *M. tuberculosis* Rv3806c in *C. glutamicum* is NCgl2781, and during compilation of this report was shown biochemically to perform the first step of DPA biosynthesis producing decaprenylphosphoryl-5-phosphoribose from 5-phosphoribofuranose pyrophosphate and decaprenol phosphate (39). To inactivate *ubiA* of *C. glutamicum*, plasmid pCg::*ubiA* was constructed and *C. glutamicum* transformed to kanamycin resistance. The resulting strain was confirmed by PCR analysis to have *ubiA* disrupted. This strain, *C. glutamicum*::*ubiA* was similar to *C. glutamicum_emb*, exhibited poor growth, and was devoid of bound cell wall corynomycolic acids (data not shown).

Glycosyl Compositional and MALDI MS Analysis of Cell Walls from C. glutamicum::ubiA—Interestingly, glycosyl compositional analysis of the resulting cell wall of *C. glutamicum::ubiA*, in contrast to *C. glutamicum*Δ*emb*, revealed a complete ablation of arabinan (Fig. 7).

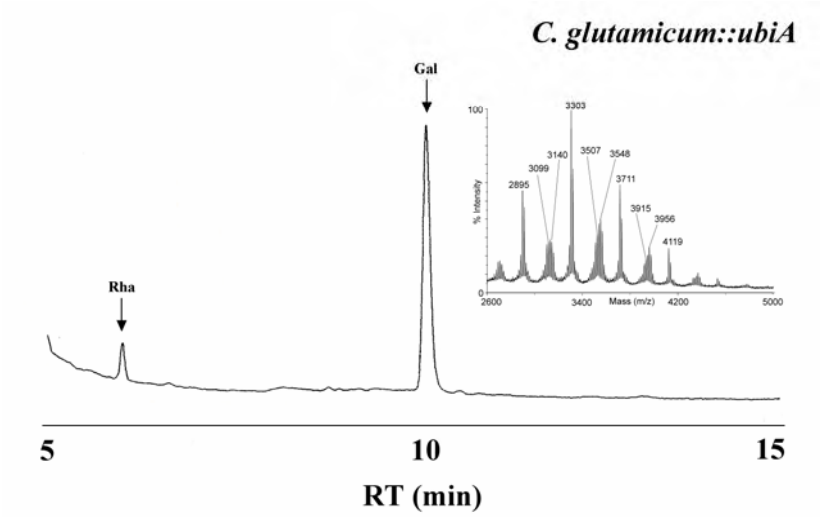

FIG. 7. Analysis of *C. glutamicum*::*ubiA* cell walls. Samples of purified cell walls were hydrolyzed with 2 M trifluoroacetic acid, reduced, per-*O*-acetylated, and subjected to GC as described under "Materials and Methods" to provide glycosyl compositional analysis. The *inset* shows the MALDI-TOF MS of per-*O*-methylated cell walls derived from *C. glutamicum*::*ubiA*.

The results support a functional role of *Cg-ubiA* in cell wall arabinan biosynthesis (39) and demonstrate that DPA is the sole donor of Ara*f* residues in cell wall biosynthesis in Corynebacterianeae. Analysis of the per-*O*-methylated galactan derived form *C. glutamicum*::*ubiA* by MALDI MS revealed a cluster of signals consistent with a galactan backbone lacking any t-Ara residues as observed for the *emb* deletion mutant (see *inset*, Fig. 7). The signals at *m*/*z* 2895, 3303, 3711, and 4199 can be assigned the compositions $Gal_{13}Rha$,

$Gal_{15}Rha$, $Gal_{17}Rha$, and $Gal_{19}Rha$, respectively. The additional signals observed can be assigned to galactan glycans lacking Rha or Gal, or retaining the GlcNAc attached to Rha.

Discussion

The mAGP represents one of the most important cell wall components of members of the Corynebacterianeae, and it is essential for the viability of *M. tuberculosis* (27–29). It acts as a fulcrum between peptidoglycan and the impermeable hydrophobic mycolic acid layer. Furthermore, its biosynthesis is the target of the anti-mycobacterial drug EMB. However, the complete biosynthetic pathway and the cellular machinery involved in AG biosynthesis are still poorly understood (9).

As evident from the genome analyses (Fig. 1*A*) in *Mycobacterium* and *Corynebacterium* species analyzed to date, Cg-*emb* and its upstream region is strictly conserved, indicative of a core function common to all Corynebacterianeae and shown in this study to be involved in the majority of arabinan deposition in AG. Previous attempts to obtain *embA*, *embB*, and *embAB* deletion mutants in *M. tuberculosis* have been unsuccessful2 and probably reflects the importance of AG in the cell wall ultrastructure of Mycobacterial species. However, individual disruptions of *embA* and *embB* in *M. smegmatis* have been obtained resulting in viable cells with observable phenotypic alterations to AG (25). The *embA* and *embB* mutants led to an alteration of the terminal Ara6 motif of AG but still produced a highly arabinosylated AG polymer. The possibility existed that in either the *embA* or *embB* mutant partial complementation could ensue through the presence of either a functional copy of *embA* and *embB*, respectively, as gene duplication and redundancy appear common in *M. tuberculosis* (9, 25, 40). As a consequence the isolation of an arabinan-deficient cell wall mutant in *M. tuberculosis* appears fraught with difficulty.

With this in mind and because *C. glutamicum* possesses only a single *emb* gene, we attempted to construct an *emb* deletion mutant of *C. glutamicum*. The resultant deletion mutant produced a viable yet slow growing phenotype with profound morphological changes. Initial analysis of the corynomycolic acid content of *C. glutamicum*Δ*emb* showed that there was a complete absence of cell wall bound corynomycolates, hinting that there was a loss of corynomycolic acid esterification sites in the mutant, consistent with the loss of the terminal Ara6 motif. Upon glycosyl compositional and linkage analysis, we observed in contrast to *M. smegmatis embA* and *embB* mutants (25) a 90% loss of cell wall arabinan, with all 5-Ara*f*, 3,5-Ara*f*, and 2,5-Ara*f* residues (also the capping t-Rha*p* residues) being absent in the cell wall of the *C. glu-tamicum*Δ*emb*, with the relative amounts of Gal unchanged. The minor

amounts of Ara*f* residues were present as t-Ara*f* units. Furthermore, the AG derived from *C. glutamicum*Δ*emb* when analyzed by MALDI-TOFMS and partial acid hydrolysis indicated for the first time the location of the Ara branches of AG. A linear galactan extends from the reducing Rha and the first Ara branch appears on the eighth Gal residue with further Ara branches appearing on the tenth and twelfth Gal residues (Fig. 8). The observation of t-Ara*f* residues in *C. glutamicum*Δ*emb* was somewhat surprising, because it has long been thought that the gene products of *embA* and *embB* in mycobacterial spp. are solely responsible for arabinan biosynthesis. Interestingly, the occurrence of arabinan deposition on an unaffected galactan backbone suggests that an unidentified arabinofuranosyltransferase might be responsible for the addition of the initial units onto the galactan domain. It is tempting to postulate that this hypothetical "priming enzyme" could fix the initial arabinan units onto the galactan chain for further elaboration by *emb* forming the fully matured AG. Interestingly, treatment of *C. glutamicum* with EMB results in a phenotype that is identical to the *C. glutamicum_emb*, with loss of esterified corynomycolic acids and a dramatically reduced arabinan content in AG. These results show that *emb* is indeed the target for EMB and that the arabinofuranosyltransferase activity of the "priming" enzyme remains unaffected. Given the importance of AG in *M. tuberculosis* viability and pathogenicity, it is tempting to suggest that this "priming" enzyme might be an ideal candidate to exploit as a drug target, because its disruption would result in a completely arabinan-deficient cell wall.

Due to the presence of t-Ara*f* residues in the *emb*-deleted strain of *C. glutamicum*, we endeavored to identify genes responsible for DPA biosynthesis, with the goal of deleting orthologues found in *C. glutamicum* for further phenotypic analysis. This was to rule out the possibility that the priming enzyme, unlike Emb, which utilizes DPA as a sugar donor, may use an alternative nucleotide sugar donor (41, 42).

Although the two gene loci depicted in Fig. 1 (*A* and *B*) are separated in *M. tuberculosis* by only two open reading frames (not shown), this part is not conserved and is at variance in *M. leprae* and other *Mycobacteria*. However, genes of the subsequent region extending from *accD4* to *glfT* are arranged in synteny in all Corynebacterianeae analyzed and are involved in some aspects of cell wall biosynthesis. For instance, *accD4* (*accD3* in *C. glutamicum*), which encodes the β-chain of an acyl carboxylase, which together with a second *accD* orthologue (*accD2* in *C. glutamicum* (31)) and the subsequent *pks13* and *fadD32*, make up the enzyme complex-activating (43) and -condensing (44) fatty acids, and these together form mycolic acids in a Claisen condensation reaction. Further upstream is the mycolyltransferase region (*fbpA* and *fbpC1* of *M. tuberculos*is), which is slightly different in

C. glutamicum with one mycolyltransferase, *cmytB*, possessing a C-terminal extension (45, 46), and a transposase between the mycolyltransferases. *In silico* analysis of the region of genes, which have previously been shown to be involved in cell wall biosynthesis, resulted in the identification of a putative polyprenyltransferase, *ubiA*. The *ubiA* gene was found to reside in the genome of *C. glutamicum* adjacent to *glfT*, the gene responsible for galactan biosynthesis (Fig. 1*B*), and the region centered around *ubiA* is common to all Corynebacterianeae.

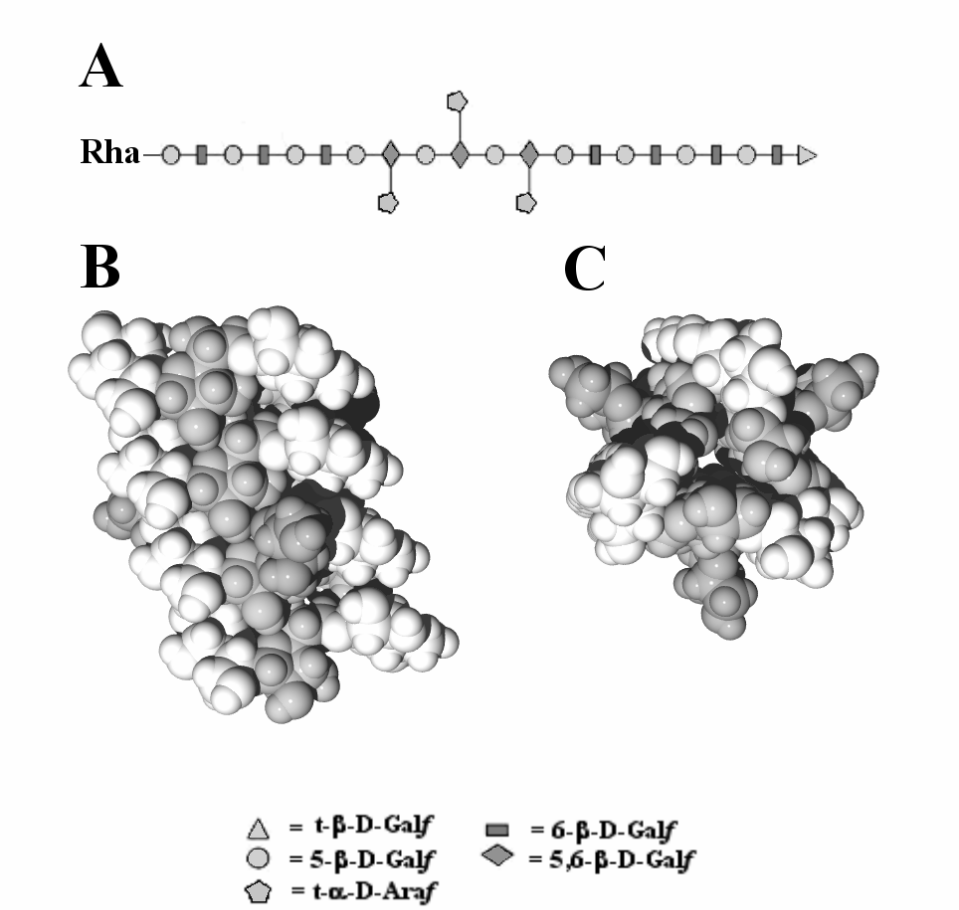

FIG. 8. Model representing truncated AG isolated from *C. glutamicum*Δ*emb*indicating the sites of arabinan attachment to the galactan moiety. *A*, diagram representing the glycosidic linkages found in truncated AG isolated from *C. glutamicum_emb*, briefly, the linkages identified were t-Ara*f*, 5-Gal*f*, 6-Gal*f*, 5,6-Gal*f*, and t-Gal*f*. ***B***, spacefilling representation of *C. glutamicum_emb*AG as viewed from side on (*perpendicular* to the peptidoglycan). ***C***, as viewed from above, with the peptidoglycan being level with the plane of the page. The space-filled model of AG was prepared using SWEET (www.dkfz-heidelberg.de /spec/sweet2/doc/index.php), manipulated with SWISS PBD Viewer, and rendered with PovRay.

UbiA is absent in Gram-negative bacteria and shares high homology with the *M. tuberculosis Rv3806c* of 53% identity, and interestingly, 49% identity with *noeC* of *Azorhizobium caulinodans* (47, 48). Recent studies have shown that UbiA is involved in the

first step of DPA biosynthesis forming decaprenylphosphoryl-5-phosphoribose from 5-phosphoribofuranose pyrophosphate and decaprenol phosphate (39). Directly upstream of *ubiA* is a gene predicted to encode a phosphatase, which presumably dephosphorylates decaprenylphosphoryl-5-phosphoribose and then is converted to DPA via an epimerization process.[2] The generation of a *ubiA* mutant of *C. glutamicum* and chemical analysis of the purified cell wall revealed a complete loss of arabinan deposition and hence, a viable arabinan-deficient strain of *C. glutamicum*. As a result, we have presented unequivocal evidence that DPA is the only arabinan donor for AG biosynthesis ruling out the possibility of some other high energy arabinose nucleotide precursor. These studies also highlight UbiA as a possible drug target due to the lack of any other compensatory mechanisms to produce DPA and arabinan. As a result its disruption would result in a completely arabinandeficient cell wall in Corynebacterianeae, such as *M. tuberculosis*.

In summary, because *C. glutamicum* and *M. tuberculosis* share a common cell wall ultrastructure and biosynthetic machinery, the deletion of *emb* and disruption of *ubiA* in *C. glutamicum*, has allowed us to shed further light on the role of these genes in cell wall AG biosynthesis in Corynebacterianeae such as *Mycobacterium* species.

References

1. Bloom, B. R., and Murray, C. J. (1992) *Science* 257, 1055–1064
2. Coyle, M. B., and Lipsky, B. A. (1990) *Clin. Microbiol. Rev.* 3, 227–246
3. Funke, G., von Graevenitz, A., Clarridge, J. E., 3rd, and Bernard, K. A. (1997) *Clin. Microbiol. Rev.* 10, 125–159
4. Sahm, H., Eggeling, L., and de Graaf, A. A. (2000) *Biol. Chem.* 381, 899–910
5. McNeil, M., Daffe, M., and Brennan, P. J. (1990) *J. Biol. Chem.* 265, 18200–18206
6. Besra, G. S., Khoo, K. H., McNeil, M. R., Dell, A., Morris, H. R., and Brennan, P. J. (1995) *Biochemistry* 34, 4257–4266
7. Daffe, M., Brennan, P. J., and McNeil, M. (1990) *J. Biol. Chem.* 265, 6734–6743
8. McNeil, M., Daffe, M., and Brennan, P. J. (1991) *J. Biol. Chem.* 266, 13217–13223
9. Dover, L. G., Cerdeno-Tarraga, A. M., Pallen, M. J., Parkhill, J., and Besra, G. S. (2004) *FEMS Microbiol. Rev.* 28, 225–250
10. Mikusova, K., Mikus, M., Besra, G. S., Hancock, I., and Brennan, P. J. (1996) *J. Biol.Chem.* 271, 7820–7828
11. Mikusova, K., Yagi, T., Stern, R., McNeil, M. R., Besra, G. S., Crick, D. C., and Brennan, P. J. (2000) *J. Biol. Chem.* 275, 33890–33897
12. Weston, A., Stern, R. J., Lee, R. E., Nassau, P. M., Monsey, D., Martin, S. L., Scherman, M. S., Besra, G. S., Duncan, K., and McNeil, M. R. (1997) *Tuber Lung Dis.* 78, 123–131
13. Sanders, D. A., Staines, A. G., McMahon, S. A., McNeil, M. R., Whitfield, C., and Naismith, J. H. (2001) *Nat. Struct. Biol.* 8, 858–863
14. Kremer, L., Dover, L. G., Morehouse, C., Hitchin, P., Everett, M., Morris, H. R., Dell, A., Brennan, P. J., McNeil, M. R., Flaherty, C., Duncan, K., and Besra, G. S. (2001) *J. Biol. Chem.* 276, 26430–26440
15. Xin, Y., Lee, R. E., Scherman, M. S., Khoo, K. H., Besra, G. S., Brennan, P. J., and McNeil, M. (1997) *Biochim. Biophys. Acta* 1335, 231–234
16. Wolucka, B. A., McNeil, M. R., de Hoffmann, E., Chojnacki, T., and Brennan, P. J. (1994) *J. Biol. Chem.* 269, 23328–23335
17. Lee, R. E., Brennan, P. J., and Besra, G. S. (1997) *Glycobiology* 7, 1121–1128
18. R. E. Lee, K. M., P. J. Brennan, G. S. Besra. (1995) *J. Am. Chem. Soc* 117, 11829–11832

19. Hancock, I. C., Carman, S., Besra, G. S., Brennan, P. J., and Waite, E. (2002) *Microbiology* 148, 3059–3067
20. Yagi, T., Mahapatra, S., Mikusova, K., Crick, D. C., and Brennan, P. J. (2003) *J. Biol.Chem.* 278, 26497–26504
21. Takayama, K., Armstrong, E. L., Kunugi, K. A., and Kilburn, J. O. (1979) *Antimicrob. Agents Chemother.* 16, 240–242
22. Takayama, K., and Kilburn, J. O. (1989) *Antimicrob. Agents Chemother.* 33, 1493–1499
23. Belanger, A. E., Besra, G. S., Ford, M. E., Mikusova, K., Belisle, J. T., Brennan, P. J., and Inamine, J. M. (1996) *Proc. Natl. Acad. Sci. U. S. A.* 93, 11919–11924
24. Telenti, A., Philipp, W. J., Sreevatsan, S., Bernasconi, C., Stockbauer, K. E., Wieles, B., Musser, J. M., and Jacobs, W. R., Jr. (1997) *Nat. Med.* 3, 567–570
25. Escuyer, V. E., Lety, M. A., Torrelles, J. B., Khoo, K. H., Tang, J. B., Rithner, C. D., Frehel, C., McNeil, M. R., Brennan, P. J., and Chatterjee, D. (2001) *J. Biol. Chem.* 276, 48854–48862
26. Zhang, N., Torrelles, J. B., McNeil, M. R., Escuyer, V. E., Khoo, K. H., Brennan, P. J., and Chatterjee, D. (2003) *Mol. Microbiol.* 50, 69–76
27. Pan, F., Jackson, M., Ma, Y., and McNeil, M. (2001) *J. Bacteriol.* 183, 3991–3998
28. Mills, J. A., Motichka, K., Jucker, M., Wu, H. P., Uhlik, B. C., Stern, R. J., Scherman, M. S., Vissa, V. D., Pan, F., Kundu, M., Ma, Y. F., and McNeil, M. (2004) *J. Biol. Chem.*279, 43540–43546
29. Vilcheze, C., Morbidoni, H. R., Weisbrod, T. R., Iwamoto, H., Kuo, M., Sacchettini, J. C., and Jacobs, W. R., Jr. (2000) *J. Bacteriol.* 182, 4059–4067
30. Eggeling, L., and Bott, M. (2005) *Handbook of Corynebacterium glutamicum*, pp. 535–566, Taylor Francis Group, CRC Press, Boca Raton, FL
31. Gande, R., Gibson, K. J., Brown, A. K., Krumbach, K., Dover, L. G., Sahm, H., Shioyama, S., Oikawa, T., Besra, G. S., and Eggeling, L. (2004) *J. Biol. Chem.* 279, 44847–44857
32. Ramaswamy, S. V., Amin, A. G., Goksel, S., Stager, C. E., Dou, S. J., El Sahly, H., Moghazeh, S. L., Kreiswirth, B. N., and Musser, J. M. (2000) *Antimicrob. Agents Chemother.* 44, 326–336
33. Sreevatsan, S., Stockbauer, K. E., Pan, X., Kreiswirth, B. N., Moghazeh, S. L., Jacobs, W. R., Jr., Telenti, A., and Musser, J. M. (1997) *Antimicrob. Agents Chemother.* 41, 1677–1681
34. Ramaswamy, S. V., Dou, S. J., Rendon, A., Yang, Z., Cave, M. D., and Graviss, E. A. (2004) *J. Med. Microbiol.* 53, 107–113
35. Cerdeno-Tarraga, A. M., Efstratiou, A., Dover, L. G., Holden, M. T., Pallen, M., Bentley, S. D., Besra, G. S., Churcher, C., James, K. D., De Zoysa, A., Chillingworth, T., Cronin, A., Dowd, L., Feltwell, T., Hamlin, N., Holroyd, S., Jagels, K., Moule, S., Quail, M. A., Rabbinowitsch, E., Rutherford, K. M., Thomson, N. R., Unwin, L., Whitehead, S., Barrell, B. G., and Parkhill, J. (2003) *Nucleic Acids Res.* 31, 6516–6523
36. Kalinowski, J., Bathe, B., Bartels, D., Bischoff, N., Bott, M., Burkovski, A., Dusch, N., Eggeling, L., Eikmanns, B. J., Gaigalat, L., Goesmann, A., Hartmann, M., Huthmacher, K., Kramer, R., Linke, B., McHardy, A. C., Meyer, F., Mockel, B., Pfefferle, W., Puhler, A., Rey, D. A., Ruckert, C., Rupp, O., Sahm, H., Wendisch, V. F., Wiegrabe, I., and Tauch, A. (2003) *J. Biotechnol.* 104, 5–25
37. Nakamura, Y., Nishio, Y., Ikeo, K., and Gojobori, T. (2003) *Gene* (*Amst.*) 317, 149–155
38. Radmacher, E., Stansen, K. C., Besra, G. S., Alderwick, L. J., Maughan, W. N., Hollweg, G., Sahm, H., Wendisch, V. F., and Eggeling, L. (2005) *Microbiology* 151, 1359–1368
39. Huang, H., Scherman, M. S., D'Haeze, W., Vereecke, D., Holsters, M., Crick, D. C., and McNeil, M. R. (2005) *J. Biol. Chem.* 280, 24539–24543
40. Belisle, J. T., Vissa, V. D., Sievert, T., Takayama, K., Brennan, P. J., and Besra, G. S. (1997) *Science* 276, 1420–1422
41. Singh, S., and Hogan, S. E. (1994) *Microbios* 77, 217–222
42. Klutts, J. S., Hatanaka, K., Pan, Y. T., and Elbein, A. D. (2002) *Arch. Biochem. Biophys.* 398, 229–239
43. Trivedi, O. A., Arora, P., Vats, A., Ansari, M. Z., Tickoo, R., Sridharan, V., Mohanty, D., and Gokhale, R. S. (2005) *Mol. Cell* 17, 631–643
44. Portevin, D., De Sousa-D'Auria, C., Houssin, C., Grimaldi, C., Chami, M., Daffe, M., and Guilhot, C. (2004) *Proc. Natl. Acad. Sci. U. S. A.* 101, 314–319
45. Kacem, R., De Sousa-D'Auria, C., Tropis, M., Chami, M., Gounon, P., Leblon, G., Houssin, C., and Daffe, M. (2004) *Microbiology* 150, 73–84
46. De Sousa-D'Auria, C., Kacem, R., Puech, V., Tropis, M., Leblon, G., Houssin, C., and Daffe, M. (2003) *FEMS Microbiol. Lett.* 224, 35–44
47. Mergaert, P., D'Haeze, W., Fernandez-Lopez, M., Geelen, D., Goethals, K., Prome, J. C., Van Montagu, M., and Holsters, M. (1996) *Mol. Microbiol.* 21, 409–419
48. Mergaert, P., Van Montagu, M., and Holsters, M. (1997) *Mol. Microbiol.* 25, 811–817

Footnotes

LJA is a BBSRC quota student. GSB acknowledges support as a Lister Institute-Jenner Research Fellow and the Medical Research Council (UK). We thank K. Krumbach, Institure of Biotechgnolgy 1 for excellent technical assistance.

[1]The abbreviations used are: AG, arabinogalactan; Ara, arabinose; CMAME, corynomycolic acid methyl ester; DPA, decaprenol phosphoarabinose; DPPR, decaprenylphosphoryl-5-phospho-ribose; EMB, ethambutol; FAB-MS, fast atom bombardment-mass spectrometry; Gal, galactose; GC, gas chromatography; GC/MS, gas chromatography/mass spectrometry; GL-1, glycolipid 1; GL-2, glycolipid 2; GlcNAc, N-acetylgalactosamine; LU, linker unit; mAGP, mycolyl arabinogalactan peptidoglycan; MALDI-TOF, matrix assisted laser desorption/ionisation-time of flight; PBS, phosphate buffered saline; PCR, polymerase chain reaction; pRpp, 5-phospho-ribofuranose-pyrophosphate; Rha, rhamnose; TBAH, tetra-butyl ammonium hydroxide; TDM, trehalose dimycolate; TFA, trifluoroacetic acid; TLC, thin layer chromatography; TMM, trehalose monomycolate.

[2]Luke. J. Alderwick (unpublished results)

2 Identification of a Novel Arabinofuranosyltransferase (AftA) Involved in Cell Wall Arabinan Biosynthesis in *Mycobacterium tuberculosis*

published in *The Journal of Biological Chemistry* 2006; **281:** 15653-15661

by Luke J. Alderwick[1#], **Mathias Seidel**[2#], Hermann Sahm[2], Gurdyal S. Besra[1] and Lothar Eggeling[2]

From the [1]School of Biosciences, University of Birmingham, Edgbaston, Birmingham, B15 2TT, UK, and [2]Institute for Biotechnology 1, Research Centre Juelich, D-52425 Juelich, Germany

Summary

The cell wall mycolyl-arabinogalactan-peptidoglycan complex is essential in mycobacterial species, such as *Mycobacterium tuberculosis* and is the target of several anti-tubercular drugs. For instance, ethambutol targets arabinogalactan biosynthesis through inhibition of the arabinofuranosyl transferases Mt-EmbA and Mt-EmbB. Following a detailed bioinformatics analysis of genes surrounding the conserved *emb* locus we present the identification and characterization of a novel arabinofuranosyl transferase AftA (Rv3792). The enzyme catalyzes the addition of the first key arabinofuranosyl residue from the sugar donor β-D-arabinofuranosyl-1-monophosphoryldecaprenol (DPA) to the galactan domain of the cell wall thus, "priming" the galactan for further elaboration by the arabinofuranosyl transferases. Since *aftA* is an essential gene in *M. tuberculosis*, we deleted its orthologue in *Corynebacterium glutamicum* to produce a slow-growing but viable mutant. Analysis of its cell wall revealed the complete absence of arabinose resulting in a truncated cell wall structure possessing only a galactan core with a concomitant loss of cell wall bound mycolates. Complementation of the mutant was fully restored to the wild type phenotype by Cg-*aftA*. In addition, by developing an *in vitro* assay using recombinant *Escherichia coli* expressing Mt-*aftA* and use of cell wall galactan as an acceptor, we demonstrated the transfer of arabinose from DPA to galactan and unlike the Mt-Emb proteins, Mt-AftA was not inhibited by ethambutol. This newly discovered glycosyltransferase represents an attractive drug target for further exploitation by chemotherapeutic intervention.

Introduction

The *Corynebacterianeae* represent a distinct group within Gram-positive bacteria, with prominent members being the human pathogens *Mycobacterium tuberculosis*, *Mycobacterium leprae*, and *Corynebacterium diphtheriae* (1). In addition, non-pathogenic

bacteria belong to this taxon, such as *Corynebacterium glutamicum* and *Corynebacterium efficiens*, which are used in the industrial production of amino acids (2). A common feature of the *Corynebacterianeae* is that they possess an unusual cell wall architecture (3-5). The cell wall is dominated by an essential heteropolysaccharide, arabinogalactan (AG)[1], linked to both peptidoglycan and mycolic acids, forming the mycolyl-arabinogalactan-peptidoglycan (mAGP) complex (3-6). The biosynthesis of the arabinan domain of AG, which is made up of $\alpha1\rightarrow5$, $\alpha1\rightarrow3$ and $\beta1\rightarrow2$ glycosyl linkages, results from the sequential addition of arabinofuranose (Ara*f*) residues from the sugar donor β-D-arabinofuranosyl-1-monophosphoryldecaprenol (DPA) (7-9), by a set of unique arabinofuranosyl transferases termed the Emb proteins, of which 3 paralogues exist in *Mycobacterium avium* (10) and *M. tuberculosis* (11).

The anti-tuberculosis drug ethambutol (EMB) specifically inhibits AG biosynthesis (12), and the molecular target of EMB occupies the *embCAB* locus in *M. tuberculosis* (11). Upon individual disruption of *embC*, *embA* and *embB* in *Mycobacterium smegmatis* the resultant mutants were viable (13,14). However, with the crucial terminal Ara_6 motif, which is the template for mycolylation in AG (5), is altered in both the Ms-*embA* and Ms-*embB* mutants (13). These results suggest that EmbA and EmbB are involved in the formation of the terminal Ara_6 motif in AG and also presumably compensated for each other in the respective Ms-*embA* and Ms-*embB* mutants, whilst Ms-*embC* is probably involved in the formation of the arabinan domains of lipoarabinomannan (LAM) (14). This is in agreement with the initial studies of the Ms-*embC* mutant (14) and recent findings that when point mutations were re-introduced into the Ms-*embC* mutant on a multi-copy plasmid expressing EmbC, a truncated LAM was synthesized which retained the basic glycosyl linkage profile of LAM (15). However, attempts to obtain deletion mutants of *embA* and *embB* in *M. tuberculosis* or *embAB* in *M. smegmatis* have proved unsuccessful[2], presumably due to the essentiality of the cell wall mAGP in these bacteria (16-19). In contrast, *C. glutamicum* has proven useful in the study of orthologous *M. tuberculosis* genes essential for cell viability. For instance, Cg-*pks* has been shown to be the key Claisen condensation enzyme involved in mycolic acid biosynthesis through the construction of a deletion mutant of *C. glutamicum* and its complementation with the Mt-*pks13* orthologue (19,20).

In a recent study (6), deletion of the single Cg-*emb* orthologue in *C. glutamicum* resulted in a slow growing yet viable mutant which synthesized a novel truncated AG structure possessing a galactan core and only t-Ara*f* residues. Moreover, partial acid hydrolysis and MALDI-TOF analysis, identified the precise location of the 3 singular *t*-Ara*f*

residues attached to the galactan core on the 8th, 10th and 12th galactofuranose (Gal*f*) residues, thus representing the anchor points of the intact arabinan domains of AG (6). Treatment of *C. glutamicum* with EMB resulted in an identical phenotype comparable to the *C. glutamicum*Δ*emb* mutant (6). Thus, in contrast to the disruption of Ms-*embA* and Ms-*embB*, deletion of Cg-*emb* leads to an almost entire absence of arabinose in the cell wall, apart from specific *t*-Ara*f* residues that are directly linked to the galactose backbone. This suggested the presence of a novel enzyme responsible for "priming" the galactan domain for further elaboration by the Emb proteins, resulting in the final maturation of the native AG polysaccharide. It is the aim of the present study to identify this novel arabinofuranosyl transferase, which catalyzes the addition of the first key Ara*f* residues to the galactan domain of AG.

Experimental Procedures

Strains and culture conditions - *C. glutamicum* ATCC 13032 (the wild type strain, and referred for the remainder of the text as *C. glutamicum*) and *Escherichia coli* DH5αMCR were grown in Luria-Bertani broth (LB, Difco) at 30°C and 37°C, respectively. The mutants generated in this study were grown on complex medium BHIS (21). Kanamycin and ampicillin were used at a concentration of 50 µg/ml. The minimal medium CGXII was used for *C. glutamicum* (21). Samples for lipid analyses were prepared by harvesting cells at an OD of 10-15, followed by a saline wash and freeze drying. Cultivation of *C. glutamicum*Δ*aftA* for lipid and cell wall analysis required 2 pre-cultures: Firstly, a 5 ml BHIS culture was grown for 8 hr which was then used to inoculate a 50 ml BHIS culture for 15 hr. This was then used to inoculate a 100 ml BHIS culture to OD 1, which was harvested after reaching OD 3.

Construction of plasmids and strains - The vectors made were pET23b-Mt-*aftA* (Rv3792), pEKEx2Cg-*aftA* (NCgl0185), pEKEx2Mt-*aftA* and pk19mobsacBΔ*aftA*, with the gene number of the *M. tuberculosis* and *C. glutamicum aftA* ortholog added in brackets. To construct the *E. coli* expression vector pET23b-Mt-*aftA* the primer pair 5'-GATCGATCCATATGCCGAGCAGACGCAAAAGCCCCCAATTC-3' and 5'-GATCGATCAAGCTTCGCGCTCTCCTGCGGCTTGCGGATGG C-3' was used with the restriction sites NdeI and HindIII underlined, with *M. tuberculosis* H37Rv chromosomal DNA as a template. The purified PCR fragment was ligated with accordingly digested pET23b (Novagen). To overexpress *C. glutamicum aftA*, the primer pair 5´-TCCCCCGGGAAGGAGATATAGATATGATTAACACCTCTGAAGATGAAG -3´ and 5´-TCCCCCGGGTTACTCATTGTGCGTTACCACCAC -3´ was used to amplify *C. glutamicum*

aftA which was ligated with SmaI cleaved pEKEx2 to generate pEKEx2Cg-*aftA*. Similarly primer pairs 5´- CAGGATCCAAGGAGATATAGATATGCCGAGCAGACGCAAAAG -3´ and 5´- CAGGATCCCCATCCGCGCTCTCCTGCGGCTTGC -3´were used to clone *M. tuberculosis aftA* into the BamHI site of pEKEx2. To construct the deletion vector pk19mobsacBΔ*aftA* cross-over PCR was applied with primer pairs AB (A: 5´- CGTGGATCCGGTGCC -3´; B: 5´- CCCATCCACTAAACTTAAACATTCAGAGGTGTTAATCAT -3´) and CD (C: 5´- TGTTTAAGTTTAGTGGATGGGGTGGGACCTTTCGTGGTGGTAACG -3´; D: 5´- GGCGTCCGTACTGTCCAG -3´) and *C. glutamicum* genomic DNA as template. Both amplificates were used in a second PCR with primer pairs AD to generate a fragment consisting of sequences adjacent to Cg-*aftA*, which was blunt end ligated with SmaI cleaved pK19mobsacB. All plasmids were finally confirmed by sequencing. The chromosomal deletion of Cg-*aftA* was performed as described using two rounds of positive selection (22), and its successful deletion verified by use of different primer pairs. Plasmid pET23b-Mt-*aftA* was used to transform chemically competent cells of *E. coli* C43 (DE3) to ampicillin resistance (100 µg/ml) and pEKEx2Cg-*aftA* was introduced into *C. glutamicum*Δ*aftA* by electroporation with selection to kanamycin resistance (25 µg/ml).

Extraction and analysis of cell wall bound mycolic acids - Cells were grown as described above, harvested, washed and freeze-dried. Cells (100 mg) were extracted by two consecutive extractions with 2 ml of $CHCl_3/CH_3OH/H_2O$ (10:10:3, v/v/v) for 3 h at 50°C. The bound lipids from the de-lipidated extracts or purified cell walls (see below) were released by the addition of 5% aqueous solution of tetra-butyl ammonium hydroxide (TBAH), followed by overnight incubation at 100°C, methylated as described previously (6) and analyzed by thin-layer chromatography (TLC) using known standards (6).

Isolation of the mAGP complex - The thawed cells were resuspended in phosphate buffered saline containing 2% Triton X-100 (pH 7.2), disrupted by sonication and centrifuged at 27000 x g (4,6,23). The pelleted material was extracted three times with 2% SDS in phosphate buffered saline at 95°C for 1 hr to remove associated proteins, successively washed with water, 80% (v/v) acetone in water, and acetone, and finally lyophilised to yield a highly purified cell wall preparation (4,6,23).

Glycosyl composition and linkage analysis of cell walls by alditol acetates - Cell wall preparations were hydrolyzed using 2 M trifluoroacetic acid (TFA), reduced with NaB_2H_4 and the resultant alditols per-*O*-acetylated and examined by gas chromatography (GC) as described previously (4,6,23). Cell wall preparations (10 mg) were per-*O*-methylated using dimethyl sulfinyl carbanion as described previously (4,6,23). The per-*O*-methylated cell walls

were hydrolyzed using 2 M TFA at 120°C for 2 hr. The resulting hydrolyzate reduced with NaB_2H_4, per-*O*-acetylated and examined by gas chromatography/mass spectrometry (GC/MS) as described previously (4,6,23). Analysis of alditol acetate sugar derivatives was performed on a CE Instruments ThermoQuest Trace GC 2000. Samples were injected in the splitless mode. The column used was a DB225 (Supelco). The oven was programmed to hold at an isothermal temperature of 275°C for a run time of 15 min (6). GC/MS was carried out on a Finnigan Polaris/GCQ PlusTM. The column used was a BPX5 (Supelco).

*DPA and Cg-Emb biosynthetic activity within membrane preparations of C. glutamicum*Δ*aftA and C. glutamicum* - Membranes from *C. glutamicum* and *C. glutamicum*Δ*aftA* were prepared as described previously to determine DPA biosynthetic activity (24,25). Membrane protein (1 mg) was added to p[^{14}C]Rpp (2×10^6 cpm), 50 µg decaprenol monophosphate, 60 µM ATP, 0.5 mM NADP in 50 mM MOPS (pH 7.9), 5 mM β-mercaptoethanol and 10 mM $MgCl_2$ (buffer A) to a final volume of 160 µl. The reaction mixture was incubated for 1 hr at 37°C and stopped by the addition of 3 ml $CHCl_3/CH_3OH$ (2:1, v/v). Radiolabelled lipid linked sugars were extracted, as described previously, prior to scintillation counting and subjected to TLC using silica gel plates (5735 silica gel $60F_{254}$, Merck) in $CHCl_3/CH_3OH/H_2O/NH_4OH$ (65:25:3.6:0.5, v/v/v/v) with reaction products visualized by autoradiography (24,25). Analysis of Cg-Emb activity was determined by using the synthetic α-D-Ara*f*-(1→5)-α-D-Araf-*O*-$C_{10:1}$ acceptor in a cell-free assay as described previously (8).

Expression and analysis of Mt-aftA gene product - *E. coli* (C43) cells were harvested by centrifugation at 5000 rpm and the resulting pellet resuspended in buffer A. Resuspended cells were sonicated, centrifuged at 23000 x g for 20 mins at 4°C, and the resulting supernatant re-centrifuged at 100000 x g for 90 mins at 4°C to isolate cell membranes which were collected and concentrated to a protein concentration of 15-20 mg/ml.

Decaprenol phospho[^{14}C]Arabinose (100.000 cpm [45 µM] prepared as described previously (9,26) and stored in $CHCl_3/CH_3OH$, 2:1 (v/v)) was dried under a stream of argon in a microcentrifuge tube (1.5 ml) and placed in a vacuum desiccator for 15 min to remove any residual solvent. The dried DP[^{14}C]A was then resuspended in 30 µl of buffer A supplemented with 10 % IgePal CA-630. An aliquot of this DP[^{14}C]A solution (10000 cpm, 4.5 µM, 3 µl) was added to the remaining constituents of the assay which included 1 mg of membranes containing Mt-AftA and increasing amounts of purified cell wall galactan polymer (0.1–1.0 mg, which represents approximately 0.015-0.15 mM galactan acceptor (6,27,28)]) from *C. glutamicum*Δ*aftA* in buffer A to a final volume of 300 µl. The reaction

mixture was incubated for 1 hr at 37°C and stopped by the addition of 1 ml $CHCl_3/CH_3OH$ (2:1, v/v) followed by centrifugation at 3000 x g. The supernatant was removed and analysed for radioactivity. The pellet was washed several times (5 in total) with $CHCl_3/CH_3OH$ (2:1, v/v) until the radioactivity was recorded as background in the organic supernatant phase (less than 30 cpm). The pellet was finally resuspended in buffer A and transferred to a scintillation vial and 10 ml of EcoScint added and the amount of [^{14}C]arabinose incorporation into cell wall galactan measured by scintillation counting.

Analysis of Mt-AftA assay product – The basic assay was repeated several times (5 assays in total) using non-radiolabelled DPA (200 µg, 0.75 mM), 1 mg of membranes containing Mt-AftA and 1 mg of cell wall galactan polymer (approximately 0.15 mM) prepared from *C. glutamicum*Δ*aftA* as described above. Following an initial incubation at 37 °C for 1 hr the assay was replenished with fresh membranes containing Mt-AftA (1 mg) and re-incubated for 1 hr at 37 °C with the entire process repeated thrice with the addition of fresh membranes. The reaction mixture was then stopped by the addition of 1 ml $CHCl_3/CH_3OH$ (2:1, v/v) followed by centrifugation at 3000 x g. The recovered pellets were then extracted several times (5 in total) using $CHCl_3/CH_3OH$ (2:1, v/v), pooled, per-*O*-methylated, hydrolyzed, reduced with NaB^2H_4, per-*O*-acetylated and analysed for by GC/MS as described earlier.

Results

Genome comparison of the emb *locus* - Based on our previous observation that *C. glutamicum*Δ*emb* possessed no known arabinofuranosyl transferase activity yet contained single *t*-Ara*f* units attached to the galactan core (6) we analyzed a 14 kb chromosomal region of *M. tuberculosis* encompassing *embC, embA* and *embB* in detail and compared it with that of other *Corynebacterianeae* (Fig. 1*A*). This region includes the recently discovered decaprenylphosphoryl-5-phosphoribose (DPPR) epimerizing enzymes encoded by Rv3790 and Rv3791, which eventually provide Ara*f* units from the sugar donor β-D-arabinofuranosyl-1-monophosphoryldecaprenol (DPA) (8,24,25,29). These genes are followed by Rv3792 which is adjacent to *embC*. This particular region consisting of four genes is syntenic with regions in *M. bovis, M. avium subsp. paratuberculosis,* and *M. leprae* as well as with those of *Corynebacterium efficiens, C. diphtheriae,* and *C. glutamicum*. In addition, *Nocardia farcinica*, also shows ample synteny to the *M. tuberculosis* gene locus, as well as *C. jeikeium,* indicating a fundamental function of Rv3792. Based on the results described below, the

Rv3792 gene and its orthologues was designated *aftA* (acronym for arabinofuranosyl transferase A).

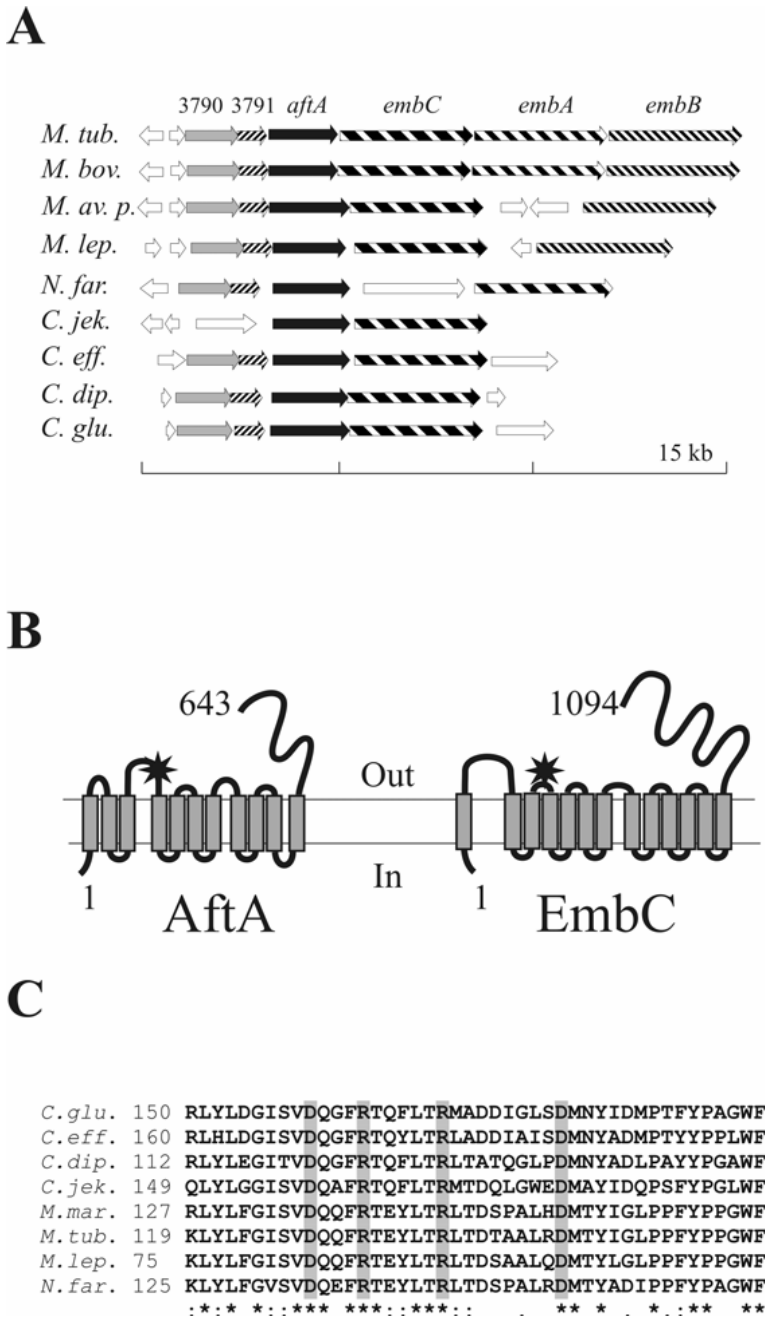

Fig. 1. Comparison of the *aftA* locus within the *Corynebacterianeae*. *A*, The locus consists in *M. tuberculosis* (*M. tub.*) of *aftA* with its 2 upstream genes Rv3790 and Rv3791 leading to the formation of DPA(24,25). Downstream of *aftA* the genes *embC*, *embA*, and *embB* are located encoding known arabinofuranosyl transferases (10,11). The organisation of *Rv3790, Rv3791, aftA* and *embC* is retained in a number of *Corynebacterianeae* indicative for a basic functional unit. In *N. farcinica* (*N. far.*), a glycosyltransferase of unknown function is located between *aftA* and *embC*. In *C. jeikeium* (*C.jek.*), *Rv3790* and *Rv3791* are clustered, but located at another locus. Abbreviations: *M. bovis* (*M. bov.*), *M. avium paratuberculosis* (*M. av. p.*), *M. leprae* (*M. lep.*), *C. efficiens* (*C. eff.*), *C. diphtheriae* (*C. dip.*) and *C. glutamicum* (*C. glu.*). *B*, Topology of AftA and EmbC of *M. tuberculosis*. The topology is predicted using DAS (39). AftA spans the membrane 11 times, EmbC 13 times, and both have a carboxy-terminal extension located in the periplasm covering about one-third of the protein. The star indicates a highly conserved region which resides in the periplasmatic loop and is probably

concerned with glycosyl transfer activity. *C*, Partial sequence comparison of region I of AftA proteins (star in Fig. 1*B*), indicating their high degree of identity. The conserved negative residues possibly involved in glycosyl transferse activity are shaded in grey. The abbreviations are as above including *Mycobacterium marinum* (*M. mar*).

In *M. tuberculosis aftA* is predicted to encode a membrane protein of 643 amino acid residues. The N-terminal region (residues 1-459) encompasses the hydrophobic segment which is predicted to form eleven transmembrane spanning helixes, whereas the C-terminal region (residues 460-643) is predicted to be directed towards the periplasm.

This domain organization and domain localization somewhat resembles that of EmbC (Fig. 1*B*). Nevertheless, the AftA proteins show no significant sequence similarity to the Emb proteins and unlike the Emb proteins, they are not included in the CAZy database of glycosyltransferases (30). However, the similarity of the AftA proteins amongst each other is very high over their entire sequence. Even for the most distant pairs, *M. tuberculosis* and *C. diphtheriae*, there is still 35.1% identity spanning 555 amino acid residues. The three regions of maximal similarity extend from 111-191 (I), 474-498 (II) and 516-551 (III) [amino acid residues of *M. tuberculosis* AftA]. These regions contain several strictly conserved acidic and polar side chains as exemplified for part of region I of AftA (Fig. 1*C*), which are also known to play roles of general base and nucleophilic residues in glycosyl hydrolysis (30). Interestingly, the region I (marked by a star in Fig. 1*B*) is within a periplasmic loop and moreover, just upstream of a transmembrane helix, which resembles the GT-C motif of EmbC (15). Taken together, the structural features of AftA as well as the localization of *aftA* within the gene cluster involved in arabinan biosynthesis indicates that AftA represents a novel glycosyltransferase involved in arabinan polymerization.

*Construction and growth of C. glutamicum*Δ*aftA* - In spite of the fact that Rv3792 is essential for *M. tuberculosis* (31), we attempted to delete its orthologue in *C. glutamicum*. The non-replicative plasmid pk19mobsacBΔ*aftA* was constructed carrying sequences adjacent to Cg-*aftA*. The vector was introduced into *C. glutamicum* and in several electroporation assays kanamycin resistant clones were obtained, indicating integration of pk19mobsacBΔ*aftA* into the genome by homologous recombination (Fig. 2*A*). The *sacB* gene enables for positive selection of a second homologous recombination event which can result either in the original wild-type genomic organization or in clones deleted of *aftA* (20). More than 200 clones were obtained after 2-4 days and analyzed by PCR, but in all of them the wild-type situation was restored, illustrating a strong disadvantage of *aftA* deletion. We continued with this analysis, to eventually obtain in 3 independent approaches 3 rough textured colonies appearing after about 15 days. These were shown by PCR to have *aftA* deleted, whereas controls either with

NCgl0186 (corresponding to Rv3791) or Cg-*emb* resulted in amplificates identical to that of controls derived from the wild type (Fig. 2*A*).

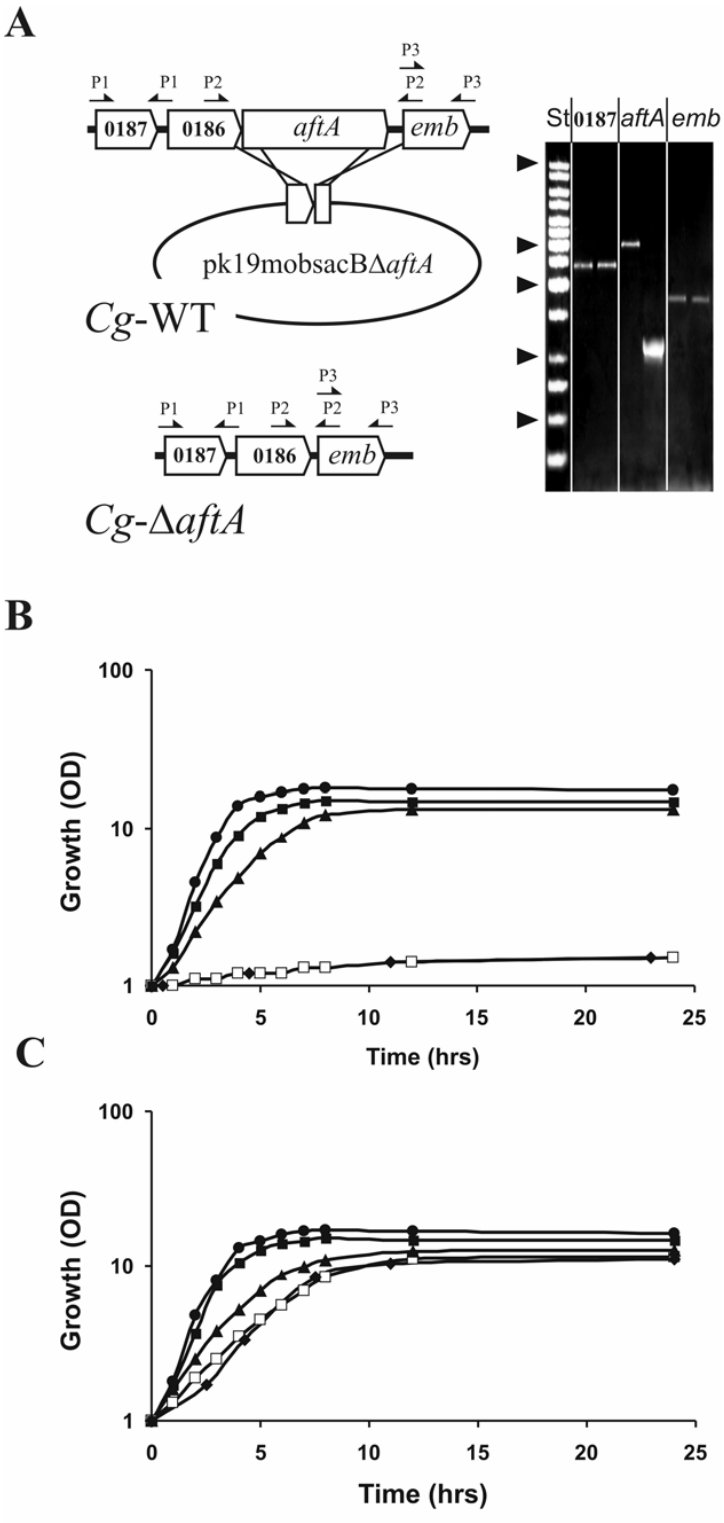

Fig. 2. Construction and characteristics of *C. glutamicum*Δ*aftA*. *A,* Illustrated is Cg-*aftA* with its adjacent genes Rv3791 and *emb* and the strategy to delete *aftA* using the deletion vector pK19mobsacBΔ*aftA*. This vector carries 18 nucleotides of the 5´-end of Cg-*aftA* and 36 nucleotides of its 3´-end thereby enabling the in-frame deletion of almost the entire Cg-*aftA* gene. The arrows marked P2 locate the primers used for the PCR analysis to confirm the absence of *aftA*. Primers P1 were used to detect NCgl0187, the orthologue of Rv3790, and P3 to

detect Cg-*emb*. Distances are not drawn to scale. The results of the PCR analysis are shown on the right, where NCgl0187 marks the result obtained with primers P1, *aftA* with P2, and *emb* with P3. Samples were applied pair wise with the amplificate obtained from the wild type applied in the left lane, and that of the deletion mutant in the right lane. St marks the standard, where the arrowheads are located at 10, 3, 2, 1, and 0.5 kb, respectively. *B,* Consequences of *aftA* deletion on growth in rich medium BHI. Growth of *C. glutamicum* (●), *C. glutamicum*Δ*aftA* (□), as well as the same strain expressing plasmid encoded Cg-*aftA* (■), Mt-*aftA* (▲), and Cg-*emb* (♦). *C,* Consequences of *aftA* deletion on growth in BHI medium as above, but supplemented with 0.5 M sorbitol for osmotic stabilization. Symbols are as above.

Growth of *C. glutamicum*Δ*aftA* in liquid brain-heart-infusion medium is shown in Fig. 2*B*. The mutant was almost unable to grow on this medium, whereas the presence of plasmid encoded Cg-*aftA* (pEKEx2Cg-*aftA*) almost fully restored growth. Also, upon complementation of the mutant with Mtb-*aftA* (pEKEx2Mt-*aftA*) growth restoration was obtained, albeit somewhat reduced, which might be due to the biased codon usage of *M. tuberculosis*.

Transformation of *C. glutamicum*Δ*aftA* with pEKEx2*emb* (6) did not restore the growth defect, showing that overexpression of Cg-*emb* is unable to substitute Cg-*aftA* thus confirming the unique specificity of both AftA and Emb. The identical strains were also grown on the same medium as before (brain-heart-infusion), but osmotically stabilized with 0.5 M sorbitol (Fig. 2*C*). Surprisingly, under these conditions, substantial growth was possible for the *C. glutamicum*Δ*aftA*, which is presumably indicative of sorbitol stabilizing the cell wall mutant. On this medium the growth rate obtained for the wild type was 0.66 h^{-1} with a final OD 17, and that for the deletion mutant 0.31 h^{-1} and a final OD of 15.

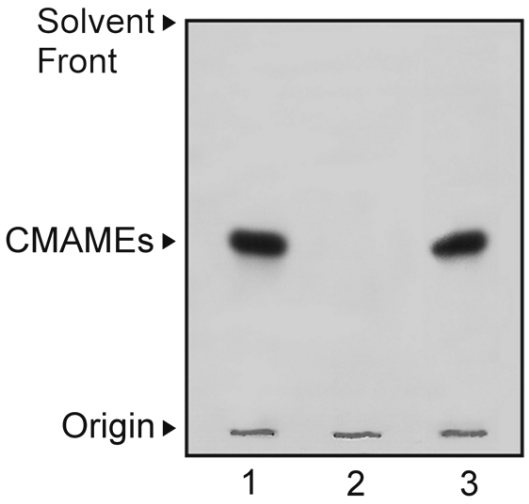

Fig. 3. Analysis of cell wall bound CMAMES from delipidated cells of *C. glutamicum, C. glutamicun*Δ*aftA*** and *C. glutamicum*Δ***aftA* pEKEx2*aftA*.** Lane 1, *C. glutamicum*; Lane 2, *C. glutamicum*Δ*aftA*; Lane 3, *C. glutamicum*Δ*aftA* pEKEx2*aftA*. The bound corynomycolic acids from the delipidated extracts or purified cell walls were released by the addition of TBAH at 100°C overnight and methylated as described in "Materials and

Methods". An aliquot from each strain was subjected to TLC using silica gel plates (5735 silica gel $60F_{254}$, Merck), and developed in petroleum ether/acetone (95:5, v/v) and charred using 5% molybdophosphoric acid in ethanol at 100°C to reveal CMAMEs and compared to known standards (6,19).

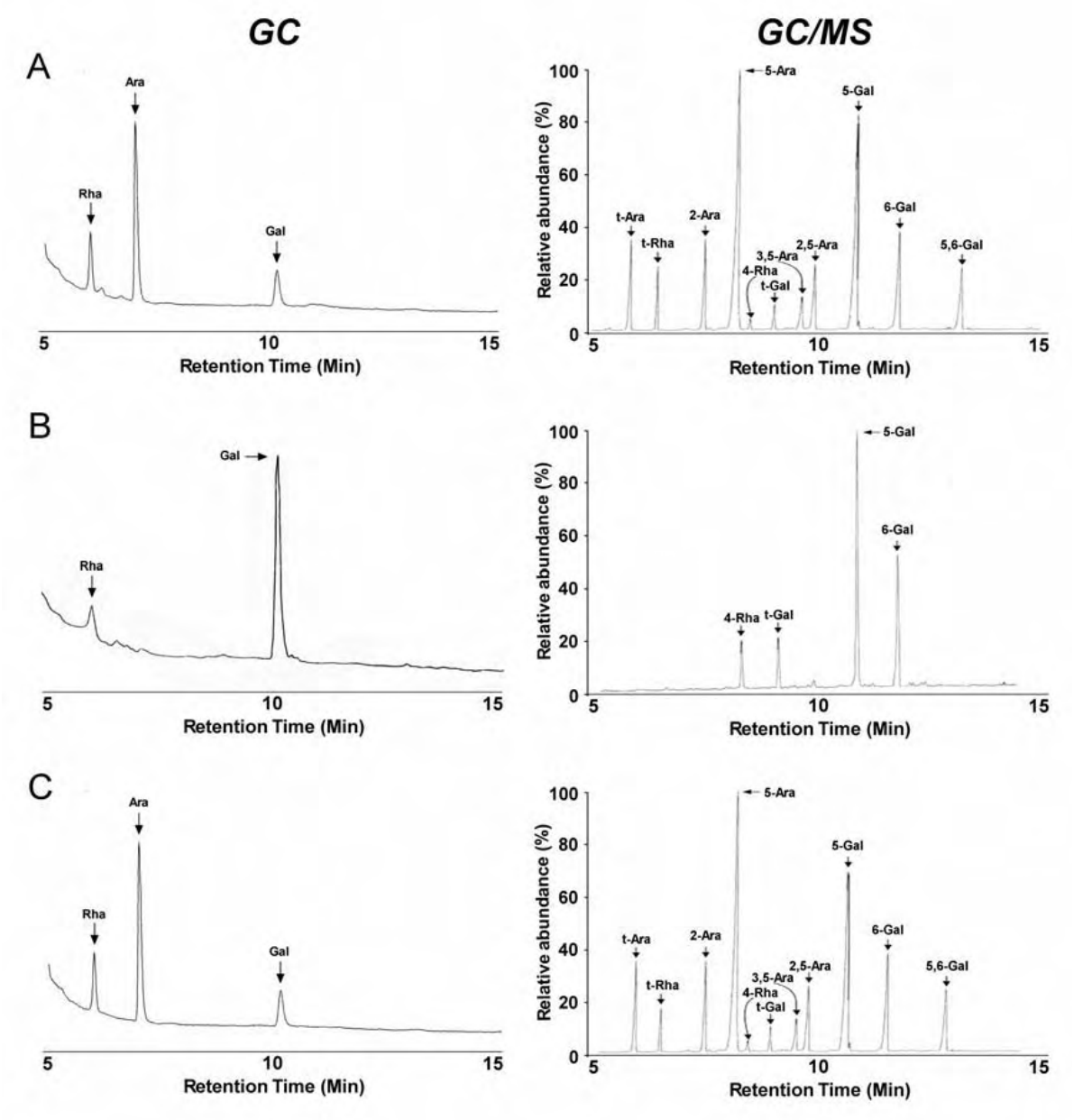

Fig. 4. Glycosyl compositional and glycosyl linkage analysis of cell walls of *C. glutamicum* (A), *C. glutamicun*Δ*aftA* (B) and *C. glutamicum*Δ*aftA* pEKEx2*aftA* (C). Samples of purified cell walls were hydrolyzed with 2M TFA, reduced, per-*O*-acetylated and subjected to GC as described under "Materials and Methods". Alditol acetate standards (Supelco) of Rha, Ara and Gal were analyzed with retention times of 6, 7 and 10.1 min respectively. Cell walls were per-*O*-methylated, hydrolyzed, reduced and per-*O*-acetylated. The resulting partially per-*O*-methylated, per-*O*-acetylated glycosyl derivatives were analyzed by GC/MS as described previously (4,6,23).

Cell wall bound corynomycolic acid, glycosyl compositional and linkage analysis of cell walls - Initially, cells were analyzed for AG esterified corynomycolic acids. *C. glutamicum* exhibited the known profile of corynomycolic acid methyl esters (CMAMEs) (Fig. 3, lane 1), whereas cell wall bound corynomycolic acids were absent in *C. glutamicum*Δ*aftA* (Fig. 3, lane 2). The complementation of *C. glutamicum*Δ*aftA* with Cg-*aftA* (Fig. 3, lane 3) led to the restoration of cell wall bound corynomycolic acids.

These results suggest that Cg-*aftA* was involved in a key aspect of arabinan biosynthesis, whereby deletion perturbs tethering of corynomycolic acids to AG. Analysis of alditol acetate derivatives prepared from purified cell walls of *C. glutamicum* by gas chromatography (GC) revealed the sugar composition, rhamnose (Rha), arabinose (Ara) and galactose (Gal) (Fig. 4*A*) (6).

GC analysis of alditol acetates prepared from *C. glutamicum*Δ*aftA* (Fig. 4*B*) revealed a total loss of cell wall arabinose, which was restored upon complementation with plasmid pEKEx2Cg-*aftA* (Fig. 4*C*). Gas chromatography-mass spectrometry (GC/MS) of per-*O*-methylated alditol acetate derivatives of *C. glutamicum*, *C. glutamicum*Δ*aftA*, and *C. glutamicum*Δ*aftA* pEKEx2Cg-*aftA* is shown in Figure 4, *A*-*C*. Apart from the presence of 2,5-Ara*f* and *t*-Rha*p* associated with the arabinan domain of AG in *C. glutamicum,* other *g*lycosidic linkages are comparable between *M. tuberculosis* (4,32) and *C. glutamicum* (6,27,32), and include t-Ara*f*, 2-Ara*f*, 5-Ara*f*, 3,5-Ara*f*, 4-Rha*p*, *t*-Gal*f*, 5-Gal*f*, 6-Gal*f* and 5,6-Gal*f* (Fig. 4*A*). As expected, *C. glutamicum*Δ*aftA* was devoid of *t*-Ara*f*, *t*-Rha*p*, 2-Ara*f*, 5-Ara*f*, 3,5-Ara*f*, 2,5-Ara*f*, while the galactan domain (apart from the 5,6-Gal*f* branching residues resulting from arabinan side chains) was completely unaffected by the deletion of *Cg-aftA* and contained 4-Rha*p*, *t*-Gal*f*, 5-Gal*f* and 6-Gal*f* (Fig. 4*B*). Complementation of *C. glutamicum*Δ*aftA* with plasmid pEKEx2Cg-*aftA* restored the glycosyl linkage profile to that of *C. glutamicum* (Fig. 4*A* and *C*). The previous deletion of *emb* in *C. glutamicum* and chemical analysis of the cell wall revealed a drastically truncated AG structure possessing only *t*-Ara*f* residues and an unaltered galactan domain (6). Thus, the results endorse that *aftA* represents the novel arabinofuranosyl transferase responsible for “priming” the galactan domain with Ara*f* residues for subsequent elaboration by Emb proteins.

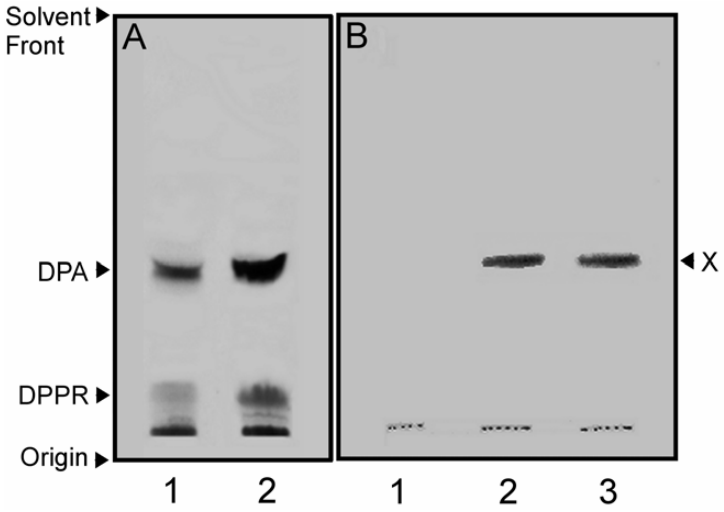

Fig. 5. Production of DPA (A) and Cg-Emb activity (B) within membrane preparations of *C. glutamicum* and *C. glutamicum*Δ*aftA*. Radiolabelled lipid linked sugars (Panel A) were extracted following incubation with membranes and p[^{14}C]Rpp, counted and subjected to TLC using silica gel plates (5735 silica gel 60F_{254}, Merck) in $CHCl_3$/CH_3OH/H_2O/NH_4OH (65:25:3.6:0.5, v/v/v/v) with reaction products [DPA and decaprenylphosphoryl-5-phospho-ribose (DPPR)] visualized by autoradiography. Lane1, *C. glutamicum* and Lane2, *C. glutamicum*Δ*aftA*. Cg-Emb activity (Panel B) was determined using the synthetic α-D-Ara*f*-(1→5)-α-D-Araf-*O*-$C_{10:1}$ acceptor in a cell-free assay as described previously (8). The product X (α-D-[^{14}C]Ara*f*-(1→2/5)-α-D-Ara*f*-(1→5)-α-D-Araf-*O*-$C_{10:1}$) was resuspended prior to scintillation counting and subjected to TLC using silica gel plates (5735 silica gel 60F_{254}, Merck) in $CHCl_3$:CH_3OH:H_2O (65/25/4, v/v/v) with the reaction products visualized by autoradiography. Lane 1, Control, no membranes, Lane 2, *C. glutamicum*, Lane 3, *C. glutamicum*Δ*aftA*.

Analysis of DPA synthesis and Cg-Emb activity - In order to ensure that in *C. glutamicum*Δ*aftA* the biosynthesis of DPA is not reduced thereby disabling Ara*f* delivery to the cell wall, we examined DPA and DPPR biosynthesis. Based on previous studies (24,25) using p[^{14}C]Rpp and decaprenol phosphate to monitor DPA formation, membranes were prepared from *C. glutamicum* and *C. glutamicum*Δ*aftA*. Both preparations afforded DPA synthesis (Fig. 5*A*), demonstrating that there was no reduced ability of *C. glutamicum*Δ*aftA* to synthesize DPA. In fact, an accumulation of DPA and DPPR was evident in *C. glutamicum*Δ*aftA* (approx. 75 and 80 % respectively) as compared to *C. glutamicum*. Using endogenous acceptors and membrane preparations of either *C. glutamicum* or *C. glutamicum*Δ*aftA* we observed no apparent Emb transferase activity with *C. glutamicum*Δ*aftA* compared to a sustained level of activity with *C. glutamicum* (data not shown). However, use of the synthetic acceptor α-D-Ara*f*-(1→5)-α-D-Araf-*O*-$C_{10:1}$ (8,9) resulted in a significant transfer of [^{14}C]arabinose from DP[^{14}C]A (8) affording an organic soluble trisaccharide product with membrane preparations from both strains (Fig. 5*B*). Thus, Emb is fully functional, as also demonstrated above by the earlier genetic experiments (Fig. 2*B*,*C*). Furthermore, these results follow our hypothesis that the galactan domain of AG requires

"priming" by the addition of a single Ara*f* unit to the C-5 OH of a β(1→6) linked Gal*f* sugar for recognition and further extension by the Emb proteins.

Cloning and functional characterization of recombinant E. coli expressed Mt-aftA - Using *M. tuberculosis* H37Rv chromosomal DNA as a template Mt-*aftA* was amplified by PCR and the purified fragment ligated with pET23b enabling expression of His_6-tagged Mt-*aftA*. For expression studies, *E. coli* was transformed with pET23b-Mt-*aftA* and cultured in Terrific Broth at 37°C until an OD of 0.5, followed by the addition of 1 mM IPTG and further incubation for 12 hours at 16°C. Membranes prepared from this culture were analysed by SDS-PAGE and revealed a weakly staining protein band with an apparent molecular weight of 69.5 kDa, which was absent in un-induced cultures, and a size predicted for Mt-His_6AftA (Fig. 6*A*). According to the current data, the reaction catalyzed by Mt-AftA is the transfer of Ara*f* from DPA to galactan. Therefore, an arabinose-free cell wall galactan acceptor was prepared from *C. glutamicum*Δ*aftA* and incubated with the *E. coli* membrane preparation expressing His_6-tagged Mt-*aftA*. Following incubation, the residual DP[^{14}C]A substrate was removed from the cell wall galactan by several repeated extractions using $CHCl_3/CH_3OH$ (2:1, v/v). The remaining insoluble cell wall core was then subjected to scintillation counting revealing an increased amount of [^{14}C]Ara*f* incorporation in the presence of increasing amounts of cell wall galactan acceptor (Fig. 6*B*). Surprisingly, a ten-fold increase in cell wall galactan acceptor resulted in only a three-fold increase in transferase activity. This poor turnover is presumably due to the inefficiency of the assay, which utilizes insoluble cell wall galactan as an acceptor. In addition, the activity of Mt-AftA remained unaffected in the presence of 100 µg/ml EMB (Fig. 6*B*), a known inhibitor of Cg-Emb (6), Mt-EmbA and Mt-EmbB (10-12).

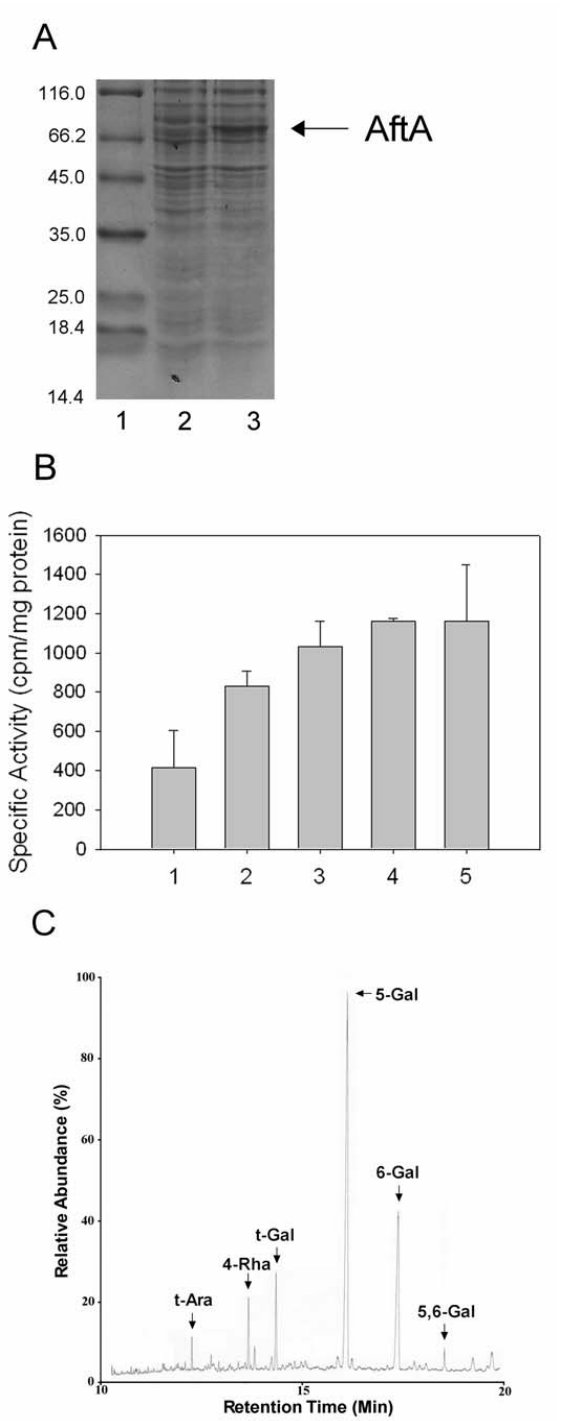

Fig. 6. Expression and functional characterization of recombinant Mt-*aftA*. *A*, Expression of Mt-*aftA* within *E. coli* (C43) membranes was confirmed by SDS-PAGE analysis. Lane 1, molecular weight standards (kDa), Lane 2, *E. coli* (C43) un-induced membranes and Lane 3, *E.coli* (C43) membranes expressing Mt-AftA. *B*, The data illustrates an increase in [^{14}C]arabinose incorporation into cell wall galactan from DP[^{14}C]A (9) with a fixed amount of *E. coli* (C43) membranes containing recombinant Mt-*aftA* (1 mg/ml). Background counts (less than30 cpm) have been subtracted to give a final value for [^{14}C]arabinose incorporation with, 0.1 mg (Lane 1), 0.25 mg (Lane 2), 0.5 mg (Lane 3) and 1.0 mg (Lane 4) of cell wall galactan. Lane 5 represents the same reaction as Lane 4 supplemented with 100 µg/ml ethambutol. In addition, control assays were performed with membranes prepared from uninduced *E. coli* or *E. coli* harbouring empty pET23b also resulted in background counts (less than 30 cpm) for the [^{14}C]Ara*f* incorporation from DP[^{14}C]A in the presence of increasing cell wall galactan acceptor. *C*, The reaction described above was scaled up using non-radiolabelled DPA (9). After incubation the reaction product was extracted, per-*O*-methylated, hydrolysed, reduced with NaB^2H_4, per-*O*-acetylated, and analysed by GC/MS as described in "Experimental Procedures".

The conversion of the galactan acceptor to a sugar polymer containing *t*-Ara*f* units was further confirmed by glycosyl linkage analysis of the enzymatic reaction product (Fig. 6*C*). The newly synthesized product of several scaled-up non-radiolabelled reactions were recovered, per-*O*-methylated and derivatized to alditol acetates, which were analysed by GC/MS. The linkages identified included those associated with the original cell wall galactan acceptor (Fig, 4*B*), plus the appearance of *t*-Ara*f*, and as a result, branched 5,6-Gal*f* residues (Fig. 6*C*).

Thus, our results describe the first report of a novel EMB-resistant arabinofuranosyl transferase, AftA as the key initial glycosyltransferase involved in cell wall arabinan biosynthesis in *Corynebacterianeae* (Fig. 7) like *M. tuberculosis* and *C. glutamicum*.

Discussion

The mAGP represents one of the most important cell wall components of the *Corynebacterianeae* and is essential for the viability of *M. tuberculosis* (16-19). It is therefore not surprising that one of the most effective anti-mycobacterial drugs, EMB, targets its biosynthesis. However, the emergence of multi drug resistant TB (MDR-TB) has accelerated the need to discover new drug targets (33). We previously hypothesized the presence of a new "priming" enzyme which would link the initial Ara*f* unit with the C-5 OH of a β(1→6) linked Gal*f* of a pre-synthesized galactan core (6). This was derived from a thorough analysis of a *C. glutamicum* mutant deleted of its single arabinofuranosyl transferase Emb (6) which still synthesizes a linear galactan extending from the reducing Rha with single *t*-Ara*f* residues attached to the 8^{th}, 10^{th} and 12^{th} Gal*f* residue. Apparently, these specific Ara*f* residues serve for recognition and extension by the known Emb proteins resulting in the formation of the mature arabinan chains (6,10,11).

The *in vivo* analysis of *C. glutamicum*Δ*aftA*, as well as the *in vitro* study with the AftA protein of *M. tuberculosis*, identifies a *bona fide* arabinofuranosyl transferase. In principle, the absence of Ara*f* residues in *C. glutamicum*Δ*aftA* could be due to the unavailability of precursors, as we previously demonstrated with a *C. glutamicum* mutant devoid of the polyprenyl transferase (UbiA) activity involved in the synthesis of β-D-arabinofuranosyl-1-monophosphoryldecaprenol (DPA) (6). However, we established that DPA biosynthesis was maintained in *C. glutamicum*Δ*aftA*, as well as Emb catalyzed arabinan biosynthesis *in vitro*.

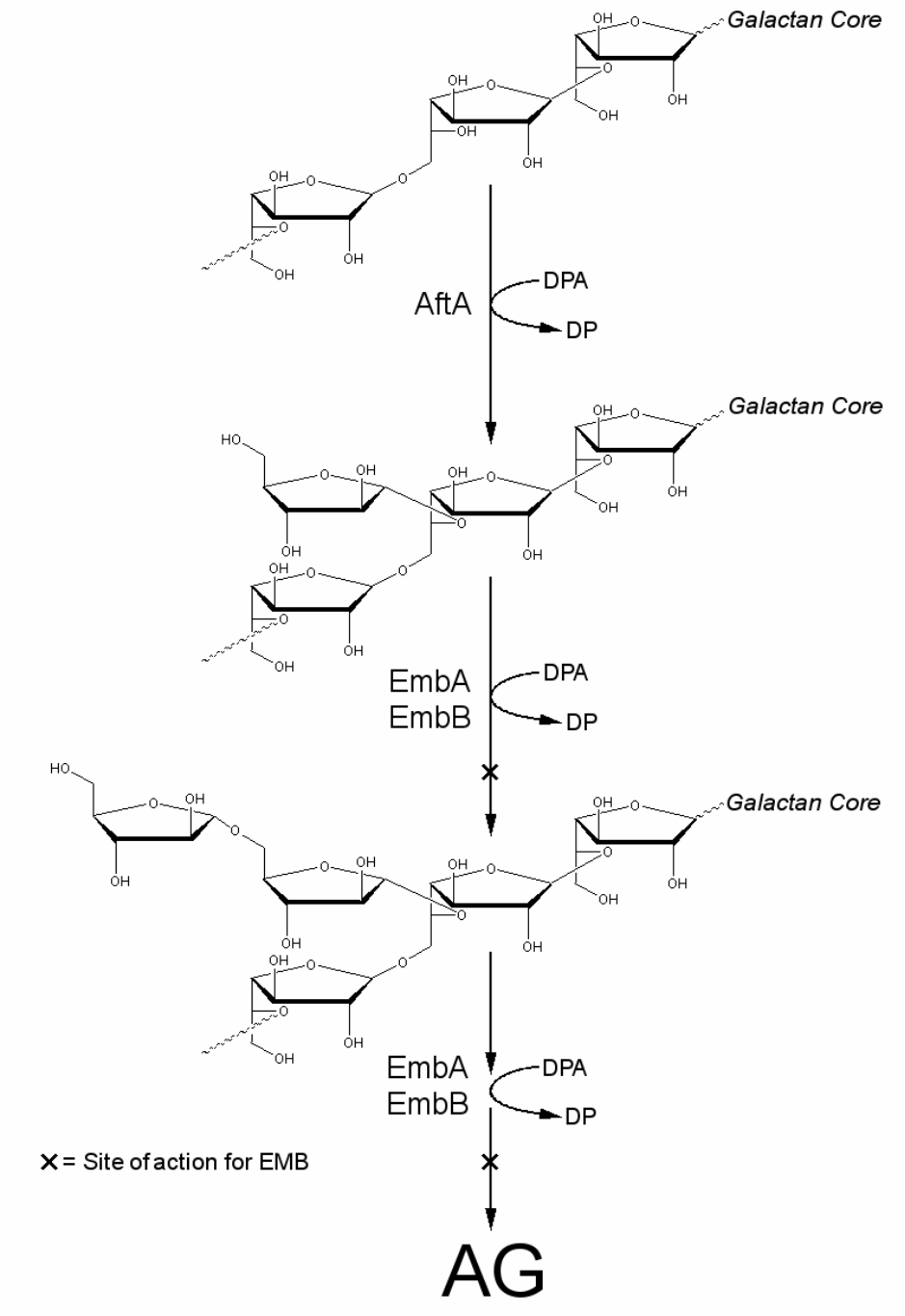

Fig. 7. Proposed biosynthetic pathway leading to arabinan formation in *M. tuberculosis* AG.

This together with our previous study on *C. glutamicum*Δ*emb* shows that AftA functions to link the first Ara*f* residue to the cell wall galactan core. More importantly, the recombinant Mt-AftA transferred Ara*f* units from DPA to a cell wall galactan core acceptor *in vivo*, thus further confirming the unique activity of the enzyme. Although, both Emb and AftA are arabinofuranosyl transferases, the proteins cannot functionally replace each other. Thus, despite some functional relationship, both glycosyltransferases have inherent specific

features as is evident from the insensitivity of Mt-AftA and Cg-AftA towards EMB, whereas the single Cg-Emb (6,34), and Mt-Emb proteins are sensitive towards EMB (10,11).

The discovery of AftA has shed new light on the key arabinofuranosyl transferases that build the arabinan domain, which is typical for *Corynebacterianeae*. An elementary structure of this sugar polymer is apparent in *C. glutamicum*, and this bacterium has proven useful for a number of studies on mAGP biosynthesis (6,19,20). It represents the archetype of the *Corynebacterianeae* andhas a low frequency of structural alterations as manifested, for instance, in a low number of gene duplications (35). *Corynebacterium* species have only one *emb* gene, whereas *Mycobacterium* species have up to three. Nevertheless, the glycosidic linkage analysis of *C. glutamicum* AG shows that 2-Ara*f*, 5-Ara*f*, and 3,5-Ara*f* linkages are present, which are analogous to those found in the AG of *M. tuberculosis* (4). Furthermore, in *C. diphtheriae* and *C. glutamicum* 2,5-Ara*f* linkages are also evident (6,36). This suggests the possibility that one single Emb glycosyltransferase enables the formation of different linkage types, a feature reminiscent of the bi-functional galactofuranosyl transferase (GlfT) of *M. tuberculosis* which produces alternating 5-Gal*f* and 6-Gal*f* linkages within the galactan core of AG (37,38). The high synteny of the *M. tuberculosis* Rv3790, Rv3791, *aftA*, and *embC* to the maps of all other *Mycobacterium* and *Corynebacterium* species is in accord with this view (Fig. 1*A*). Also in *Nocardia farcinica* this general organization is retained with an additional membrane protein-encoding gene. This largely retained organization, as well as the separation of the paralogous *embAB* genes in *M. leprae* and *M. avium subsp. paratuberculosis* is indicative of an ancient core function of Rv3790, Rv3791, *aftA*, and *embC* within the *Corynebacterianeae* involved in the synthesis of Ara*f* donors and their use to assemble a basic periplasmic arabinan domain which serves as a scaffold to tie mycolic acids. The identification of new cell wall biosynthetic drug targets is of great importance, especially with the emergence of multi-drug-resistant tuberculosis (MDR-TB). This newly discovered DPA dependent arabinofuranosyl transferase represents a promising candidate for further exploitation as a potential drug target to disrupt the essential mycolyl-arabinogalactan-peptidoglycan complex in mycobacterial species, such as *Mycobacterium tuberculosis.*

References

1. Bloom, B. R., and Murray, C. J. (1992) Science **257**, 1055-1064
2. Sahm, H., Eggeling, L., and de Graaf, A. A. (2000) Biol Chem **381**, 899-910
3. McNeil, M., Daffe, M., and Brennan, P. J. (1990) J Biol Chem **265**, 18200-18206
4. Besra, G. S., Khoo, K. H., McNeil, M. R., Dell, A., Morris, H. R., and Brennan, P. J. (1995) Biochemistry **34**, 4257-4266
5. McNeil, M., Daffe, M., and Brennan, P. J. (1991) J Biol Chem **266**, 13217-13223
6. Alderwick, L. J., Radmacher, E., Seidel, M., Gande, R., Hitchen, P. G., Morris, H. R., Dell, A., Sahm, H., Eggeling, L., and Besra, G. S. (2005) J Biol Chem **280**, 32362- 32371
7. Wolucka, B. A., McNeil, M. R., de Hoffmann, E., Chojnacki, T., and Brennan, P. J. (1994) J Biol Chem **269**, 23328-23335
8. Lee, R. E., Brennan, P. J., and Besra, G. S. (1997) Glycobiology **7**, 1121-1128
9. R. E. Lee, K. M., P. J. Brennan, G. S. Besra. (1995) J. Am. Chem. Soc **117**, 11829-11832
10. Belanger, A. E., Besra, G. S., Ford, M. E., Mikusova, K., Belisle, J. T., Brennan, P. J., and Inamine, J. M. (1996) Proc Natl Acad Sci U S A **93**, 11919-11924
11. Telenti, A., Philipp, W. J., Sreevatsan, S., Bernasconi, C., Stockbauer, K. E., Wieles, B., Musser, J. M., and Jacobs, W. R., Jr. (1997) Nat Med **3**, 567-570
12. Takayama, K., and Kilburn, J. O. (1989) Antimicrob Agents Chemother **33**, 1493-1499
13. Escuyer, V. E., Lety, M. A., Torrelles, J. B., Khoo, K. H., Tang, J. B., Rithner, C. D., Frehel, C., McNeil, M. R., Brennan, P. J., and Chatterjee, D. (2001) J Biol Chem **276**, 48854-48862
14. Zhang, N., Torrelles, J. B., McNeil, M. R., Escuyer, V. E., Khoo, K. H., Brennan, P. J., and Chatterjee, D. (2003) Mol Microbiol **50**, 69-76
15. Berg, S., Starbuck, J., Torrelles, J. B., Vissa, V. D., Crick, D. C., Chatterjee, D., and Brennan, P. J. (2005) J Biol Chem **280**, 5651-5663
16. Pan, F., Jackson, M., Ma, Y., and McNeil, M. (2001) J Bacteriol **183**, 3991-3998
17. Mills, J. A., Motichka, K., Jucker, M., Wu, H. P., Uhlik, B. C., Stern, R. J., Scherman, M. S., Vissa, V. D., Pan, F., Kundu, M., Ma, Y. F., and McNeil, M. (2004) J Biol Chem **279**, 43540-43546
18. Vilcheze, C., Morbidoni, H. R., Weisbrod, T. R., Iwamoto, H., Kuo, M., Sacchettini, J. C., and Jacobs, W. R., Jr. (2000) J Bacteriol **182**, 4059-4067
19. Gande, R., Gibson, K. J., Brown, A. K., Krumbach, K., Dover, L. G., Sahm, H., Shioyama, S., Oikawa, T., Besra, G. S., and Eggeling, L. (2004) J Biol Chem **279**, 44847-44857
20. Portevin, D., De Sousa-D'Auria, C., Houssin, C., Grimaldi, C., Chami, M., Daffe, M., and Guilhot, C. (2004) Proc Natl Acad Sci U S A **101**, 314-319
21. Eggeling, L., and Bott, M. (2005) Handbook of Corynebacterium glutamicum., CRC Press, Taylor Francis Group
22. Schafer, A., Tauch, A., Jager, W., Kalinowski, J., Thierbach, G., and Puhler, A. (1994) Gene **145**, 69-73
23. Daffe, M., Brennan, P. J., and McNeil, M. (1990) J Biol Chem **265**, 6734-6743
24. Mikusova, K., Huang, H., Yagi, T., Holsters, M., Vereecke, D., D'Haeze, W., Scherman, M. S., Brennan, P. J., McNeil, M. R., and Crick, D. C. (2005) J Bacteriol **187**, 8020-8025
25. Huang, H., Scherman, M. S., D'Haeze, W., Vereecke, D., Holsters, M., Crick, D. C., and McNeil, M. R. (2005) J Biol Chem **280**, 24539-24543
26. Lee, R. E., Brennan, P. J., and Besra, G. S. (1998) Bioorg Med Chem Lett **8**, 951-954
27. Puech, V., Chami, M., Lemassu, A., Laneelle, M. A., Schiffler, B., Gounon, P., Bayan, N., Benz, R., and Daffe, M. (2001) Microbiology **147**, 1365-1382
28. Acharya, P. V., and Goldman, D. S. (1970) J Bacteriol **102**, 733-739
29. Cole, S. T., Brosch, R., Parkhill, J., Garnier, T., Churcher, C., Harris, D., Gordon, S. V., Eiglmeier, K., Gas, S., Barry, C. E., 3rd, Tekaia, F., Badcock, K., Basham, D., Brown, D., Chillingworth, T., Connor, R., Davies, R., Devlin, K., Feltwell, T., Gentles, S., Hamlin, N., Holroyd, S., Hornsby, T., Jagels, K., Barrell, B. G., and et al. (1998) Nature **393**, 537-544
30. Liu, J., and Mushegian, A. (2003) Protein Sci **12**, 1418-1431
31. Sassetti, C. M., Boyd, D. H., and Rubin, E. J. (2003) Mol Microbiol **48**, 77-84
32. Daffe, M., McNeil, M., and Brennan, P. J. (1993) Carbohydr Res **249**, 383-398
33. Brennan, P. J., and Nikaido, H. (1995) Annu Rev Biochem **64**, 29-63
34. Radmacher, E., Stansen, K. C., Besra, G. S., Alderwick, L. J., Maughan, W. N., Hollweg, G., Sahm, H., Wendisch, V. F., and Eggeling, L. (2005) Microbiology **151**, 1359-1368
35. Nakamura, Y., Nishio, Y., Ikeo, K., and Gojobori, T. (2003) Gene **317**, 149-155
36. Dover, L. G., Cerdeno-Tarraga, A. M., Pallen, M. J., Parkhill, J., and Besra, G. S. (2004) FEMS Microbiol Rev **28**, 225-250
37. Kremer, L., Dover, L. G., Morehouse, C., Hitchin, P., Everett, M., Morris, H. R., Dell, A., Brennan, P. J., McNeil, M. R., Flaherty, C., Duncan, K., and Besra, G. S. (2001) J Biol Chem **276**, 26430-26440

38. Mikusova, K., Yagi, T., Stern, R., McNeil, M. R., Besra, G. S., Crick, D. C., and Brennan, P. J. (2000) J Biol Chem **275**, 33890-33897
39. Cserzo, M., Wallin, E., Simon, I., von Heijne, G., and Elofsson, A. (1997) Protein Eng **10**, 673-676

FOOTNOTES

[#]LJA and MS contributed equally to this work. LJA is a Biotechnology and Biological Sciences Research Council Quota Student. GSB acknowledges support as a Lister Institute-Jenner Research Fellow and the Medical Research Council (UK) and HS support from the Fonds der Chemischen Industrie for support. M. tuberculosis H37Rv DNA was obtained from the Tuberculosis Research Materials Contract (NIH) at Colorado State University. We thank Graham Burns for technical assistance.

[1]The abbreviations used are: AG, arabinogalactan; Ara, arabinose; CMAME, corynomycolic acid methyl ester; DPA, decaprenol phosphoarabinose; DPPR, decaprenylphosphoryl-5-phospho-ribose; EMB, ethambutol; Gal, galactose; GC, gas chromatography; GC/MS, gas chromatography/mass spectrometry; mAGP, mycolyl-arabinogalactan-peptidoglycan; pRpp, 5-phospho-ribofuranose-pyrophosphate; Rha, rhamnose; TLC, thin layer chromatography.

[2]GSB (unpublished results)

3 Topology and mutational analysis of the single Emb arabinofuranosyltransferase of *Corynebacterium glutamicum* as a model of Emb proteins of *Mycobacterium tuberculosis*

published in *Glycobiology* 2007; **17:** 210–219

by **Mathias Seidel**[1], Luke J. Alderwick[2], Hermann Sahm[1], Gurdyal S. Besra[2], and Lothar Eggeling[1]

From the [1]Institute for Biotechnology 1, Research Centre Juelich, D-52425 Juelich, Germany and [2]School of Biosciences, University of Birmingham, Edgbaston, Birmingham B15 2TT, UK

Summary

The cell wall mycolyl-arabinogalactan (AG)–peptidoglycan complex is essential in mycobacterial species, such as *Mycobacterium tuberculosis*, and is the target of several antitubercular drugs. For instance, ethambutol (EMB) targets AG biosynthesis through inhibition of the arabinofuranosyltransferases Mt-EmbA and Mt-EmbB, as well as the single Emb from *Corynebacterium glutamicum*. Here, we present for the first time an experimental analysis of the membrane topology of Emb. The domain organization clearly positions highly conserved loop regions, like the recognized glycosyltransferase C motif and the hydrophilic C-terminus towards the periplasmic side of the cell. Moreover, the assignment and orientation of hydrophobic segments identified a loop region, which might dip into the membrane and could possibly line a transportation channel for the emerging substrate. Site-directed mutations introduced into plasmid-encoded Cg-emb were analyzed in a *C. glutamicum*Δ*emb* strain for their AG glycosyl composition and linkage analysis. Mutations analyzed did not perturb galactan synthesis; however, D297A produced a dramatically reduced arabinan content and prevented growth, indicating an inactive Emb. A second D298A mutation also drastically reduced arabinan content; however, growth of the corresponding mutant was not altered, indicating a certain tolerance of this mutation in terms of Emb function. A W659L–P667A–Q674E triple mutation in the chain length regulation motif (Pro-motif) resulted in a reduced arabinose deposition in AG but retained all arabinofuranosyl linkages. Taken together, the data clearly define important residues of Emb involved in arabinan domain formation and, for the first time, shed new light on the topology of this important enzyme.

Introduction

The Corynebacterianeae represent a distinct group within Gram-positive bacteria, with prominent members being the human pathogens *Mycobacterium tuberculosis, M. leprae*, *Corynebacterium diphtheriae*, and *C. jeikeium* (Bloom and Murray 1992). In addition, nonpathogenic bacteria belong to this taxon, such as *C. glutamicum, C. efficiens*, and *C. ammoniagenes* which are used in the industrial production of amino acids and nucleotides (Eggeling and Bott 2005). A common feature of the Corynebacterianeae is that they possess an unusual cell wall architecture (McNeil et al. 1990, 1991; Besra et al. 1995). The cell wall is dominated by mycolic acids and an essential heteropolysaccharide arabinogalactan (AG) linked to peptidoglycan *via* a disaccharide linker unit, L-Rha*p*-(1→4)-α-D-GlcNAc-phosphate, thus forming the mycolyl-AG–peptidoglycan (mAGP) complex (McNeil et al. 1990, 1991; Besra et al. 1995; Alderwick et al. 2005). The AG is composed of approximately 30 galactofuranosyl residues of alternating β(1→6) and β(1→5)-Galf linkages (Mikusova et al., 2000; Kremer et al. 2001). The galactan domain is further glycosylated at the 8^{th}, 10^{th}, and 12^{th} residue by arabinan motifs, made up primarily of α(1→5), α(1→3), and β(1→2)-Araf residues (Alderwick et al. 2005), yielding arabinan domains of approximately 25 residues in size (Besra et al. 1995).

The antituberculosis drug ethambutol (EMB) was shown to specifically inhibit AG biosynthesis (Takayama and Kilburn 1989). The precise molecular target of EMB occupies the *embCAB* locus in *M. tuberculosis* and its encoded proteins (Telenti et al. 1997). To further define the role of the EmbCAB proteins in cell wall arabinan biosynthesis, the *embC*, *embA*, and *embB* genes were disrupted individually in *M. smegmatis*, however, with the sequences in the genome retained (Escuyer et al. 2001; Zhang et al. 2003). Although all three mutants were viable, only the crucial terminal Ara_6 motif, which is the template for mycolylation in AG (McNeil et al. 1991), was altered in both Ms-*embA* and Ms-*embB* mutants (Escuyer et al. 2001). This suggested that EmbA and EmbB are involved in the formation of the terminal Ara_6 motif in AG and also presumably compensated for each other in the Ms-*embA* and Ms-*embB* mutants, whereas Ms-*embC* was involved in the formation of arabinan domains of lipoarabinomannan (LAM) (Zhang et al. 2003). Attempts to obtain deletion mutants of *embA* and *embB* in *M. tuberculosis* and *embAB* in *M. smegmatis* have proved unsuccessful (GSB, unpublished results), thus preventing the analysis of a simple defined sytem to further unravel the apparent complex Emb functions in *Mycobacterium*. In this respect, *Corynebacterium glutamicum* has proved useful, as it represents one of the simplest Corynebacterianeae with respect to cell wall structure and genomic organization. It possesses the basic cell wall

components and lipids characteristic of this peculiar group of bacteria, and often a limited number of paralogous genes,when compared with *Mycobacterium* species, are present (Kalinowski et al. 2003). Moreover, it is more tolerable with respect to deletion of essential genes. In contrast to *M. tuberculosis*, deletion of the single Cg-*emb* ortholog was possible and chemical analysis of the cell wall revealed the entire absence of the arabinan domain in AG except terminal t-Ara*f* residues, thus representing a novel truncated AG structure (Alderwick et al. 2005). More recent studies have led to the identification and characterization of the novel arabinofuranosyltransferase AftA in *C. glutamicum* conserved in the Corynebacterianeae, including *M. tuberculosis*, which catalyzes the addition of the first key arabinofuranosyl residue from the sugar donor β-D-arabinofuranosyl-L-monophosphoryl-decaprenol to the galactan domain of the cell wall, thus "priming" the galactan for further elaboration by Cg-Emb and Mt-EmbA/B, respectively (Alderwick, Seidel et al. 2006).

Despite the importance of the arabinofuranosyltransferases Emb and AftA, there is little information on the structure and mechanism of these membrane-located enzymes. Overall, the Emb proteins of Corynebacterianeae are similar in size, 1094–1146 aa residues, and predictions suggest a very similar topology with transmembrane spanning helices dominating the N-terminal domain followed by a large hydrophilic C-terminal domain, probably directed towards the periplasmic side. Interestingly, in clinical isolates of EMB-resistant *M. tuberculosis* strains, mutations are found within *embC*, *embA*, and *embB*, with prominent mutations in the putative membrane embedded N-terminal part of EmbB, specifically Met 306 (Ramaswamy et al. 2000). However, mutational studies to date have focussed on Ms-EmbC, which has been shown to be involved in LAM biosynthesis (Zhang et al. 2003). Interestingly, in this regard, when point mutations within a motif characteristic for the glycosyltransferase C (GT-C) family (Liu and Mushegian 2003) were introduced into a complementing plasmid in the Ms-*embC* mutant, LAM synthesis was completely abolished (Berg et al. 2005). The GT-C motif is predicted to face the periplasmic side of the membrane, as does a second chain length regulation praline motif (Pro-motif) (Berg et al. 2005). In addition, point mutations within the Pro-motif when introduced into the complementing plasmid in the Ms-*embC* mutant led to a truncation in LAM. More recently, truncated *embC* alleles within the hydrophilic extracytoplasmic C-terminal domain when introduced into the complementing plasmid in the Ms-*embC* mutant have afforded highly truncated LAMs (Shi et al. 2006).

It is clear that there is a need to deepen our knowledge on the structure and function of arabinofuranosyltransferases within the Corynebacterianeae. In the present study, we have

used the *C. glutamicum* mutant deleted of the single emb ortholog as it provides a strong phenotypic background in terms of arabinan biosynthesis to perform a topological analysis of Cg-Emb together with a mutational study of this protein to clarify the role of emb in AG biosynthesis for the first time.

Material and Methods

Strains and culture conditions

Corynebacterium glutamicum ATCC 13032 (the wild type strain) and *C. glutamicum*Δ*emb* (Alderwick et al. 2005) together with its recombinant derivatives with *emb* alleles were grown on brain–heart infusion (BHI, Difco, Detroit, MI) containing 0.5 M sorbitol at 30 °C (Eggeling and Bott 2005). *Escherichia coli* DH5α was grown on Luria-Bertani (LB) medium (Difco) at 37 °C. When appropriate, kanamycin was used at a concentration of 25 µg/mL and ampicillin at a concentration of 50 µg/mL. Samples for cell wall analyses of *C. glutamicum* strains were prepared by harvesting cells at an OD of 5–8, followed by a saline wash and freeze-drying.

Construction of emb-phoA–lacZ fusion and exonuclease treatment

To make vector pMS3 suitable for exonuclease treatment of Cg-*emb*, pMA632 (Alexeyev and Winkler 1999) was *Nru*I/ *Nra*I digested and ligated with a mixture of CGACCGCGGGG (all oligonucleotides are given in direction 50 to 30) and GGCGCCCCGCGGTCG to generate the new restriction site *Ksp*I in vector pMA632-1. This vector was prepared by a *Sma*I–*Ksp*I digest and treated with alkaline phosphatase. To obtain *emb* with appropriate restriction sites attached, pEKEx2emb was ScaI/EcoRI cleaved and ligated with a mixture of oligonucleotide CGACCGCGGGG and GGCGCCCCGCGGTCG to generate pEKEx2*emb*-2. From this vector, emb was obtained as a SwaI–KspI fragment that was purified and ligated with pMA632-1 to generate pMS3. The integrity of the *emb-phoA–lacZ* fusion was verified by sequencing.

To construct progressive unidirectional deletions of the 3´ end of *emb*, pMS3 was cleaved with *Fse*I–*Sca*I and treated for various times with exonuclease III (Henikoff 1984). Subsequently, single-stranded protruding DNA ends were digested with nuclease S1 and DNA blunted and religated. The ligation mixture was electroporated into *E. coli* DH5α and plated on dual indicator plates containing blue alkaline phosphatase and red β-galactosidase

chromogenic substrates (Alexeyev and Winkler 1999). The plates contained 1.5% Bacto-agar, 1% Bacto-tryptone, 0.5% yeast extract, 1% NaCl, 80 µg/mL 5-bromo-4-chloro-3-indolyl-β-D-galactoside disodium salt (Roche, Palo Alto, CA), 100 µg/mL, chloro-3-indolyl-β-D-galactopyranoside (rose-Gal, AppliChem Inc., Cheshire, CT), and 50 µg/mL kanamycin. The plasmid DNA was isolated from different colored colonies and insertion points mapped by restriction digests and confirmed by sequencing.

Site-directed mutagenesis

Using pEKEx2*emb* as a template (Radmacher et al. 2005), mutations in *emb* were introduced in a two-step polymerase chain reaction (PCR) (Landt et al. 1990). The following mutation primers were used (with the mutated codon underlined): For D297A, AACACCTC-TGCCGACGGCTTCATC; D298A, AACACCTCTGACGCC-GGCTTCATC, D297AD298A, AACACCTCTGCCGCCGG-CTTCATC, in all cases with CGCAAGTAGAGCTCCCA-TCGC as the identical second primer. The resulting megaprimers were purified and used with GCTTGCATGCCTGCAG GTCGA in a second PCR to yield mutated *emb* fragments. These were treated with *Sbf*I and *Sac*I and ligated with pEKEx2*emb* from which the GT-C site containing *Sbf*I–*Sac*I fragment had been previously removed. Similarly, mutations were introduced into the *Asp*I–*Sca*I fragment of emb using primers: W659L, GGAGGTGTACAAGAATCCGTT; P667A, ATCCCACCATGCCACGGCGTA; I673A, CTTGATCTGGGCGGTTTTATC; Q674E, CTTGATCTCGATGGTTTTATCCC. The second primer in the first PCR was CGATCAGACTCTGTCAACCGT, and the additional primer for the second PCR was TCCGGTTCCAGTACTGAAGGT. After cloning, the integrity of all replaced fragments with their adjacent sites was verified by sequencing. The triple mutation was obtained commercially from 4base lab, Reutlingen, Germany.

Enzyme assays

For alkaline phosphatase and β-galactosidase activity determinations, 1 mL LB overnight cultures of E. coli cells bearing fusion constructs and unfused plasmid (background control) were harvested by centrifugation, washed, and resuspended in 10 mM Tris–HCl, 10 mM $MgSO_4$, pH 8 to an OD 600 of 1. Cells in 100 µL of this suspension were permeabilized by addition of 50 µL 0.1% sodium dodecyl sulphate (SDS) and 50 µL of chloroform. After incubation for 5 min at 37 °C, cells were stored on ice for enzyme activity determinations. Alkaline phosphatase activity was assayed essentially as described by Brickman and

Beckwith (1975), except using an extinction coefficient of ε_{405}nm = 1.85 x 10^4 $M^{-1}cm^{-1}$ with 5-bromo-4-chloro-3-indolyl phosphate disodium salt as a substrate, whereas β-galactosidase was assayed according to Miller (1992) with nitrophenyl-β-galactoside using an extinction coefficient of ε_{420}nm = 2.13 x 10^4 M^{-1} cm^{-1}. Protein was determined by the bicinchoninic method, and specific activities expressed in micromoles per minute per milligram.

Extraction and analysis of cell wall associated and cell wall bound lipids

Cells were grown as described earlier, harvested, washed, and freeze-dried. Cells (100 mg) were extracted by two consecutive extractions using 2 ml of $CHCl_3/CH_3OH/H_2O$ (10:10:3, v/v/v) for 3 h at 50 °C and the resulting delipidated cells stored for further use (as described subsequently). Organic extracts were combined with 1.75 mL $CHCl_3$ and 0.75 mL H_2O, mixed and centrifuged. The lower organic phase was recovered, washed twice with 2 mL of $CHCl_3/CH_3OH/H_2O$ (3:47:48, v/v/v), dried, and resuspended in 200 µL of $CHCl_3/CH_3OH/H_2O$ (10:10:3, v/v/v). An aliquot (20 µL) was analyzed by TLC using silica gel plates (5735 silica gel $60F_{254}$, Merck, Darmstadt, Germany) developed in $CHCl_3/CH_3OH/H_2O$ (60:16:2, v/v/v). TLCs were visualized by charring with 5% molybdophosphoric acid in ethanol at 100 °C to reveal cell wall associated lipids.

The bound lipids from delipidated extracts or purified cell walls (Isolation of the mAGP complex) were released by the addition of a 5% aqueous solution of tetra-butyl ammonium hydroxide, followed by overnight incubation at 100 °C, and methylated as described in Alderwick et al. (2005). CMAMEs were analyzed by TLC using silica gel plates (5735 silica gel $60F_{254}$, Merck) developed in petroleum ether/acetone (95:5, v/v). TLCs were visualized by charring with 5% molybdophosphoric acid in ethanol at 100 °C to reveal CMAMEs.

Isolation of the mAGP complex

The thawed cells were resuspended in phosphate-buffered saline containing 2% Triton X-100 (pH 7.2), disrupted by sonication, and centrifuged at 27 000g (Daffe et al. 1990; Besra et al. 1995). The pelleted material was extracted three times with 2% SDS in phosphate-buffered saline at 95 °C for 1 h to remove associated proteins, successively washed with water, 80% (v/v) acetone in water, and acetone, and finally lyophilized to yield a highly purified cell wall preparation (Besra et al. 1995; Alderwick et al. 2005).

Glycosyl composition and linkage analysis of cell walls

Cell wall preparations were hydrolyzed using 2 M trifluoroacetic acid (TFA), reduced with NaB_2H_4 and the resultant alditols per-O-acetylated and examined by GC as described in Daffe et al. (1990), Besra et al. (1995), and Alderwick et al. (2005). Cell wall preparations were per-O-methylated using dimethyl sulfinyl carbanion (Daffe et al. 1990; Besra et al. 1995; Alderwick et al. 2005). The per-O-methylated cell walls were hydrolyzed using 2 M TFA, reduced with NaB_2H_4, per-O-acetylated, and examined by GC/MS. Analysis of alditol acetate sugar derivatives was performed on a CE Instruments ThermoQuest Trace GC 2000 in the splitless mode using a DB225 column (Supelco, Pennsylvania, PA). The oven was programmed to hold at an isothermal temperature of 275 °C for a run time of 15 min (Alderwick et al. 2005). GC/MS was carried out on a Finnigan Polaris/GCQ PlusTM using a BPX5 column (Supelco).

Results

Reporter fusions to Cg-*emb*

A clear advantage of our studies is that *C. glutamicum* has only one single arabinofuranosyltransferase, with identities to the Emb proteins of *M. tuberculosis*, and which is proved to be involved in AG biosynthesis (Alderwick et al. 2005), whereas *M. tuberculosis* has three Emb proteins (Telenti et al. 1997). They all share a high degree of sequence similarity among each other. Interestingly, Cg-Emb exhibits the highest similarity of 58% to Mt-EmbC, thought to be involved in LAM biosynthesis (Zhang et al. 2003), which is remarkable. We therefore compared the wild type of *C. glutamicum* and its *emb* deletion mutant *C. glutamicum*Δ*emb* in terms of their lipoglycan content. *Corynebacterium glutamicum* has lipomannan (Gibson et al. 2003) and a very specific LAM. Gas chromatography (GC) and GC/mass spectrometry (MS) analyses showed that LAM of *C. glutamicum* possesses a linear mannan backbone with only single t-Ara*f* residue attached and this structure is retained in *C. glutamicum*Δ*emb* (data not shown), whereas LAM of *M. tuberculosis* has a branched mannan core with chains of Araf residues attached (Chatterjee et al. 1992). This confirms that the single *emb* of *C. glutamicum* contributes to the formation of the arabinan domain in AG (Alderwick, Dover et al. 2006; Alderwick, Seidel et al. 2006), but does not affect LAM synthesis. Because of the importance of Emb proteins in terms of drug targeting and resistance to EMB (Takayama and Kilburn 1989) as well as their

importance for mAGP biosynthesis, supportive information on their structure and activity is urgently needed.

To this end, we fused Cg-*emb* in pMS3 with an alkaline phosphatase-β-galactosidase reporter cassette (Alexeyev and Winkler 1999). This system enables to localize the fusion point to the periplasmic side when alkaline phosphatase is active and β-galactosidase is inactive or to the cytoplasmic side when the enzyme activities are reversed.

Tab. I. Analysis of Cg-Emb topology using phoA-lacZ reporters

Fusion[a]	Color	Phosphatase[b], sp A ($\mu mol \cdot min^{-1} \cdot mg^{-1}$)	Galactosidase[b], sp A ($\mu mol \cdot min^{-1} \cdot mg^{-1}$)	Ratio[c]
Control	No	0.30	0.08	–
V67	Blue	3.75	0.31	12.1
W288	Blue	3.90	0.26	15.0
Y317	Blue	1.95	0.26	7.5
L395	Blue	1.72	0.70	2.5
G410	Blue	3.00	0.98	3.1
L454	Blue	1.46	0.24	6.1
L471	Red	0.76	1.90	0.4
D508	Blue	1.87	0.23	8.1
V565	Blue	1.93	0.27	7.1
R585	Red	0.75	3.21	0.2
M598	Blue	2.31	0.33	7.0
A615	Blue	2.20	0.41	5.4
A619	Blue	1.68	0.67	2.5
R637	Purple	0.89	3.34	0.3
W668	Blue	4.01	0.40	10.0
G677	Blue	2.50	0.25	10.0

Fusion points in Cg-Emb were determined by DNA sequencing and colony coloration on dual indicator plates judged after 48 h (Alexeyev and Winkler 1999).
[a]Position of the last residue of Cg-Emb followed by reporter.
[b]Enzyme activities of the fusions, determined as described in Materials and methods, average of at least two independent experiments.
[c]Normalized activity ratio rounded to the first decimal place.

Using introduced restriction sites (see Materials and methods) and a set of exonuclease III treatments, Cg-*emb* was digested from its 3´ end, thus creating a collection of truncated Emb proteins with the fusion at their C-terminus. A total of 62 fusions were chosen conferring a blue, red, or purple color to *Escherichia coli* DH5α indicator plates due to an apparent alkaline phosphatase activity (Table I). Sequencing identified that these fusions cover the entire length of the polypeptide sequence from 67 to 1146 aa. The location of all fusions is

given in Figure 1, with all fusion sites listed in Supplementary Table S1. Red colonies indicative of β-galactosidase activity were obtained with fusions at L471 and R585. To confirm the color appearance of the colonies, a direct enzyme assay for 16 selected clones was performed concentrating on the first two-thirds of the protein, where topology predictions were strongly deviating from each other. As shown in Table I, both phosphatase and b-galactosidase activities were well above the control and generally agreed with colony coloration. An exception was the fusion at R637, which resulted in an ambiguous purple color on plates. However, the absolute specific β-galactosidase activity, as well as the ratio of activities, directs this fusion to the cytoplasmic side.

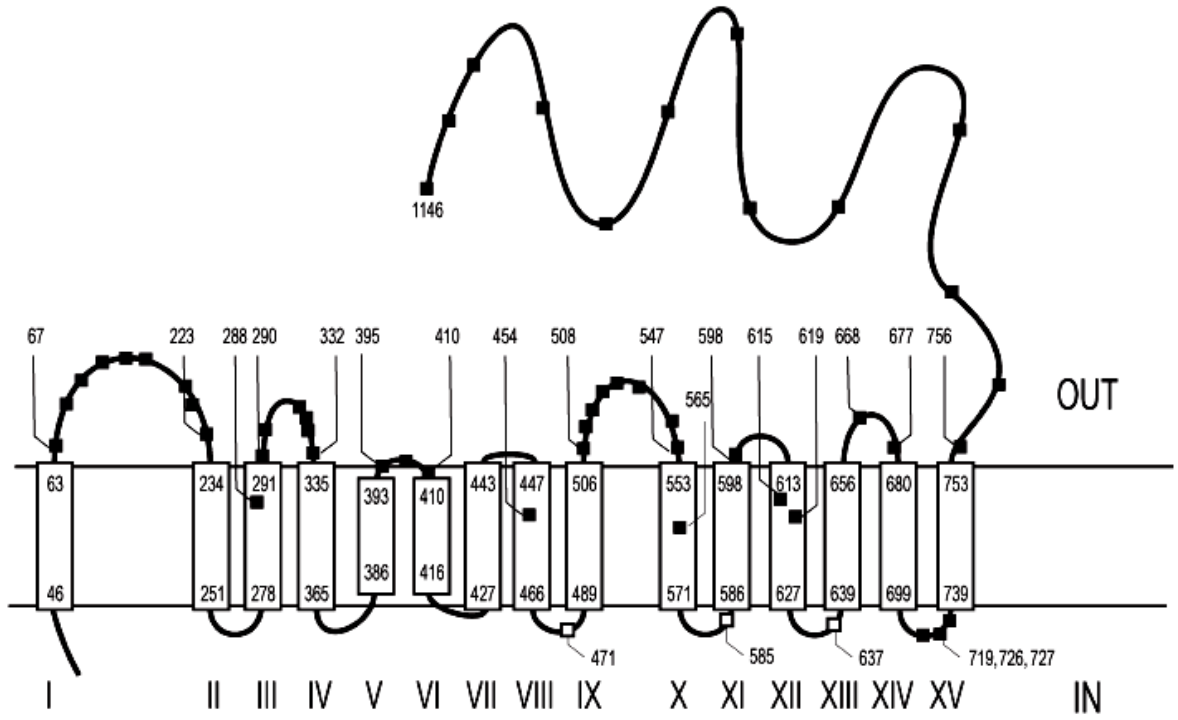

Fig. 1. Topological model of the Cg-emb arabinofuranosyltransferase of C. glutamicum. Filled squares give positions in the Emb polypeptide where fusions resulted in alkaline phosphatase activity, with selected positions numbered (all fusions are given in the Supplementary data). The three numbered open squares give positions in the Emb polypeptide where fusions resulted in b-galactosidase activity. The numbers in the large rectangles give the amino acid positions delimiting the hydrophobic segments numbered I–XV. IN denotes the cytoplasmic side of the membrane and OUT the periplasmic side.

Localization of fusions

To locate the fusions in a topology model, a number of predictions were applied to Cg-Emb based on a variety of algorithms available at the Swiss Institute of Bioinformatics (data not shown). Method PHDhtm predicted the C-terminus to be cytosolic. This prediction was

not considered due to the large number of active PhoA fusions between aa 756 and 1145, clearly indicating the C-terminus to be located towards the periplasmic side. Similarly, the TMHMM prediction was not considered, as was the case with other predictions due to their strong divergence from the experimental data. The highest consistency of the information derived from the fusions was obtained with the Dense Alignment Surface algorithm (Cserzö et al. 1997), which is based on low-stringency dot-plots of the query sequence against a collection of library sequences derived from nonhomologous membrane proteins. Almost all 62 fusions analyzed provide a best fit to the model shown in Figure 1. There are only a very limited number of exceptions, like the set of fusions at V719, R726, and E727. However, these fusions result in the absence of at least two of the Arg residues present in the original Emb protein in positions R726, R728, and R731. The absence of positively charged residues, dominating the cytosolic side of polytopic membrane proteins, is well known to disable proper membrane integration via the sec-translocon (Pohlschröder et al. 2005). Also, the fusion at position R637 replaces a positive Arg residue, which may thus lead in part to improper localization and explain the high phosphatase activity and vague colony color. In the case of phosphatase activity within transmembrane helical fusions, such as L454, V565, and A619, the mere length of the remaining hydrophobic stretch is expected to be too short to enable pulling of the reporter protein through the membrane to the cytosolic side. This is in accordance with a study on the *E. coli* Lac permease where at least half of a helix is necessary for insertion into the membrane (Calamia and Manoil 1990). Overall, there is a very good consistency of the experimental data with the model.

Growth characteristics of Cg-emb mutants

The availability of *C. glutamicum*Δ*emb*, and its feature that solely due to plasmid-encoded Cg-*emb* the arabinan domain in mAGP is fully restored (Alderwick et al. 2005), is an ideal tool to study the consequences of Cg-*emb* mutations on Ara*f* delivery to the mAGP complex. To this end, we introduced eight mutations into Cg-*emb* (Figure 2B) based on the mutations introduced into *embC* of *M. smegmatis* which affect LAM biosynthesis (Berg et al. 2005). These mutations together with their locations in the topological model are given in Table II. Cg-*emb* and alleles of this gene cloned in pEKEx2 were introduced into *C. glutamicum*Δ*emb* and growth of the recombinant clones judged on plates (Table II). Whereas without *emb* present colonies of *C. glutamicum*Δ*emb* were small with rough appearance, the single mutations W659L, P667A, I673A, and Q674E introduced into the Pro-motif of plasmid-encoded emb resulted in glossy large colonies characteristic for wild type Cg-*emb*.

The triple mutation W627L–P667A–Q674E analyzed in the same manner produced colonies of intermediate size. D297A and D297A-D298A in the GT-C motif produced only tiny mate colonies indistinguishable from the negative control indicating a distortion of cell wall biosynthesis, whereas the D298A mutation resulted in colony size and surface characteristics of wild type Cg-*emb*. In addition, growth was analyzed in liquid culture. Again the positive control with plasmid-encoded *emb* in *C. glutamicum*Δ*emb* exhibited growth comparable to the wild type, whereas growth rate and final optical clensity (OD) were significantly reduced with *emb* carrying the triple mutation (Figure 2A). The mutation D297A-D298A prevented growth, whereas D298A again restored growth (Figure 2A).

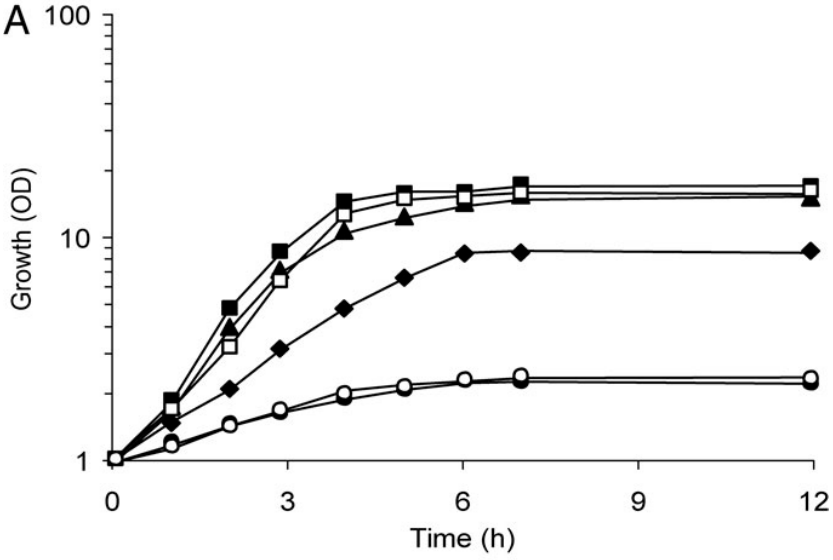

B

Loop connecting helices III-IV

```
Cglu_emb   291  LGANTSDDGFIMTMARVSQNADYMANYYRWFGVPESPFGAPYYDL  335
Mmar_embC  269  VGANTSDDGYILTMARVSEHAGYMANYYRWFGTPEAPFG-WYYDL  329
Mtub_embC  287  VGANTSDDGYILTMARVSEHAGYMANYYRWFGTPEAPFG-WYYDL  330
Mlep_embC  286  VGANTSDDGYILTMARVSEHAGYMANYYRWFGTPEAPFG-WYYDL  312
                :*********:::·**:·*  :·**********·**:***::*****·
```

Loop connecting helices XIII-XIV

```
Cglu_emb   656  GFWYTSSYAVPWWDKTIQIKGIEA  680
Mmar_embC  637  GWWYVSNFGVPWSNSFPRLR-WSL  660
Mtub_embC  638  GWWYVSNFGVPWSNSFPKWR-WSL  661
Mlep_embC  620  GWWYVSNFGVPWSNSFPKLR-WSL  643
                *:** *·:·:** :·  :  ·
```

Fig. 2. Mutations and growth analysis of mutant Emb arabinofuranosyltransferases in *C. glutamicum*Δ*emb*. (**A**) Growth analysis due to mutated Emb arabinofuranosyltransferases in *C. glutamicum*Δ*emb* containing the plasmid-encoded *emb* alleles. Growth was analyzed in BHI medium supplemented with 0.5 M sorbitol, followed by measuring the OD at 600 nm. ■, controls of the wild type; F, the mutant *C. glutamicum*Δ*emb* without emb encoded arabinofuranosyltransferase activity (Alderwick et al. 2005); □, the same mutant with pEKEx2*emb* overexpressing *emb*. With the plasmid encoded *emb* carrying the D297A-D298A mutation (M) no complementation was obtained, whereas with the D298A mutation (□), growth was almost identical as obtained with unmutated *emb*. With the triple mutation P659L–P667A–Q674E in *emb* (♦), an intermediate growth was obtained. (**B**) Sequence identities among the Emb proteins and mutations introduced in

the periplasmic loop regions identified connecting helices III–IV, with the GT-C motif (Liu and Mushegian 2003) and XIII–XIV with the Pro-motif (Berg et al. 2005), respectively. The amino acid substitutions introduced in Cg-Emb are indicated by white letters on a black background. Beneath the alignments, the degree of conservation is indicated. Cglu stands for *C. glutamicum*, Mmar for *M. marinum*, Mtub for *M. tuberculosis*, and Mlep for *M. leprae*. Growth performance due the other mutations is given in Table II.

Growth was also restored with the individual W659L, P667A, I673A, and Q674E mutations (data not shown). Interestingly, already truncation of the C-terminus by 159 amino acids of Cg-Emb resulted in inactive arabinosyltransferase as judged from the inability of *C. glutamicum*Δ*emb* carrying the corresponding pEKEx2*emb* derivative to grow (data not shown).

Tab. II. Mutations in Cg-emb and consequences of colony formation of C. glutamicumDemb complemented with Cg-emb alleles

Strain	Mutation	Localization of mutation	Motif	Colony size of strain[a] (mm)
*C.g.*Δ*emb* pEKEx2	Negative control			<0.4
*C.g.*Δ*emb* pEKEx2*emb*	Positive control			3
*C.g.*Δ*emb* pEKEx2*emb*-D297A	D297A	Loops III–IV	GT-C	<0.4
*C.g.*Δ*emb* pEKEx2*emb*-D298A	D298A	Loops III–IV	GT-C	3
*C.g.*Δ*emb* pEKEx2*emb*-D297A-D298A	D297A-D298A	Loops III–IV	GT-C	<0.4
*C.g.*Δ*emb* pEKEx2*emb*-R350A	R350A	Helix IV		3
*C.g.*Δ*emb* pEKEx2*emb*-K603A	K603A	Loops XI–XII		3
*C.g.*Δ*emb* pEKEx2*emb*-W659L	W659L	Loops XIII–XIV	Pro	3
*C.g.*Δ*emb* pEKEx2*emb*-P667A	P667A	Loops XIII–XIV	Pro	3
*C.g.*Δ*emb* pEKEx2*emb*-I673A	I673A	Loops XIII–XIV	Pro	3
*C.g.*Δ*emb* pEKEx2*emb*-Q674E	Q674E	Loops XIII–XIV	Pro	3
*C.g.*Δ*emb* pEKEx2*emb*-W659L-P667A-Q674E	W659L-P667A-Q674E	Loops XIII–XIV	Pro	1
*C.g.*Δ*emb* pEKEx2*emb*-D1031A	D1031A	C-terminus		3

Most mutations are localized according to the model in periplasmic loop regions (Figure 1) and correspond to a GT-C and proline Pro-motif, respectively (Berg et al. 2005; Liu and Mushegian 2003).
[a]Phenotype was determined after incubation for 1 week on plates containing BHI (Difco) plus 0.5 M sorbitol.

Analysis of cell wall associated lipids

To obtain an initial phenotypic composition of the cell wall, the “free lipids” from each of the strains studied underwent lipid extraction and analysis by thin layer chromatography (TLC) (Figure 3). A clear increase in free trehalose monocorynomycolates (TMCM) could be observed in *C. glutamicum*Δ*emb*, and the same strain carrying plasmidencoded Cg-*emb* with the D297A mutation or the D297AD298A mutation. A slight increase could be observed due to the P659L–P667A–Q674E mutation. This apparent increase in the amount of free TMCM in the cell wall is indicative of an altered cell wall

ultrastructure, particularly when considering the removal of sites for mycolic acid attachment McNeil et al. 1991; Alderwick et al. 2005; Alderwick, Dover et al. 2006). Although this view appears plausible, it could not be excluded that additional effects due to the, in part, altered growth characteristics of the mutants are present. Normal levels of TMCM could be observed with plasmids carrying the D298A, W659L, P667A, or the Q674E mutation, which is indicative of an intact cell wall and its associated free lipids.

Cell wall bound corynomycolic acid compositional analysis

It has previously been reported that a good indicator for the disruption of the arabinan component of the cell wall is the absence of AG-esterified corynomycolic acids (Alderwick et al. 2005; Alderwick, Dover et al. 2006). We therefore analyzed these bound lipids derivatized as corynomycolic acid methyl esters (CMAMEs) in *C. glutamicum*Δ*emb* carrying the plasmid-encoded *emb* mutations. *Corynebacterium glutamicum* and *C. glutamicum*Δ*emb* exhibited the expected presence and absence of CMAMEs, respectively (Figure 4, Lanes 1 and 2). No CMAMEs could be observed with the D297A mutation in Cg-*emb* (Figure 4, Lane 3). However, CMAMEs were detectable with the D298A mutation indicating the presence of mycolation sites (Figure 4, Lane 4), although the absolute amount of CMAMEs in comparison to *C. glutamicum* (Figure 4, Lane 1) hinted to a reduced number of possible CMAME-linkage sites. The D297A-D298A mutation resulted also in the absence of CMAMEs (Figure 4, Lane 5), thus confirming again that D297 is the more important amino acid residue within the GT-C motif. Although slightly reduced, the CMAMEs for the remaining mutants studied remained largely unaffected, apart from the triple mutant, which did exhibit a moderate decrease in the amount of apparent CMAMEs esterified in the cell wall (Figure 4, Lane 9).

Glycosyl compositional analysis

To directly observe the effects of the mutated arabinosyltransferase Cg-*emb* on the arabinan domain structure, the mutants together with controls were subjected to glycosyl compositional analysis. *Corynebacterium glutamicum* and *C. glutamicum*Δ*emb* afforded Ara:Gal ratios of 3.1 : 1 and 0.2 : 1, respectively (Figure 5, Lanes 1 and 2).

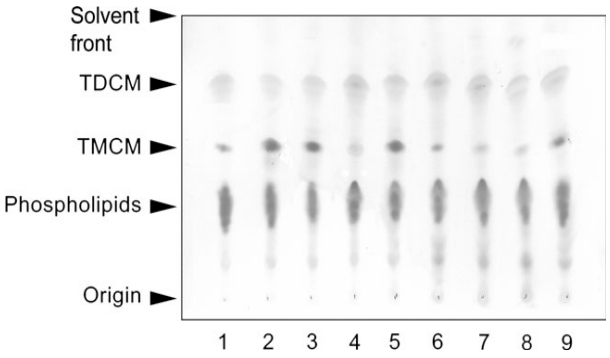

Fig. 3. Analysis of cell wall associated lipids from *C. glutamicum*, *C. glutamicumΔemb*, and *C. glutamicumΔemb* carrying mutated *emb* alleles. Cell wall associated free lipids were analyzed as described in Materials and methods. The strains analyzed are as follows: 1, *C. glutamicum*; 2, *C. glutamicumΔemb*; 3, *C. glutamicumΔemb* pEKEx2*emb*-D297A; 4, *C. glutamicumΔemb* pEKEx2*emb*-D298A; 5, *C. glutamicumΔemb* pEKEx2*emb*-D297A-D298A; 6, *C. glutamicumΔemb* pEKEx2*emb*-W659L; 7, *C. glutamicumΔemb* pEKEx2*emb*-P667A; 8, *C. glutamicumΔemb* pEKEx2*emb*-Q674E; 9, *C. glutamicumΔemb* pEKEx2*emb*-W659L-P667AQ674E.

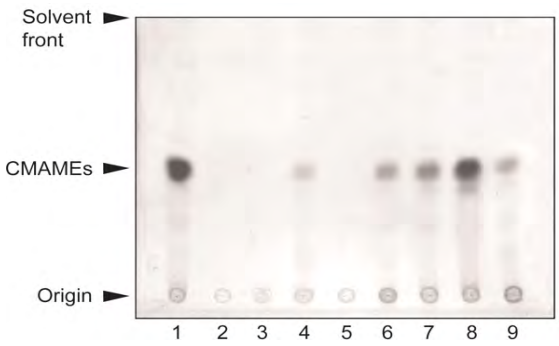

Fig. 4. Analysis of cell wall bound CMAMEs of delipidated cells. An aliquot of the released cell wall bound CMAMEs from each strain was analyzed by TLC as described in Materials and methods. 1, *C. glutamicum*; 2, *C. glutamicumΔemb*; 3, *C. glutamicumΔemb* pEKEx2*emb*-D297A; 4, *C. glutamicumΔemb* pEKEx2*emb*-D298A; 5, *C. glutamicumΔemb* pEKEx2*emb*-D297A-D298A; 6, *C. glutamicumΔemb* pEKEx2*emb*-W659L; 7, *C. glutamicumΔemb* pEKEx2*emb*-P667A; 8, *C. glutamicumΔemb* pEKEx2*emb*-Q674E; 9, *C. glutamicumΔemb* pEKEx2*emb*-W659L-P667AQ674E.

The D297A mutation in *emb* produced a cell wall with a dramatically reduced arabinose content (Figure 5, Lane 3) almost identical to *C. glutamicumΔemb*. Also, with the D298A mutation, the level of arabinose was significantly reduced by approximately 80% to give an Ara:Gal ratio of 0.8 : 1 (Figure 5, Lane 4). The D297A-D298A mutation caused a phenotype identical to the D297A mutation, thus reinforcing the importance of the D297 residue in catalysis (Figure 5, Lane 5). Analysis of cell walls isolated from strains carrying mutations within the proline motif gave a varying profile of sugar composition (Figure 5, Lanes 6–9). W659L, P667A, and Q674E gave Ara:Gal ratios of 1.2:1, 1.5:1, and 1.9:1, respectively, whereas the triple mutation caused a further reduction of arabinose resulting in an Ara:Gal ratio of 0.56 : 1. In summary, there is a reduction of Ara in the mutants and therefore the Gal ratio relative to Ara is higher in the glycosyl compositional analysis. Moreover, it has to be borne in mind that the decreased Rha content with respect to Gal (Figure 5) can also be explained by the fact that we have additional Rha residues that are not in the linker region, i.e. not 4-linked Rha but are terminal Rha residues that are located at the terminal ends of the arabinan domains. So, the *C. glutamicum emb* deletion strain will retain a small amount of Rha as 4-Rha from the linker unit but will have decreased t-Rha.

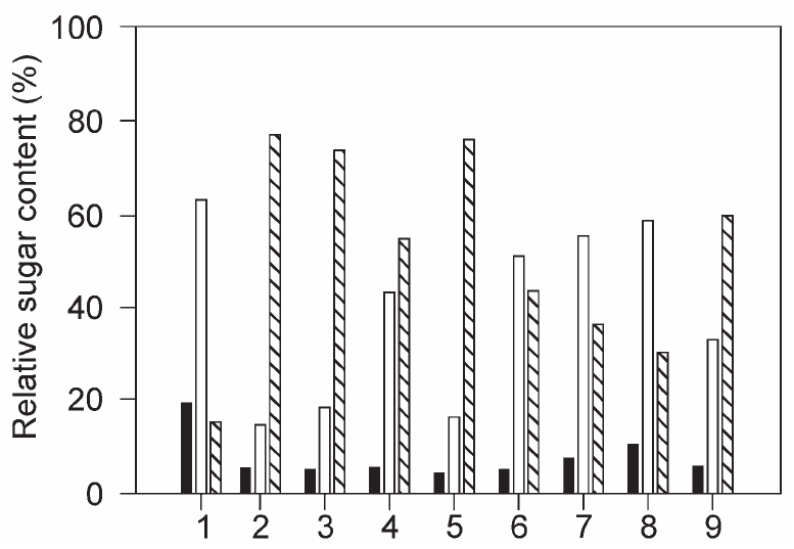

Fig. 5. Glycosyl compositional analysis of cell walls from *C. glutamicum*, *C. glutamicum*Δ*emb*, and *C. glutamicum*Δ*emb* carrying mutated *emb* alleles. Samples were prepared and analyzed as described in Materials and methods. The data represent the relative sugar composition as a percentage in graphical format. The bars are tinted as follows: rhamnose, black; arabinose, white; galactose, hatched. 1, *C. glutamicum*; 2, *C. glutamicum*Δ*emb*; 3, *C. glutamicum*Δ*emb* pEKEx2*emb*-D297A; 4, *C. glutamicum*Δ*emb* pEKEx2*emb*-D298A; 5, *C. glutamicum*Δ*emb* pEKEx2*emb*-D297A-D298A; 6, *C. glutamicum*Δ*emb* pEKEx2*emb*-W659L; 7, *C. glutamicum*Δ*emb* pEKEx2*emb*-P667A; 8, *C. glutamicum*Δ*emb* pEKEx2*emb*-Q674E; 9, *C. glutamicum*Δ*emb* pEKEx2*emb*-W659L-P667A-Q674E.

Glycosyl linkage analysis

To further define the role of amino acid residues from Cg-Emb in the biosynthesis of cell wall arabinan, glycosidic linkages from cell walls isolated from *C. glutamicum*Δ*emb* strains carrying mutations in plasmid-encoded Cg-*emb* were analyzed by GC/MS. For all such mutants studied, the 5-Gal*f*, 6-Gal*f*, and 5,6-Gal*f* residues could be accounted for, which as expected represent an unmodified galactan domain (data not shown). As previously reported (Alderwick et al. 2005), deletion of Cg-*emb* resulted in a severely truncated arabinan domain with only single *t*-Ara*f* residues attached to the galactan domain. The D298A mutation results in an increase in the relative *t*-Ara*f* content with a reduced degree of branching while generally retaining other glycosidic linkages, which indicates abrogated Cg-Emb activity. However, the D297A and the D297A-D298A mutations fully abolished the Araf linkages of AG of *C. glutamicum*, excluding *t*-Ara*f* (Table III). Thus, it is clear that D297 is a major catalytic residue in terms of arabinan deposition, albeit D298 also influences this activity. Typical glycosidic linkages in comparison with *C. glutamicum* are observed with each of the W627L, P667A, and Q674E mutations (Table III). Taken together with the reduced Ara:Gal ratio (Figure 5), this may imply that these residues in some way moderate the size of the arabinan chains in AG. This is substantiated by the fact that, when all three residues are

mutated together, a severe reduction in arabinose can be observed by GC (Figure 5), but with all glycosidic linkages remaining present (Table III).

Tab. III. Glycosyl linkage analysis of cell wall arabinan from C. glutamicum, C. glutamicum deleted of emb (C.g.Demb), and the plasmid-encoded mutant alleles in the C.g.Demb background as determined by GC/MS

Strain	*t*-Ara*f*	2-Ara*f*	5-Ara*f*	3,5-Ara*f*	2,5-Ara*f*
C. glutamicum	8.7	9.3	52.9	11.9	17.2
*C.g.*Δ*emb*	100	0.0	0.0	0.0	0.0
*C.g.*Δ*emb* pEKEx2*emb*-D297A	100	0.0	0.0	0.0	0.0
*C.g.*Δ*emb* pEKEx2*emb*-D298A	20.6	9.9	45.4	13.4	10.7
*C.g.*Δ*emb* pEKEx2*emb*-D297A-D298A	100	0.0	0.0	0.0	0.0
*C.g.*Δ*emb* pEKEx2*emb*-W659L	16.7	10.8	51.7	10.3	10.3
*C.g.*Δ*emb* pEKEx2*emb*-P667A	13.7	11.4	51.0	11.2	12.7
*C.g.*Δ*emb* pEKEx2*emb*-Q674E	13.9	6.1	55.1	12.8	12.1
*C.g.*Δ*emb* pEKEx2*emb*-W659L-P667A-Q674E	34.2	9.3	45.8	6.2	4.5

Values are given as relative glycosyl linkages in percentage.

Discussion

The mAGP complex represents one of the most important cell wall components of the Corynebacterianeae and is essential for the viability of *M. tuberculosis* (Vilcheze et al. 2000; Pan et al. 2001; Gande et al. 2004; Mills et al. 2004). It is therefore not surprising that one of the most effective antimycobacterial drugs, EMB, targets its biosynthesis. An elementary structure of this mAGP polymer is apparent in *C. glutamicum*, and this bacterium has proved useful for a number of studies on mAGP biosynthesis (Gande et al. 2004; Portevin et al. 2004; Alderwick et al. 2005; Alderwick, Seidel et al. 2006). It represents the archetype of the Corynebacterianeae with respect to a core cell wall structure and also a low number of gene duplications (Nakamura et al. 2003) when compared with *M. tuberculosis* which has a much more elaborated cell wall and also a significantly larger genome.

Although, arabinofuranosyltransferases are of prime interest for arabinan formation in Corynebacterianeae, functional and structural studies of these glycosyltransferases are scarce. The sequences of Mt-EmbC, Mt-EmbA, Mt-EmbB, and Cg-Emb exhibit a high degree of similarity among each other (54–58%) (Berg et al. 2005), with Mt-EmbC probably closest to the single Cg-Emb. There are two domains predicted for the Emb proteins. They consist of a

hydrophilic C-terminus and a hydrophobic N-terminus as typical for membrane-embedded proteins. Predictions of the hydrophobic part of Mt-EmbC range from 11 to 14 hydrophobic segments (HSs) which may span the membrane (Berg et al. 2005). Interestingly, in all the predictions we compared (data not shown), these were largely on par with respect to HSs corresponding to helices I–III and VII-XV of our current model (Figure 1), whereas for the regions in between variations existed. The fusions obtained (Table 1 and Supplementary Table S1) are consistent with three HSs in this part, because the large number of fusions obtained with PhoA activity of the entire remaining Emb protein would have to be located on the cytoplasmic side. In addition, a single HS does not match the experimental data due to active PhoA fusions at L395, P396, and G410. This allows a clear assignment of specific loop regions and the C-terminus to the periplasmic side as shown in Figure 1. As HS I has the strongest hydrophobicity score (Cuff et al. 1998) of all the HSs, we regard this as membrane spanning and not as a segment located in the periplasm.

Application of a segment-based multiple sequence alignment (Subramanian et al. 2005) identified particularly conserved regions within the Emb proteins (data not shown). The highest conservation is present in the segment covering aa 286–410 of Mt-EmbC, which is consistent in part with the GT-C motif of glycosyltransferases (Liu and Mushegian 2003). The clear assignment of HSs and their orientation enables a further delineation of the structure–function aspects of the Emb proteins. Within HSs IV, the fully conserved motif WMRLP (343–347 aa in Mt-EmbC) is present. It is known that proline residues in membrane spanning helices introduce kink angles of about 208 which may position functionally important residues in the three-dimensional structure (Grigorieff et al. 1996). For example, Pro50 in helix B in bacteriorhodopsin positions an unpaired carbonyl oxygen of Thr46 which forms part of the channel (Deisenhofer and Michel 1989). Therefore, it is very likely that this part of Emb is of functional importance. A further indication is the fact that the adjacent HSs V and VI are short or represent loop regions that dip into the membrane. As the three-dimensional structures of membrane proteins, such as that of either aquaporin or the glutamate transporter, illustrate (Yernool et al. 2004), there are regions which do not simply form transmembrane spanning HSs but which span only a portion of the membrane which are mechanistically of great significance. Thus, the charged residues in the motif NGLRPE between HSs V and VI (394–399 aa in Mt-EmbC) could be involved in translocation of a substrate related to EMB function. We recently identified AftA as a new mycobacterial arabinosyltransferase, which like the Emb proteins incorporates single Araf residue onto the galactan domain (Alderwick, Seidel et al. 2006). The introduction of these Ara*f* residues by Emb and AftA activity is fully

dependent on the donor decaprenol phosphoarabinose (DPA). Although some similarities between AftA and the Emb proteins exist (Alderwick, Seidel et al. 2006), our sequence and topology comparison did not reveal a region obvious for translocation of the assumed DPA precursor but could, for instance, be related to the accepting glycosyl unit(s).

In terms of catalytic mechanism, the details of arabinofuranosyl transfer to the accepting polymer remain to be defined. There is a lack of experimental data regarding the mechanism of glycosyl transfer within the GT-C super family of glycosyltransferases, probably due to the fact that these are large membrane proteins and that their function within Corynebacterianeae is only now becoming clearer. A conserved element of these proteins is a modified DXD motif (Liu and Mushegian 2003), which is DDG in the Emb proteins (Figure 2B), which we are now able to locate between the third and fourth HS. Within this motif, the first Asp residue, D297, is clearly the most important residue for a fully functional Emb protein, with the second Asp, D298, having a less pronounced effect on arabinose deposition and linkage establishment of AG. In a study with a eukaryotic mannosyltransferase of *Trypanosoma brucei*, both Asp residues of the DXD motif have been demonstrated to be of comparable importance for glycosyltransferase activity (Maeda et al. 2001). As both Asp residues are adjacent in the Emb proteins, one might expect the functional group of these residues to face in opposite directions; therefore, the notion of these acidic residues being involved in sugar–phosphate coordination via a divalent metal ion requires further clarification (Liu and Mushegian 2003).

Mutagenic analysis of the amino acids, in the proposed proline motif of Cg-*emb* (Figure 2B) (Berg et al. 2005), resulted in indistinct phenotypes. The mutation of W659L caused an overall decrease in CMAMEs and arabinose but resulted in a cell wall retaining all AG-specific glycosyl linkages. The same phenotype could be observed for P667L and Q674E, but with differing levels of glycosidic linkages, but again with the retention of a wild type glycosidic linkage profile. The triple W659L–P667A–Q674E mutation, however, did result in a marked reduction in arabinose and CMAMEs, with a concomitant increase in cell wall associated TMCM. This suggests that the residues of this periplasmic loop region are clearly implicated in the coordination of polysaccharide chain length formation or regulation, respectively, rather than the maturation of the terminal Ara6 motif (Morona et al. 1995; Becker and Pühler 1998; Daniels and Morona 1999; Oriol et al. 2002; Berg et al.2005). The fact that the glycosyl linkage types of all mutants are largely retained could indicate that Cg-Emb and possibly also the other Emb proteins are mostly involved in establishing a linear Ara chain as that in mature AG attached to the single Ara residue introduced by AftA. It has not

gone unnoticed that the occurrence of several other arabinofuranosyltransferases could exist which work in concert with the Emb protein in the biosynthesis of AG. Clearly, the mode of arabinan decoration requires further investigation, because it cannot be expected that a single arabinofuranosyltransferase (Cg-Emb) would be responsible for such a plethora of arabinofuranosyl glycosidic linkages, including the *C. glutamicum* specific 2,5-Araf linkages.

The identification of new cell wall biosynthetic drug targets is of great importance, especially with the emergence of multidrug-resistant tuberculosis. As a result, a clearer understanding of the Emb-related DPA-dependent arabinofuranosyltransferase structure and function is of paramount importance for the further exploitation of potential drug targets to disrupt the essential mAGP complex in mycobacterial
species such as *M. tuberculosis*.

References

Alderwick LJ, Dover L, Seidel M, Gande R, Sahm H, Eggeling L, Besra GS. 2006. Arabinan deficient mutants of Corynebacterium glutamicum and the consequent flux in decaprenylmonophosphoryl-D-arabinose metabolism. Glycobiology. 16:1073–1081.

Alderwick LJ, Radmacher E, Seidel M, Gande R, Hitchen PG, Morris HR, Dell A, Sahm H, Eggeling L, Besra GS. 2005. Deletion of Cg-emb in Corynebacterianeae leads to a novel truncated cell wall arabinogalactan, whereas inactivation of Cg-ubiA results in an arabinan-deficient mutant with a cell wall galactan core. J Biol Chem. 280:32362–32371.

Alderwick LJ, Seidel M, Sahm H, Besra GS, Eggeling L. 2006. Identification of a novel arabinofuranosyltransferase (AftA) involved in cell wall arabinan biosynthesis in Mycobacterium tuberculosis. J Biol Chem. 281: 15653–15661.

Alexeyev MF, Winkler HH. 1999. Membrane topology of the Rickettsia prowazekii ATP/ADP translocase revealed by novel dual pho-lac reporters. J Mol Biol. 285:1503–1513.

Becker A, Pühler A. 1998. Specific amino acid substitutions in the praline rich motif of the Rhizobium meliloti ExoP protein result in enhanced production of low-molecular-weight succinoglycan at the expense of high-molecular-weight succinoglycan. J Bacteriol. 180:395–399.

Berg S, Starbuck J, Torrelles JB, Vissa V, Crick DC, Chatterjee D, Brennan PJ. 2005. Roles of conserved proline and Glycosyltransferase motifs of EmbC in biosynthesis of lipoarabinomannan. J Biol Chem. 280: 5651–5663.

Besra GS, Khoo KH, McNeil MR, Dell A, Morris HR, Brennan PJ. 1995. A new interpretation of the structure of the mycolyl-arabinogalactan complex of Mycobacterium tuberculosis as revealed through characterization of oligoglycosylalditol fragments by fast-atom bombardment mass spectrometry and 1H nuclear magnetic resonance spectroscopy. Biochemistry. 34:4257–4266.

Bloom BR, Murray CJ. 1992. Tuberculosis: commentary on a reemergent killer. Science. 257:1055–1064.

Brickman E, Beckwith J. 1975. Analysis of the regulation of Escherichia coli alkaline phosphatase synthesis using deletions and phi80 transducing phages. J Mol Biol. 96:307–316.

Calamia J, Manoil C. 1990. Lac permease of Escherichia coli: topology and sequence elements promoting membrane insertion. Proc Natl Acad Sci USA. 87:4937–4941.

Chatterjee D, Hunter SW, McNeil M, Brennan PJ. 1992. Lipoarabinomannan. Multiglycosylated form of the mycobacterial mannosylphosphatidylinositols. J Biol Chem. 267:6228–33.

Cserzö M, Wallin E, Simon I, von Heijne G, Elofsson A. 1997. Prediction of transmembrane alpha-helices in prokaryotic membrane proteins: the dense alignment surface method. Protein Eng. 10:673–676.

Cuff JA, Clamp ME, Siddiqui AS, Finlay M, Barton GJ. 1998. JPred: a consensus secondary structure prediction server. Bioinformatics. 14: 892–893.

Daffe M, Brennan PJ, McNeil M. 1990. Predominant structural features of the cell wall arabinogalactan of Mycobacterium tuberculosis as revealed through characterization of oligoglycosyl alditol fragments by gas chromatography/ mass spectrometry and by 1H and 13C NMR analyses. J Biol Chem. 265:6734–6743.

Daniels C, Morona R. 1999. Analysis of Shigella flexneri wzz (Rol) function by mutagenesis and cross-linking: wzz is able to oligomerize. Mol Microbiol. 34:181–194.

Deisenhofer J, Michel H. 1989. Nobel lecture. The photosynthetic reaction centre from the purple bacterium Rhodopseudomonas viridis. EMBO J. 8: 2149–2170.

Eggeling L, Bott M. 2005. Handbook of Corynebacterium glutamicum. Boca Raton (FL): CRC Press, Taylor Francis Group. Escuyer VE, Lety MA, Torrelles JB, Khoo KH, Tang J, Rithner CD, Frehel C, McNei MR, Brennan PJ, Chatterjee D. 2001. The role of the embA and embB gene products in the biosynthesis of the terminal hexaarabinofuranosyl motif of Mycobacterium smegmatis arabinogalactan. J Biol Chem. 276:48854–48862.

Gande R, Gibson KJ, Brown AK, Krumbach K, Dover LG, Sahm H, Shioyama S, Oikawa T, Besra GS, Eggeling L. 2004. Acyl-CoA carboxylases (accD2 and accD3), together with a unique polyketide synthase (Cg-pks), are key to mycolic acid biosynthesis in Corynebacterianeae such as Corynebacterium glutamicum and Mycobacterium tuberculosis. J Biol Chem. 279:44847–44857.

Gibson KJ, Eggeling L, Maughan WN, Krumbach K, Gurcha SS, Nigou J, Puzo G, Sahm H, Besra GS. 2003. Disruption of Cg-Ppm1, a polyprenyl monophosphomannose synthase, and the generation of lipoglycan-less mutants in Corynebacterium glutamicum. J Biol Chem. 278: 40842–40850.

Grigorieff N, Ceska TA, Downing KH, Baldwin JM, Henderson R. 1996. Electron-crystallographic refinement of the structure of bacteriorhodopsin. J Mol Biol. 259:393–421.

Henikoff S. 1984. Unidirectional digestion with exonuclease III creates targeted breakpoints for DNA sequencing. Gene. 28:351–359.

Kalinowski J, Bathe B, Bartels D, Bischoff N, Bott M, Burkovski A, Dusch N, Eggeling L, Eikmanns BJ, Gaigalat L, et al. 2003. The complete Corynebacterium glutamicum ATCC 13032 genome sequence and its impact on the production of L-aspartate-derived amino acids and vitamins. J Biotechnol. 104:5–25.

Kremer L, Dover LG, Morehouse C, Hitchin P, Everett M, Morris HR, Dell A, Brennan PJ, McNeil MR, Flaherty C, et al. 2001. Galactan biosynthesis in Mycobacterium tuberculosis. Identification of a bifunctional UDP-galactofuranosyltransferase. J Biol Chem. 276:26430–26440.

Landt O, Grunert HP, Hahn U. 1990. A general method for rapid site-directed mutagenesis using the polymerase chain reaction. Gene. 96:125–128.

Liu J, Mushegian A. 2003. Three monophyletic superfamilies account for the majority of the known glycosyltransferases. Protein Sci. 12:1418–1431.

Maeda Y, Watanabe R, Harris CL, Hong Y, Ohishi K, Kinoshita K, Kinoshita T. 2001. PIG-M transfers the first mannose to glycosylphosphatidylinositol on the lumenal side of the ER. EMBO J. 20:250–261.

McNeil M, Daffe M, Brennan PJ. 1990. Evidence for the nature of the link between the arabinogalactan and peptidoglycan of mycobacterial cell walls. J Biol Chem. 265:18200–18206.

McNeil M, Daffe M, Brennan P. 1991. Location of the mycolyl ester substituents in the cell walls of mycobacteria. J Biol Chem. 266:13217–13223.

Mikusova K, Yagi T, Stern R, McNeil MR, Besra GS, Crick DC, Brennan PJ. 2000. Biosynthesis of the galactan component of the mycobacterial cell wall. J Biol Chem. 275:33890–33897.

Miller JH. 1992. A Short Course in Bacterial Genetics. Cold Spring Harbor (NY): Cold Spring Harbor Laboratory.

Mills JA, Motichka K, Jucker M, Wu HP, Uhlik BC, Stern RJ, Scherman MS, Vissa VD, Pan F, Kundu M et al. 2004. Inactivation of the mycobacterial rhamnosyltransferase, which is needed for the formation of the arabinogalactan-peptidoglycan linker, leads to irreversible loss of viability. J Biol Chem. 279:43540–43546.

Morona R, van den Bosch L, Manning PA. 1995. Molecular, genetic, and topological characterization of O-antigen chain length regulation in Shigella flexneri. J Bacteriol. 177:1059–1068.

Nakamura Y, Nishio Y, Ikeo K, Gojobori T. 2003. The genome stability in Corynebacterium species due to lack of the recombinational repair system. Gene. 317:149–155.

Oriol R, Martinez-Duncker I, Chantret I, Mollicone R, Codogno P. 2002. Common origin and evolution of glycosyltransferases using Dol-P-monosaccharides as donor substrate. Mol Biol Evol. 19:1451–1463.

Pan F, Jackson M, Ma Y, McNeil M. 2001. Cell wall core galactofuran synthesis is essential for growth of mycobacteria. J Bacteriol. 183: 3991–3998.

Pohlschröder M, Hartmann E, Hand NJ, Dilks K, Haddad A. 2005. Diversity and evolution of protein translocation. Annu Rev Microbiol. 59:91–111.

Portevin D, De Sousa-D'Auria C, Houssin C, Grimaldi C, Chami M, Daffe M, Guilhot C. 2004. A polyketide synthase catalyzes the last condensation step of mycolic acid biosynthesis in mycobacteria and related organisms. Proc Natl Acad Sci USA. 101:314–319.

Radmacher E, Stansen KC, Besra GS, Alderwick LJ, Maughan WN, Hollweg G, Sahm H, Wendisch VF, Eggeling L. 2005. Ethambutol, a cell wall inhibitor of Mycobacterium tuberculosis, elicits L-glutamate efflux of Corynebacterium glutamicum. Microbiology. 151:1359–1368.

Ramaswamy SV, Amin AG, Goksel S, Stager CE, Dou SJ, El Sahly H, Moghazeh SL, Kreiswirth BN, Musser JM. 2000. Molecular genetic analysis of nucleotide polymorphisms associated with ethambutol resistance in human isolates of Mycobacterium tuberculosis. Antimicrob Agents Chemother. 44:326–336.

Shi L, Berg S, Lee A, Spencer JS, Zhang J, Vissa V, McNeil MR, Khoo KH, Chatterjee D. 2006. The carboxy terminus of EmbC from Mycobacterium smegmatis mediates chain length extension of the arabinan in lipoarabinomannan. J Biol Chem. 281:19512–19526.

Subramanian AR, Weyer-Menkhoff J, Kaufmann M, Morgenstern B. 2005. DIALIGN-T: an improved algorithm for segment-based multiple sequence alignment BMC. Bioinformatics. 6:66.

Takayama K, Kilburn JO. 1989. Inhibition of synthesis of arabinogalactan by ethambutol in Mycobacterium smegmatis. Antimicrob Agents Chemother. 33:1493–1499.

Telenti A, Philipp WJ, Sreevatsan S, Bernasconi C, Stockbauer KE, Wieles B, Musser JM, Jacobs WR Jr. 1997. The emb operon, a gene cluster of Mycobacterium tuberculosis involved in resistance to ethambutol. Nat Med. 3:567–570.

Vilcheze C, Morbidoni HR, Weisbrod TR, Iwamoto H Kuo M, Sacchettini JC, Jacobs WR Jr. 2000. Inactivation of the inhA-encoded fatty acid synthase II (FASII) enoyl-acyl carrier protein reductase induces accumulation of the FASI end products and cell lysis of Mycobacterium smegmatis. J Bacteriol. 182:4059–4067.

Yernool D, Boudker O, Jin Y, Gouaux E. 2004. Structure of a glutamate transporter homologue from Pyrococcus horikoshii. Nature. 431: 811–818.

Zhang N, Torrelles JB, McNeil MR, Escuyer VE, Khoo KH, Brennan PJ, Chatterjee D. 2003. The Emb proteins of mycobacteria direct arabinosylation of lipoarabinomannan and arabinogalactan via an N-terminal recognition region and a C-terminal synthetic region. Mol Microbiol. 50: 69–76.

Supplementary data

Supplementary data are available at Gycobiology online (http://glycob.oxfordjournals.org/).

Acknowledgments

L.J.A. and M.S. contributed equally to this work. L.J.A. is a Biotechnology and Biological Sciences Research Council Quota Student. G.S.B. acknowledges support in the form of a Personal Research chair from Mr James Bardrick and as a former Lister Institute-Jenner Research Fellow, the Medical Research Council (UK). H.S. acknowledges the support from the Fonds der Chemischen Industrie. We thank Graham Burns and Karin Krumbach for technical assistance.

Abbreviations

AG, arabinogalactan; Ara, arabinose; BHI, brain–heart infusion; CMAME, corynomycolic acid methyl ester; DPA, decaprenol phosphoarabinose; EMB, ethambutol; Gal, galactose; GC, gas chromatography; GT-C, glycosyltransferase-C; HS, hydrophobic segment; LAM, lipoarabinomannan; LB, Luria-Bertani; mAGP, mycolyl-arabinogalactan–peptidoglycan; MS, mass spectrometry; OD, optical density; PCR, polymerase chain reaction; Rha, rhamnose; SDS, sodium dodecyl sulfate; TFA, trifluoroacetic acid; TLC, thin layer chromatography; TMCM, trehalose monocorynomycolates

4 Identification of a novel arabinofuranosyltransferase AftB involved in a terminal step of cell wall arabinan biosynthesis in C*orynebacterianeae*, such as *Corynebacterium glutamicum* and *Mycobacterium tuberculosis*

Accepted in *The Journal of Biological Chemistry Papers in press*; on 26 March 2007 as Manuscript M700271200

by **Mathias Seidel**[1#], Luke J. Alderwick[2#], Helen L. Birch[2], Hermann Sahm[1], Lothar Eggeling[1] and Gurdyal S. Besra[2]

From the [1]Institute for Biotechnology 1, Research Centre Juelich, D-52425 Juelich, Germany, and [2]School of Biosciences, University of Birmingham, Edgbaston, Birmingham, B15 2TT

Summary

Arabinofuranosyltransferase enzymes, such as EmbA, EmbB and AftA play pivotal roles in the biosynthesis of arabinogalactan, and the antituberculosis agent ethambutol (EMB) targets arabinogalactan biosynthesis through inhibition of Mt-EmbA and Mt-EmbB. Herein, we describe the identification and characterization of a novel arabinofuranosyltransferase, now termed AftB (Rv3805c). Deletion of itsorthologue NCgl2780 in the closely related species *Corynebacterium glutamicum* resulted in a viable mutant. Analysis of the cell wall associated lipids from the deletion mutant revealed a decreased abundance of cell wall bound mycolic acids, consistent with a partial loss of mycolylation sites. Subsequent glycosyl linkage analysis of arabinogalactan also revealed the complete absence of terminal β(1→2) linked arabinofuranosyl residues. The deletion-mutant's biochemical phenotype was fully complemented by either Mt-AftB or Cg-AftB, but not with muteins of Mt-AftB, where the two adjacent aspartic acid residues, which have been suggested to be involved in glycosyltransferase activity, were replaced by alanine. In addition, the use of *C. glutamicum* and *C. glutamicum*Δ*aftB* in an *in vitro* assay utilizing the sugar donor β-D-arabinofuranosyl-1-monophosphoryldecaprenol (DPA) together with the neoglycolipid acceptor α-D-Ara*f*-(1→5)-α-D-Ara*f*-*O*-C_8 as a substrate, confirmed AftB as a terminal β(1→2) arabinofuranosyltransferase, which was also insensitive to EMB. Altogether, these studies have shed further light on the complexities of *Corynebacterianeae* cell wall biosynthesis and Mt-AftB represents a potential new drug target.

Introduction

Mycobacterial diseases, such as tuberculosis and leprosy, still represent a severe public health problem (1). For instance, the recent emergence of multidrug resistant tuberculosis (MDR-TB)1 strains, and more recently, extensively drug-resistant tuberculosis (XDR-TB) clinical isolates (2,3), has prompted the need for new drugs, and drug targets. The causative agent of these diseases, *Mycobacterium tuberculosis* and *Mycobacterium leprae*, respectively, are characterized by an intricate cell envelope (4-6). This characteristic mycobacterial cell envelope is composed of four macromolecules, lipoarabinomannan (LAM), mycolic acids, arabinogalactan (AG) and peptidoglycan (4-7). The galactan domain of AG is linked to peptidoglycan *via* a specialized "linker unit", L-Rha*p*-(1→4)-α-D-GlcNAc, and its distal arabinan domain to mycolic acids, forming the mycolylarabinogalactan-peptidoglycan (mAGP) complex (4-6). The arabinan domain contains α(1→), α(1→3) and β(1→2) arabinofuranosyl (Ara*f*) linkages, arranged in several distinct structural motifs (5,8,9). The non-reducing arabinan termini of AG consists of *t*-Ara*f*, 2-Ara*f*, 5-Ara*f*, and 3,5-Ara*f* residues arranged into a characteristic terminal Ara6 motif, with the 5-OH of the *t*-Ara*f* and 2-Ara*f* residues representing sites of mycolylation (6). The packing and ordering of mycolic acids within the mAGP and additional lipids within the outer envelope results in a highly impermeable barrier (10). It is interesting to note that several front-line antitubercular drugs, such as ethambutol (EMB) (11-13) and isoniazid (INH) (14,15), target aspects of the biosynthesis of the mAGP complex.

Corynebacterium glutamicum has proven useful in the study of orthologous *M. tuberculosis* genes essential for viability (16,17). This bacterium together with *Corynebacterium diphtheriae*, *Corynebacterium jeikeium*, as well as, *M.tuberculosis* and *M. leprae*, and a number of other closely related species form the well-defined taxon *Corynebacterianeae*. The bacteria within this taxon share many characteristic cell wall features, such as AG and mycolic acids. In addition, the use of *C. glutamicum* together with its low number of paralogous genes (18), has proven useful in the study of the mAGP complex within this peculiar group of organisms (9). For instance, we recently identified a novel mycobacterial arabinofuranosyltransferase AftA using *C.glutamicum* due to the fact that it is largely tolerable with respect to the deletion of Cg-*emb* (9) and Cg-*aftA* (19), which are otherwise essential in *M. tuberculosis*[2].

The structural basis of AG is now well defined (4,5,8), conversely, aspects of its biogenesis remained poorly resolved. The biosynthesis of AG involves the formation of a linear galactan chain with alternating β(1→5) and β(1→6)-D-galactofuranosyl (Gal*f*) residues

of approximately 30 residues in length from the specialized 'linker unit', L-Rha*p*-(1→4)-α-D-GlcNAc (20,21). MALDI-TOF MS analyzes of per-*O*-methylated AG of *C. glutamicum* deleted of its single arabinofuranosyltransferase, Cg-*emb*, revealed that the 8th, 10th and 12th Gal*f* residue possessed singular Ara*f* residues (9). These specific Ara*f* residues, were recently shown to be transferred by a specialized arabinofuranosyltransferase AftA, whose gene in all *Corynebacterianeae* analyzed to date is adjacent to the *emb* cluster (19). These initial Ara*f* residues "prime" the galactan backbone for further attachment of α(1→5) linked Ara*f* residues. These reactions require the arabinofuranosyltransferase activities of Mt-EmbA and Mt-EmbB, or Cg-Emb, respectively, which are also targets of EMB (9,13,22), to eventually result in mature AG. The Emb and AftA proteins utilize the specialized sugar donor, β-Darabinofuranosyl-1-monophosphoryldecaprenol (DPA) (23-25), and is a characteristic feature found only in *Corynebacterianeae* (26-28). In addition, these proteins also belong to the GT-C superfamily of integral membrane glycosyltransferases (29). A recent topological analysis of Cg-Emb (30), which together with a mutational study of Mt-EmbC (31), revealed for the first time a clear domain organization of these proteins, with the Glycosyltransferase DDX signature evident in the extracellular loop which connects helixes III-IV, and the chain elongation "Pro-motif", in the extracellular loop connecting helixes XIIIXIV (31).

It is interesting to note that the arabinan domain of AG utilizes several different Ara*f* linkages, which suggests that additional arabinofuranosyltransferases must be required to form a fully matured AG. Moreover, initial Ara*f* residues at branching sites could require specialized arabinofuranosyltransferases as already observed for AftA (19), and it has to be considered that even further specialized arabinofuranosyltransferases might exist to incorporate Ara*f* into LAM. Clearly additional arabinofuranosyltransferases still remain to be identified in *Corynebacterianeae*. Indeed, Liu and Musheginan (29) identified fifteen members of the GT-C superfamily, representing candidates involved in the biosynthesis of cell wall related glycans and lipoglycans in *M. tuberculosis*. We have continued our earlier studies (9,16,19) to identify genes required for the biosynthesis of the core structural elements of the mAGP complex in *Corynebacterianeae* by studying mutants of *C. glutamicum* and the orthologous genes and enzymes of *M. tuberculosis*. Herein, we present Rv3805c as a new arabinofuranosyltransferase of the GT-C superfamily which is responsible for the transfer of Ara*f* residues from DPA to the arabinan domain to form terminal β(1→2) linked Ara*f* residues, which marks the "end-point" for AG arabinan biosynthesis before decoration with mycolic acids.

Experimental Procedures

Strains and culture conditions – M. tuberculosis H37Rv DNA was obtained from the Tuberculosis Research Material Contract (NIH) at Colorado State University. *C. glutamicum* ATCC 13032 (the wild type strain, and referred for the remainder of the text as *C. glutamicum*) and *Escherichia coli* DH5α were grown in Luria-Bertani broth (LB, Difco) at 30 °C and 37 °C, respectively. The mutants generated in this study were grown on complex Brain Heart Infusion (BHI) medium (32). Kanamycin and ampicillin were used at a concentration of 50 µg/ml. Samples for lipid analyzes were prepared by harvesting cells at an OD of 10-15, followed by a saline wash and freeze drying.

Construction of plasmids and strains – The vectors made were, pMSX-Cg-*aftB* (NCgl2780), pMSX-Mt-*aftB* (Rv3805c), and pK19mobsacBΔ*aftB*, with the gene number of the *M. tuberculosis* and *C. glutamicum aftB* orthologue added in parentheses.

To express *M. tuberculosis aftB* in *C. glutamicum* the primer pair GTATGAGCATATGGTCCGGGTCAGCTTGTGG (all primers in 5' - 3'direction) ATTGCCCCTCACTCGAGCTCCCGCGGTGGC GGG was used with the restriction sites NdeI and XhoI underlined, using *M. tuberculosis* H37Rv chromosomal DNA as a template. The purified PCR fragment was ligated with accordingly digested pMSX to give pMSX-Mt-*aftB*. pMSX was preparedfrom pEKEx2 (33) to generate a derivative providing an appropriate ribosome binding site together with a carboxy-terminal Histag. It was created by the individual cleavage of pEKEx2 with NdeI and XhoI, each followed by Klenow treatment and religation. The intermediate construct was SalI/DraI cleaved, treated with MungBeanNuclease and ligated with the XbaI/MroI fragment from pET22b (Novagen), which before use was treated with the Klenow fragment to eventually yield pMSX.

To overexpress Cg-*aftB*, the primer pair ATGTGGCCATATGACGTTTAGCCCCCA GCGTC and TGTTTACTCGAGCTGAGAGCTATATAAAGGTTCTCCGC was used to amplify *C. glutamicum aftB*, which was ligated with NdeI and XhoI cleaved pMSX to generate pMSX-Cg-*aftB*.

To construct the deletion vector pK19mobsacBΔ*aftB* cross-over PCR was applied with primer pairs AB (A: ACGCCAAGCTTTGCTAGTCGCTGCGTTTGGTTC; B: CCCATCCACTAAACACTGGG GGCTAAACGTCATGAG) and CD (C: TGTTTAAGTTTAGTGGATGGGGAACCTCG CGGAGAACCTTTATATA; D: GCCAGTGAATTCGGCGCGCAGCGTTGGTATC) and *C. glutamicum* genomic DNA as template. Both amplified products were used in a second PCR with primer pairs AD to generate a fragment consisting of sequences adjacent to Cg-*aftB*, which was blunt end ligated

with SmaI cleaved pK19mobsacB. All plasmids were confirmed by sequencing. The chromosomal deletion of Cg-*aftB* was performed as described previously using two rounds of positive selection (34), and its successful deletion verified by use of different primer pairs. Plasmid pMSX-Mt-*aftB* and pMSX-Cg-*aftB* were introduced into *C. glutamicum*Δ*aftB* by electroporation with selection to kanamycin resistance (25 µg/ml).

Site-specific mutations were introduced in Mt-*aftB* using appropriate mutagenic primers and pMSX-Mt-*aftB* as the doublestranded template (Quikchange-Kit, Stratagene). Following linear amplification of the newly synthesized strands and DpnI digestion of parental strands, plasmids pMSX-Mt-*aftB*-D29A and pMSX-Mt-*aftB*-D30A were generated, carrying the mutations as indicated. All plasmids were verified by sequencing.

Protein analysis - Recombinant *C. glutamicum* strains deleted of the chromosomal Cg-*aftB* copy, but carrying either pMSX, pMSX-Mt-*aftB*, pMSX-Mt*aftB*-D29A or pMSX-Mt-*aftB*-D30A were each grown in LB up to an OD of 4. Cells were harvested by centrifugation, washed and resuspended in 30 ml of 50 mM TrisHCl pH 7.4 buffer, containing 200 mM NaCl and 50 mM imidazole, and disrupted by probe sonication. Centrifugation at 27,000 x *g* resulted in a clear supernatant, which was applied to a 1 ml HiTrap™ Chelating HP column (GE Healthcare) using an ÅKTA chromatography system. The column was initially washed with 10 ml of the aforementioned buffer, and bound proteins subsequently eluted with 2 ml of the same buffer but containing 500 mM imidazole. Eluted proteins were precipitated, dried, and resuspended in 10 µl loading buffer and SDS-PAGE carried out on a 10% polyacrylamide gel, which was subsequently stained using 0.05% coomassie-G250 in 10% acetic acid and 25% isopropanol. Bands of interest were excised and subjected to in-gel digestion with trypsin before peptide mass fingerprinting. Peptides were extracted by sequential addition of water (12 µl) and 0.1% (v/v) trifluoroacetic acid (TFA) in 30% (v/v) acetonitrile (10 µl), and analyzed manually using an Applied Biosystems Voyager STR MALDI-TOF mass spectrometer (Weiterstadt, Germany).

Extraction and analysis of cell wall associated and cell wall bound lipids – Cells (100 mg) were extracted by two consecutive extractions using 2 ml of $CHCl_3/CH_3OH/H_2O$ (10:10:3, v/v/v) for 3 h at 50 °C and the resulting de-lipidated cells stored for further use (as described below). Organic extracts were combined with 1.75 ml $CHCl_3$ and 0.75 ml H_2O, mixed and centrifuged. The lower organic phase was recovered, washed twice with 2 ml of $CHCl_3/CH_3OH/H_2O$ (3:47:48, v/v/v), dried and resuspended in 200 µl of $CHCl_3/CH_3OH/H_2O$ (10:10:3, v/v/v). An aliquot (20 µl) was analyzed by thin layer chromatography (TLC) using silica gel plates (5735 silica gel $60F_{254}$, Merck) developed in $CHCl_3/CH_3OH/H_2O$ (60:16:2,

v/v/v). TLCs were visualized by charring with 5% molybdophosphoric acid in ethanol at 100 °C to reveal cell wall associated lipids.

The bound corynomycolic acids from delipidated extracts or purified cell walls (see below) were released by the addition of a 5% aqueous solution of tetra-butyl ammonium hydroxide (TBAH), followed by overnight incubation at 100 °C, and methylated as described previously (9). Corynomycolic acid methyl esters (CMAMEs) were analysed by TLC using silica gel plates (5735 silica gel $60F_{254}$, Merck) developed in petroleum ether/acetone (95:5, v/v). TLCs were visualized by charring with 5% molybdophosphoric acid in ethanol at 100°C to reveal CMAMEs.

Alternatively, [^{14}C]labeling of cell wall associated lipids and cell wall bound corynomycolic acids was performed by growing cultures initially at 30 °C in 5 ml of BHI media supplemented with antibiotic where appropriate. Once the OD reached ~0.5, cultures were labeled with 5 µCi of [14C]-acetic acid (50-62 µCi/mmol, Amersham Radiochemicals) and further incubated for 8 h. Cells were harvested by centrifugation and the cell wall associated lipids extracted as described above. The cell wall associated [14C]-labeled lipidswere resuspended in 200 µl of $CHCl_3/CH_3OH/H_2O$ (10:10:3, v/v/v) and an aliquot (5 µl) dried in a scintillation vial and then mixed with 10 ml of EcoScintA scintillation fluid (National Diagnostics, Atlanta) and counted. Equal counts (25,000 cpm) of each sample were analyzed by TLC using silica gel plates (5735 silica gel $60F_{254}$, Merck) developed in $CHCl_3/CH_3OH/H_2O$ (60:16:2, v/v/v) and quantified using a phosphorimager following exposure to Kodak X-Omat film for 24 h. The bound [^{14}C]corynomycolic acids from the delipidated extracts were released by base treatment and methylated as described above to afford [^{14}C]CMAMEs. The[^{14}C]CMAMEs were resuspended in 100 µl of CH_2Cl_2 and an aliquot (5 µl) dried in a scintillation vial and then mixed with 10 ml of EcoScintA scintillation fluid (National Diagnostics, Atlanta) and counted to quantify cell wall bound [^{14}C]corynomycolic acids. A 5 µl aliquot of [^{14}C]CMAMES was also analyzed by TLC using silica gel plates (5735 silica gel $60F_{254}$, Merck) developed in petroleum ether/acetone (95:5, v/v). TLC autoradiograms were obtained by exposing TLCs to Kodak X-Omat film for 24 h.

Isolation of the mAGP complex – The thawed cells were resuspended in phosphate buffered saline containing 2% Triton X-100 (pH 7.2), disrupted by sonication and centrifuged at 27,000 x *g* (5,8,9). The pelleted material was extracted three times with 2% SDS in phosphate buffered saline at 95 °C for 1 h to remove associated proteins, successively washed with water, 80% (v/v) acetone in water, and acetone, and finally lyophilized to yield a highly purified cell wall preparation (5,8,9).

Glycosyl composition and linkage analysis of cell walls by alditol acetates - Cell wall preparations were hydrolyzed using 2M TFA, reduced with NaB_2H_4 and the resultant alditols per-*O*-acetylated and examined by gas chromatography (GC) (5,8,9). Cell wall preparations were per-*O*methylated using dimethyl sulfinyl carbanion (5,8,9). The per-*O*-methylated cell walls were hydrolyzed using 2M TFA, reduced with NaB_2H_4, per-*O*-acetylated and examined by gas chromatography/mass spectrometry (GC/MS) (5,8,9). Analysis of alditol acetate sugar derivatives were performed on a CE Instruments ThermoQuest Trace GC 2000. Samples were injected in the splitless mode. The column used was a DB225 (Supelco). The oven was programmed to hold at an isothermal temperature of 275 °C for a run time of 15 min (9). GC/MS was carried out on a Finnigan Polaris/GCQ PlusTM (9). The column used was a BPX5 (Supelco).

Arabinofuranosyltransferase activity with membrane preparations of C. glutamicum, C. glutamicumΔaftB, and C. glutamicumΔaftB pMSX-Mt-*aftB* - Membranes were prepared as described previously (19,24) and resuspended in 50 mM MOPS (pH 7.9), containing 5 mM β-mercaptoethanol and 10 mM MgCl2 (buffer A) to a final concentration of 15-10 mg/ml. The neoglycolipid acceptor α-DAra*f*-(1→5)-α-D-Ara*f*-*O*-C8 (24,35) (stored in C_2H_5OH) and DP[^{14}C]A (25,35) (stored in $CHCl_3/CH_3OH$, 2:1, v/v) were aliquoted into a 1.5 ml eppendorf tube to a final concentration of 2 mM and 200,000 cpm (90 µM), respectively, and dried under nitrogen. The basic arabinofuranosyltransferase assay was carried out as described previously (24) with modifications. IgePalTM (Sigma-Aldrich) was added (0.1%, v/v) with the appropriate amount of buffer A (final volume 80 µl). Tubes were sonicated for 15 min to resuspend lipid linked substrates and then mixed with the remaining assay components, which included membrane protein (1 mg) from either *C. glutamicum*, *C. glutamicumΔaftB* or *C. glutamicumΔaftB* pMSX-Mt-*aftB*, 1 mM ATP, 1 mM NADP and in some cases EMB (0-1 mg/ml). Assays were incubated for 1 h at 37 °C and quenched by the addition of 533 µl $CHCl_3/CH_3OH$ (1:1, v/v). After mixing and centrifugation at 27,000 x *g* for 15 min at 4 °C, the supernatant was removed and dried under nitrogen. The residue was then resuspended in 700 µl of CH_3CH_2OH/H_2O (1:1, v/v) and loaded onto a 1 ml SepPak strong anion exchange cartridge (Supelco),pre-equilibrated with CH_3CH_2OH/H_2O (1:1, v/v). The column was washed with 2 ml CH_3CH_2OH and the eluate collected, dried and partitioned between the two phases arising from a mixture of *n*-butanol (3 ml) and water (3 ml). The resulting organic phase was recovered following centrifugation at 3,500 x *g* and the aqueous phase again extracted twice with 3 ml of water-saturated *n*-butanol. The pooled extracts were back-washed twice with *n*-butanol-saturated water (3 ml). The *n*-butanol fraction was dried and

resuspended in 200 µl butanol. The extracted radiolabeled material was quantified by liquid scintillation counting using 10 % of the labelled material and 5 ml of EcoScintA (National Diagnostics, Atlanta). The incorporation of [^{14}C]Ara*f* was determined by subtracting counts present in control assays (incubations in the absence of acceptor). The remaining labeled material was subjected to TLC using silica gel plates (5735 silica gel 60F_{254}, Merck) developed in $CHCl_3$:CH_2OH:H_2O:NH_4OH (65:25:3.6:0.5, v/v/v/v). TLC autoradiograms were obtained by exposing TLCs to Kodak X-Omat film for 3 days.

Characterization of arabinofuranosyltransferase products A and B formed with membranes prepared from C. glutamicum and *C. glutamicumΔaftB* - Large-scale reaction mixtures containing cold DPA (200 µg, 0.75 mM) (24) and 50 mM of the acceptor α-D-Ara*f*-(1→5)-α-D-Ara*f*-*O*-C_8 were mixed and given an initial incubation at 37 °C with membranes prepared from either *C. glutamicum* (EMB also added to reaction mixtures at a concentration of 100 µg/ml) or *C. glutamicumΔaftB* for 1 h. The assays were replenished with fresh membranes (1 mg) and re-incubated for 1 h at 37 °C with the entire process repeated thrice. Products were extracted from reaction mixtures by *n*-butanol/water phase separation as described earlier to extract products. Products were applied to preparative TLC plates, developed in $CHCl_3$:CH_3OH:H_2O:NH_4OH (65:25:3.6:0.5, v/v/v/v) and sprayed with 0.01% 1,6-diphenylhexatriene in petroleum-ether:acetone (9:1, v/v), and the products localized under long-wave (366 nm) UV light (24). The plate was then redeveloped in toluene to remove the reagent and the bands recovered from the plates by extraction with *n*-butanol. The butanol phases were washed with water saturated with *n*-butanol and the dried products subjected to ^{1}H-NMR, ES-MS and GC/MS as previously described (24).

RESULTS

Genome comparison of the Rv3805c locus – We recently identified AftA as a novel arabinofuranosyltransferase present in *Corynebacterianeae* (19). Based on the fact that AftA is present in a highly conserved cell wall locus (19), we concentrated our studies to identify other cell wall related genes, and subsequently identified Rv3805c (Fig. 1*A*), which is located in close proximity to the antigen 85 complex-encoding genes *fbpA* and *fbpD* (36). Furthermore, Rv3805c is likely to form an operon together with *ubiA*, which is required for prenyl transfer to 5-phosphoribose pyrophosphate (PRPP) to form decaprenylphosphoryl-5-phosphoribose (DPPR), before conversion to DPA (27,28), and *glfT,* which is responsible for establishing the galactan backbone of AG (20,21). The apparent fundamental function of *aftB* is indicated by the fact that the genome organization of this particular region is syntenic in

Corynebacterianeae, including all *Mycobacterium* and *Corynebacterium* species analyzed to date (see Fig. 1*A*), and also in *Norcardia farcinica* IFM 10152 and *Rhodococcus* sp. RHA1.

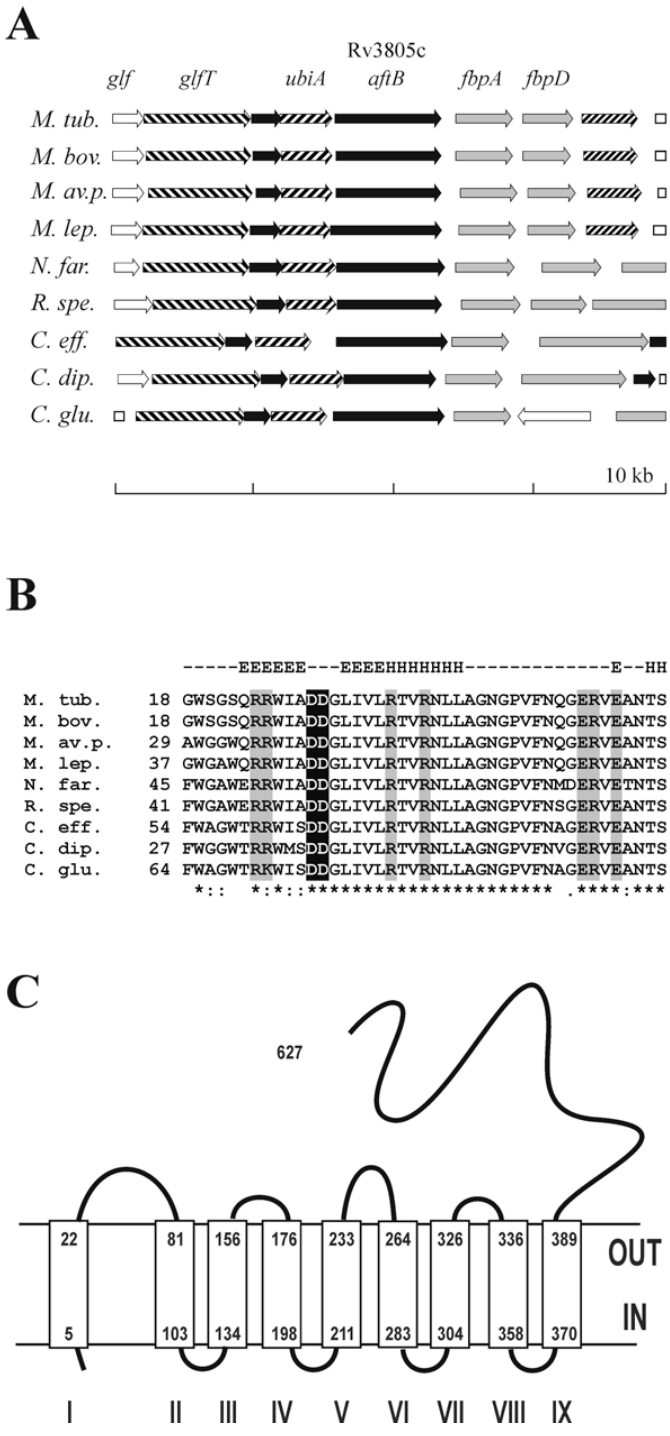

Fig. 1. Comparison of the *aftB* locus within *Corynebacterianeae*. *A*, the locus consists in *M. tuberculosis* (*M. tub.*) of *aftB* with the upstream located *ubiA* gene product catalyzing prenylation of 5-phosphoribose pyrophosphate (PRPP) (26,27), and the known galactofuranosyltransferase *glfT* (20,21) and UDP-Gal*p* mutase enzyme *glf* (45). Downstream of *aftB* the genes *fbpA*, and *fbpD* are located which encode mycolyltransferases for decoration of the terminal arabinose residues with mycolic acids (6,36). The organization of these genes is largely retained in a number of *Corynebacterianeae* indicative for a basic functional unit. In *N. farcinica* (*N. far.*), a third paraloguous mycolyltransferase is present, and in *C. glutamicum* (*C. glu.*) a transposon is inserted between the two mycolyltransferases. Orthologuous genes are shaded accordingly. The *M. tuberculosis* region

derived from NC_000962 extends from nucleotide 4,262,896 to 4,272,896. Abbreviations: *M. bovis* (*M. bov.*), *M. avium paratuberculosis* (*M. av. p.*), *M. leprae* (*M. lep.*), *Rhodococcus* sp. RHA1 (*R. spe.*), *C. efficiens* (*C. eff.*), and *C. diphtheriae* (*C. dip.*). *B*, Partial sequence comparison of the first loop region of AftB. The conserved charged residues possibly involved in Glycosyltransferase activity are shaded in grey, and the adjacent aspartate residues possibly directly involved in glycosyl transfer are in white on black background (29). On top are the predicted structural properties of the peptide with E indicating β-sheet, and H α-helix structure. The abbreviations are as above. *C*, Topology of Mt-AftB based on dense alignment surface (DAS) analysis (46). The membrane spanning helixes are given in Roman numbers, and their amino acyl residues in Arabic.

The gene product of Rv3805c, termed AftB, is predicted to form nine transmembrane (TM) spanning helixes, in its amino-terminal part, whereas a 237 amino acid carboxy-terminal part is directed towards the periplasm (see Fig. 1*C*). Interestingly, AftB shows no obvious sequence similarity to the previously identified arabinofuranosyltransferases, such as Emb (9) and AftA (19), although the topology, with the C-terminus directed towards the periplasmic side, is to some degree comparable.

However, the similarity of the AftB proteins amongst each other is very high, even for the most distant pairs, *M. tuberculosis* and *C. diphtheriae*, exhibiting 33% identity over the entire length of the proteins. Even stronger conservation is found in the first periplasmic loop region (Fig. 1*B*), exhibiting a modified motif of the GT-C superfamily of glycosyltransferases consisting of two adjacent aspartic acid residues (29). Also, the periplasmic loop regions following helix V and VII are strongly conserved, which may play a role in presenting the nascent arabinose domain to the catalytic glycosyltransferase site. Taken together, the features of AftB and the locus where the gene is localized suggests that it represents a glycosyltransferase involved in AG biosynthesis.

Construction and growth of C. glutamicumΔaftB - In an attempt to delete *aftB* in *C. glutamicum* the non-replicative plasmid pK19mobsacBΔ*aftB* was constructed carrying sequences adjacent to Cg-*aftB*. The vector was introduced into *C. glutamicum* and in several electroporation assays kanamycin resistant clones were obtained, indicating integration of pK19mobsacBΔ*aftB* into the genome by homologous recombination (Fig. 2*A*). The *sacB* gene enables for positive selection of a second homologous recombination event, which can result either in the original wild-type genomic organization or in clones deleted of *aftB* (34). Forty-eight clones exhibiting the desired phenotype of vector-loss (KanS, SucR) were analyzed by PCR and twentyone of them were found to have Cg-*aftB* excised. These numbers indicate that the loss of Cg-*aftB* is apparently not a serious disadvantage for viability, in contrast with Cg-*aftA*, where deletion was rather difficult to obtain (19). As a result, one clone was subsequently termed *C. glutamicumΔaftB* and confirmed by PCR to have Cg-*aftB* deleted,

whereas controls with *C. glutamicum* wild type and genes adjacent to Cg-*aftB* resulted in the expected amplification products (Fig. 2*A*).

Growth of wild type *C. glutamicum* and *C. glutamicum*Δ*aftB* were compared in BHI medium as well as salt medium CGXII (32). Both strains exhibited comparable growth rates and the final cell densities reached were comparable (data not shown). Single colonies of the deletion mutant appeared less glossy. In streak-outs on BHI plates the surface of the deletion mutant appeared rough with a coarsely granular surface, as compared to wild type *C. glutamicum* (Fig. 2B).

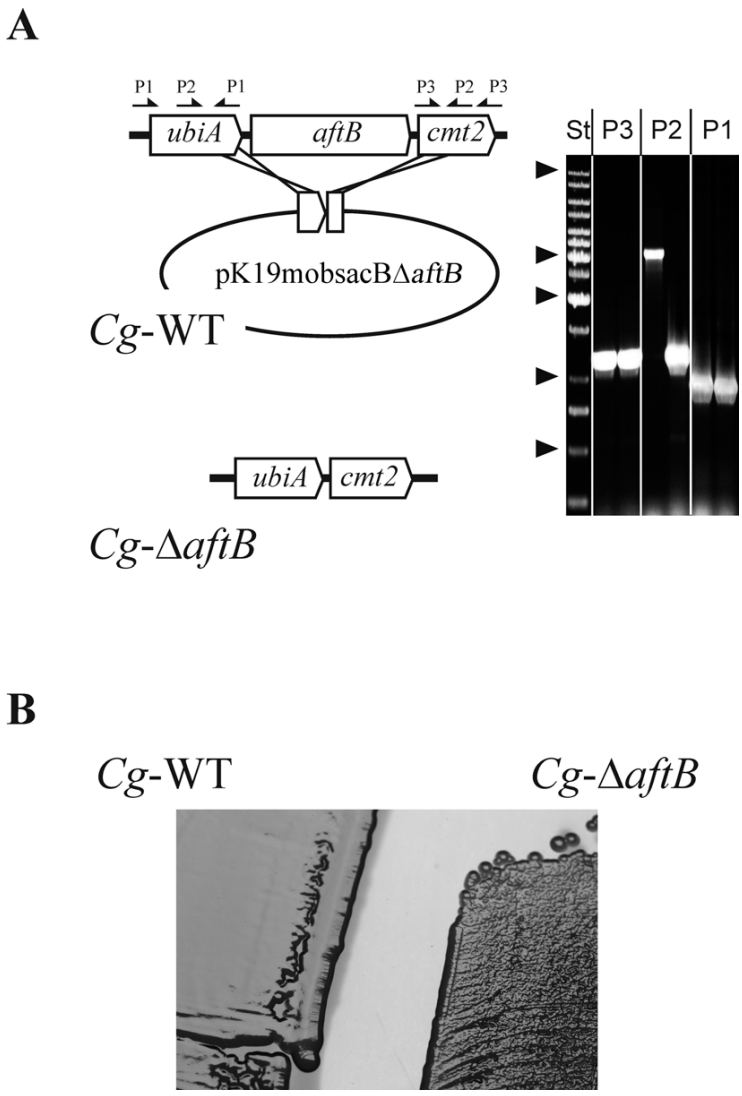

Fig. 2. Construction and characteristics of *C. glutamicum*Δ*aftB*. *A*, Genomic illustration of Cg-*aftB* with its adjacent genes *ubiA* and *cmt2*, which is the orthologue of mycobacterial *fbpA* (Fig. 1*A*), and the strategy to delete Cg-*aftB* using the deletion vector pK19mobsacBΔ*aftB*. This vector carries 18 nucleotides of the 5´-end of Cg-*aftB* and 36 nucleotides of its 3´-end thereby enabling the in-frame deletion of almost the entire Cg-*aftB* gene. The arrows marked P2 locate the primers used for the PCR analysis to confirm the absence of Cg-*aftB*. PrimersP1 were used to detect *ubiA*, and P3 to detect *cmt2*. Distances are not drawn to scale. The results of the PCR analysis are shown on the right, where the results obtained with the corresponding primer pairs are marked accordingly. Samples were applied pair wise with the amplification products obtained from the wild type applied

in the left lane, and that of the deletion mutant in the right lane. St marks the standard, where the arrowheads are located at 10, 3, 2, 1, and 0.5 kb, respectively. *B*, Phenotype of *C. glutamicum*Δ*aftB* cells spread on BHI medium and incubated for 3 days. On the left is shown wild type *C. glutamicum* (*Cg*-WT) and on the right the deletion mutant *C. glutamicum*Δ*aftB* (*Cg*-Δ*aftB*). The picture shows an area of about 1.5 cm square.

Taken together *C. glutamicum*Δ*aftB* possesses only a slight growth defect under the conditions assayed indicating a degree of tolerance to the deletion of Cg-*aftB.* Complementation of *C. glutamicum*Δ*aftB* with either pMSXCg-*aftB* or pMSX-Mt-*aftB* restored the mutant to a wild type phenotype. For the purpose of significance, *C.glutamicum*Δ*aftB* complemented with Mt*aftB* was used throughout this investigation to study the corresponding mutant phenotype, however, similar results were also obtained with *C. glutamicum*Δ*aftB* complemented with Cg*aftB* (data not shown).

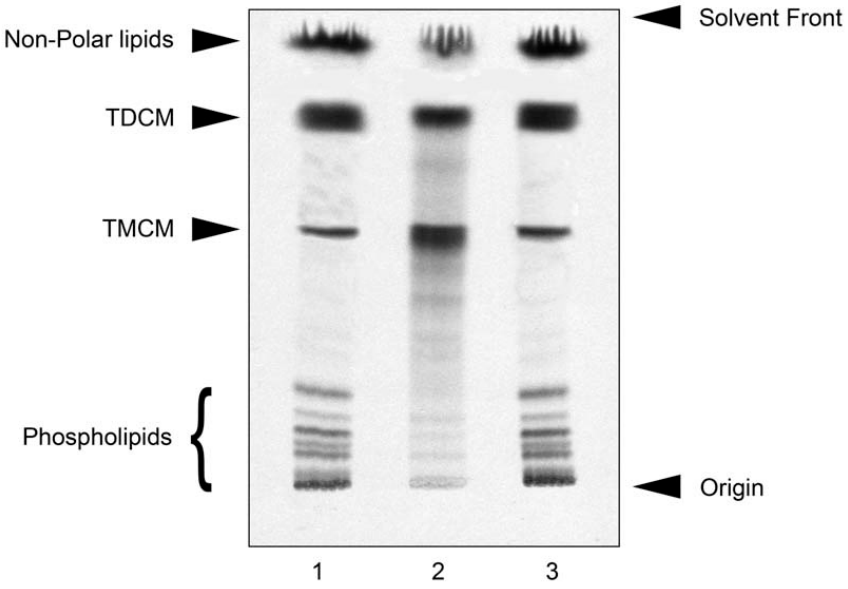

Fig. 3. Quantitative analysis of extractable [^{14}C]lipids from *C. glutamicum*, *C. glutamicun*Δ*aftB* and *C. glutamicum*Δ*aftB* pMSX-Mt-*aftB*. Lipids were extracted from cells by a series of organic washes as described in "Experimental Procedures". An aliquot (25,000 cpm) from each strain was subjected to TLC using silica gel plates (5735 silica gel 60F_{254}, Merck) developed in $CHCl_3$/CH_3OH/H_2O (60:16:2, v/v/v) and either charred using 5% molybdophosphoric acid in ethanol at 100 ^oC to reveal the extracted lipids and compared to known standards (9,16) or quantified using a phosphorimager following exposure to Kodak X-Omat film for 24 h. The TLC-autoradiogram is representative of 3 independent experiments. Lane 1, *C. glutamicum*; lane 2, *C. glutamicum*Δ*aftB*; and lane 3, *C.glutamicum*Δ*aftB* pMSX-Mt-*aftB.*

Cell wall associated and bound corynomycolic acid analysis – Our initial qualitative investigations involved the analysis of cell wall associated lipids and bound CMAMEs following TLC analysis. Analysis of free lipids from other previously identified cell wall

mutants, such as *C. glutamicum*Δ*emb* (9) and *C. glutamicum*Δ*aftA* (19), highlighted an apparent increase in trehalose monocorynomycolate (TMCM) indicating a defect in cell wall biosynthesis. This phenotype was also consistently observed for the *aftB* deletion mutant, in several independent experiments (data not shown).

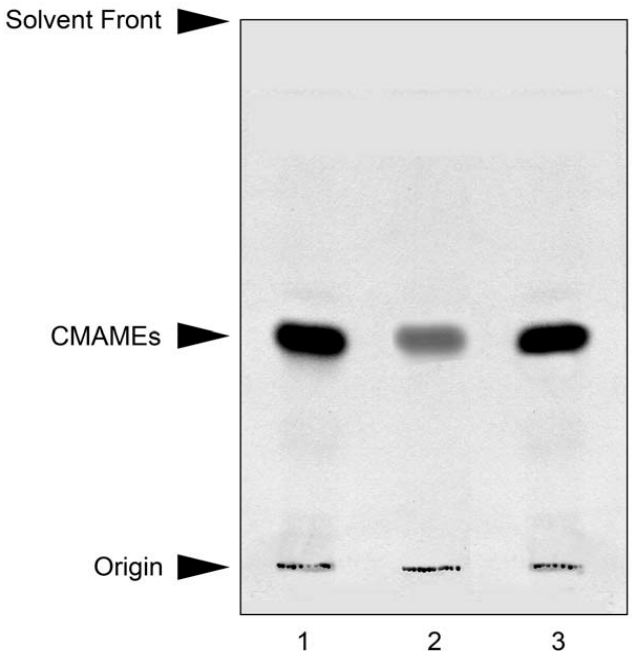

Fig. 4. Quantitative analysis [^{14}C]CMAMEs from *C. glutamicum*, *C. glutamicun*Δ*aftB* and *C. glutamicum*Δ*aftB* pMSX-Mt-*aftB*. The bound [^{14}C]corynomycolic acids from [^{14}C] delipidated extracts were released by the addition of TBAH at 100 °C overnight and methylated as described in "Experimental Procedures". A 5% aliquot from each strain was subjected to TLC using silica gel plates (5735 silica gel 60F_{254}, Merck) developed in petroleum ether/acetone (95:5, v/v) and either charred using 5% molybdophosphoric acid in ethanol at 100 °C to reveal [^{14}C]CMAMEs and compared to known standards (9,16) or quantified using a phosphorimager following exposure to Kodak X-Omat film for 24 h. The TLC-autoradiogram is representative of 3 independent experiments. Lane 1, *C. glutamicum*; lane 2, *C. glutamicum*Δ*aftB*; and lane 3, *C. glutamicum*Δ*aftB* pMSX-Mt-*aftB.*

In addition, we also compared quantitatively through [^{14}C]-acetate labeling of cultures and equal loading of radioactivity, the extractable free lipids from *C. glutamicum*, *C. glutamicum*Δ*aftB* and the complemented *C. glutamicum*Δ*aftB* pMSX-Mt-*aftB* strains. Typically, *C. glutamicum* exhibited the known free lipid profile for wild type *C. glutamicum*, including phospholipids (3945 cpm), TMCM (3217 cpm), trehalose dicorynomycolate (TDCM) (8619 cpm) and non-polar lipids migrating at the solvent front (8753 cpm) (Fig. 3, lane 1).

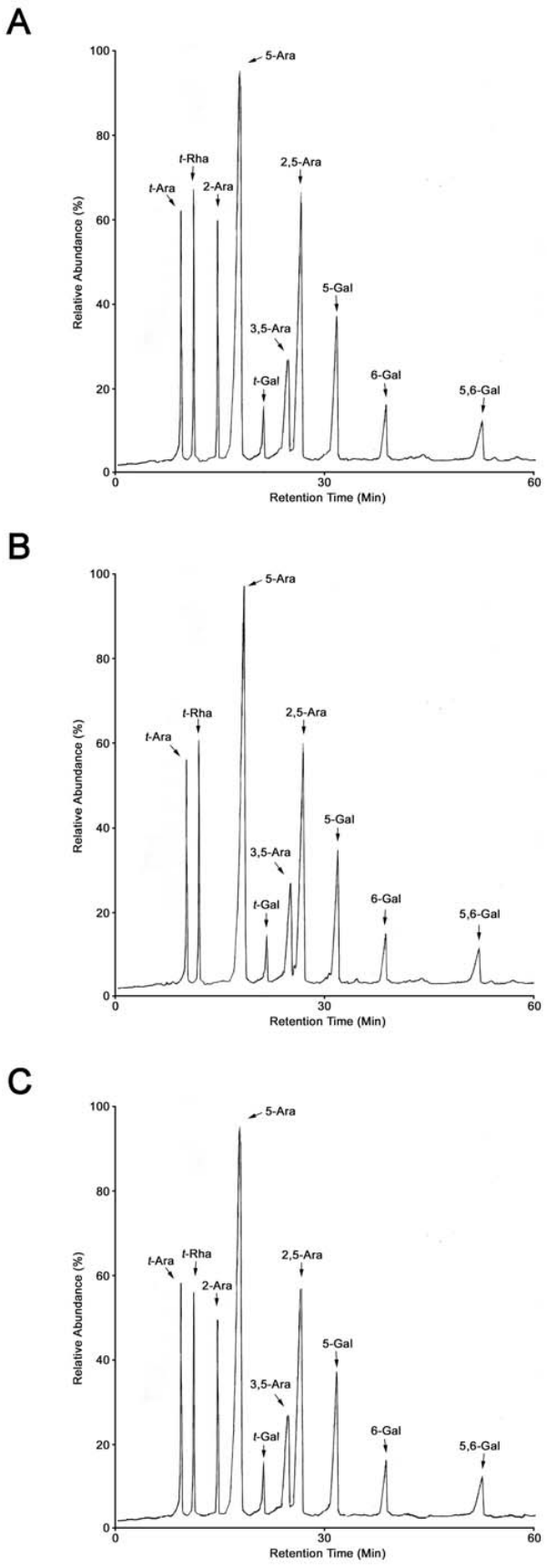

Fig. 5. Glycosyl linkage analysis of cell walls of *C. glutamicum* (*A*), *C. glutamicun aftB* (*B*), *C. glutamicumΔaftB* pMSX-Mt-*aftB* (*C*). Cell walls were per-*O*-methylated, hydrolyzed using 2M TFA, reduced and per-*O*-acetylated. The resulting partially per-*O*-methylated, per-*O*acetylated glycosyl derivatives were analyzed by GC/MS as described previously (5,8,9).

In contrast, following equivalent loading of radioactivity and quantitative analysis by phosphorimager analyzes, *C. glutamicum*Δ*aftB* possessed an approximate significant three-fold increase in TMCM (10185 cpm) and a decrease in TDCM (6539 cpm), phospholipids (1275 cpm) and non-polar lipids (5439 cpm) (Fig. 3, lane 2). Complementation of *C. glutamicum*Δ*aftB* with pMSX-Mt-*aftB*, reverted the deletion mutant back to a phenotype similar to the wild type, TMCM (3331 cpm), TDCM (9123 cpm), phospholipids (4011 cpm) and non-polar lipids (8901 cpm) (Fig. 3, lane 3).

To relate the above growth phenotypic changes of *C. glutamicum*Δ*aftB* to its cellular composition, *C. glutamicum*Δ*aftB* and *C. glutamicum*Δ*aftB* pMSX-Mt-*aftB*, along with wild type *C. glutamicum*, were analyzed for arabinogalactan esterified corynomycolic acids released from the above [^{14}C]-delipidated cells. As expected, the wild type exhibited a typical profile of CMAMEs (Fig. 4, lane 1, 28562 cpm), whereas these products were significantly reduced in *C. glutamicum*Δ*aftB* (Fig. 4, lane 2, 8947 cpm). In addition, complementation of *C. glutamicum*Δ*aftB* with pMSX-Mt-*aftB* (Fig. 4, lane 3, 27523 cpm) led to the restoration of normal 'levels' of cell wall bound corynomycolic´acids. These results suggested that Mt-*aftB* was involved in a key aspect of arabinan biosynthesis, whereby deletion perturbs tethering of corynomycolic acids to AG, but not as severely as in *C. glutamicum*Δ*emb* and *C. glutamicum*Δ*aftA* mutants (9,19).

Cell wall glycosyl compositional and linkage analysis of cell walls – Alditol acetate derivatives of highly purified mAGP from *C. glutamicum*, *C. glutamicum*Δ*aftB* and *C. glutamicum*Δ*aftB* pMSX-Mt-*aftB* were prepared for glycosyl compositional analysis. All strains exhibited a similar Ara:Gal ratio of 3.7:1. However, glycosyl linkage analysis of per-*O*-methylated alditol acetate derivatives of mAGP extracted from these strains highlighted an obvious difference inlinkage profiles (Fig. 5). All glycosyl linkages could be accounted for in wild type *C. glutamicum* (Fig. 5*A*) as described previously (9,19), however, mAGP from *C. glutamicum*Δ*aftB* was devoid of β(1→2) Ara*f* linkages (Fig. 5*B*). Complementation of *C. glutamicum*Δ*aftB* with pMSX-Mt-*aftB* restored the β(1→2) Ara*f* linkage thus reverting the deletion mutant to a wild type phenotype (Fig. 5*C*). Further to this, we analyzed the cell wall glycosyl composition of *C. glutamicum*Δ*aftB* complemented with either pMSX-Mt-*aftB*-D29A or pMSXMt-*aftB*-D30A. Each of these complemented stains exhibited a phenotype identical to that of *C. glutamicum*Δ*aftB*, with a complete loss of 2-Ara*f* linkages (data not shown). As confirmed in Figure 6 the Mt-AftB muteins are synthesized *in vivo* and the failure to establish the β(1→2) Ara*f* linkage is therefore most likely due to a catalytically inactive

AftB, thus highlighting the importance of these particular aspartic acid residues in enzyme function.

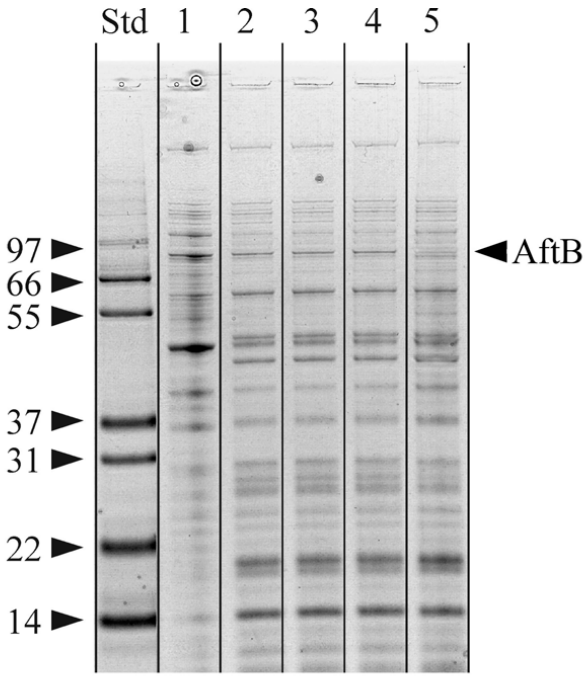

Fig. 6. Formation of Mt-AftB in *C. glutamicum*. Extracts of *C. glutamicum*Δ*aftB* expressing His-tagged *M. tuberculosis* Aft*B* and AftB muteins were subjected to Ni^{2+}-NTA chromatography and analyzed by SDS-PAGE. Lane 1, 20 µg of clarified extract of *C. glutamicum*Δ*aftB* pMSX-Mt-*aftB* prior to chromatography. Lane 2-5 received the entire protein isolated from a 2 L culture of the respective recombinant strain *via* Ni^{2+}-NTA chromatography, which was approximately 20 µg in each case. Lane 2 *C. glutamicum*Δ*aftB* pMSX-Mt-*aftB*; lane 3, *C. glutamicum*Δ*aftB* pMSX-Mt-*aftB*-D29A; lane 4, *C. glutamicum*Δ*aftB* pMSX-Mt-*aftB*-D30A; and lane 5, *C. glutamicum*Δ*aftB* pMSX (control). Standards (Std) along with their molecular weights in kDa are shown. The expected molecular weight for Mt-AftB is 72 kDa and the faint band at this location in lanes 2-4 is shown by an arrow and was verified by peptide mass fingerprinting as *M. tuberculosis* AftB (data not shown).

*In vitro arabinofuranosyltransferase activity of C. glutamicum, C. glutamicum*Δ*aftB, and C. glutamicum*Δ*aftB* pMSX-*Mt-aftB* – Initial attempts to develop an *in vitro* assay using either purified recombinant expressed Mt-AftB or *E. coli* membranes expressing Mt*aftB*, have thus far proved unsuccessful. As an alternative approach, we assessed the capacity of membrane preparations from *C. glutamicum, C. glutamicum*Δ*aftB* and *C. glutamicum*Δ*aftB* complemented with pMSX-Mt-*aftB* to catalyze arabinofuranosyltransferase activity in the presence of an exogenous synthetic α-D-Ara*f*-(1→5)-α-D-Ara*f*-*O*-C^8, neoglycolipid acceptor (24) and DP[^{14}C]A (35). TLC analysis of the products, when assayed with wild type *C. glutamicum* membranes, resulted in the formation of two products (A and B) (Fig. 7*A*) when analyzed by TLC (Fig. 7*B*). The enzymatic synthesis of products A and B are consistent with our previous studies (24) using mycobacterial membrane preparations resulting in trisaccharide products as a result of the addition of α(1→5) and β(1→2) linked Ara*f* residues

to the disaccharide acceptor (Fig. 7*A*) (24). Addition of EMB in several experiments, even at high concentrations of up to 1 mg/ml to the reaction mixture, resulted in the complete loss of only product A. However, when assays were performed using membranes prepared from *C. glutamicum*Δ*aftB,* only a single band migrating to a position akin to that of product A could be observed and no product formation could be identified upon the addition of 100 µg/ml of EMB, (Fig. 7*B*). Membranes prepared from *C. glutamicum*Δ*aftB* complemented with pMSX-Mt-*aftB* restored product A and B formation back to that of the wild type (Fig. 7*B*) and only product B was synthesized when EMB (up to 1 mg/ml) was added to the reaction mixtures.

ES-MS and GC/MS analysis of product A and B – Newly synthesized products A and B prepared using *C. glutamicum* treated with EMB and *C. glutamicum*Δ*aftB* membranes, as described above, were further characterized. ES-MS analysis of the reaction products A (data not shown) and B extracted through preparative TLC (Fig. 8*A*), revealed a strong molecular ion *m/z* 549.3 ($M+Na^+$), which corresponds to a trisaccharide product Ara*f*-(1→?)-Ara*f*-(1→5)-α-D-Ara*f*-*O*-C_8. GC/MS analysis of the partially per-*O*-methylated, per-*O*acetylated alditol acetate derivative of product A, synthesized in assays with *C. glutamicum*Δ*aftB* membranes revealed the addition of only an α(1→5) linked Ara*f* residue (Fig. 8*B* and Fig. 7*A*) (24). However, GC/MS analysis of the partially per-*O*-methylated, per-*O*-acetylated alditol acetate derivative of product B, synthesized in enzyme assays utilizing membranes from *C. glutamicum* and EMB, identified the new glycosyl linkage as a β(1→2)-linked Ara*f* residue (Fig. 8*C* and Fig. 7*A*). By analogy, this new glycosidic linkage corresponds to a terminal β(1→2) linked Ara*f* residue (24). These analyses were further confirmed by ^{1}H-NMR studies (data not shown) by the assignment of α(1→5) and β(1→2) Ara*f* anomeric protons in comparison to the acceptor Ara*f*-(1→5)-α-D-Ara*f*-*O*-C_8, and are consistent with our previous studies (24). Finally, the results clearly establish both from *in vivo* and *in vitro* experiments that Mt-AftB catalyzes the addition of a β(1→2) Ara*f* unit, and that this enzyme is resistant to EMB (Fig. 7*B*).

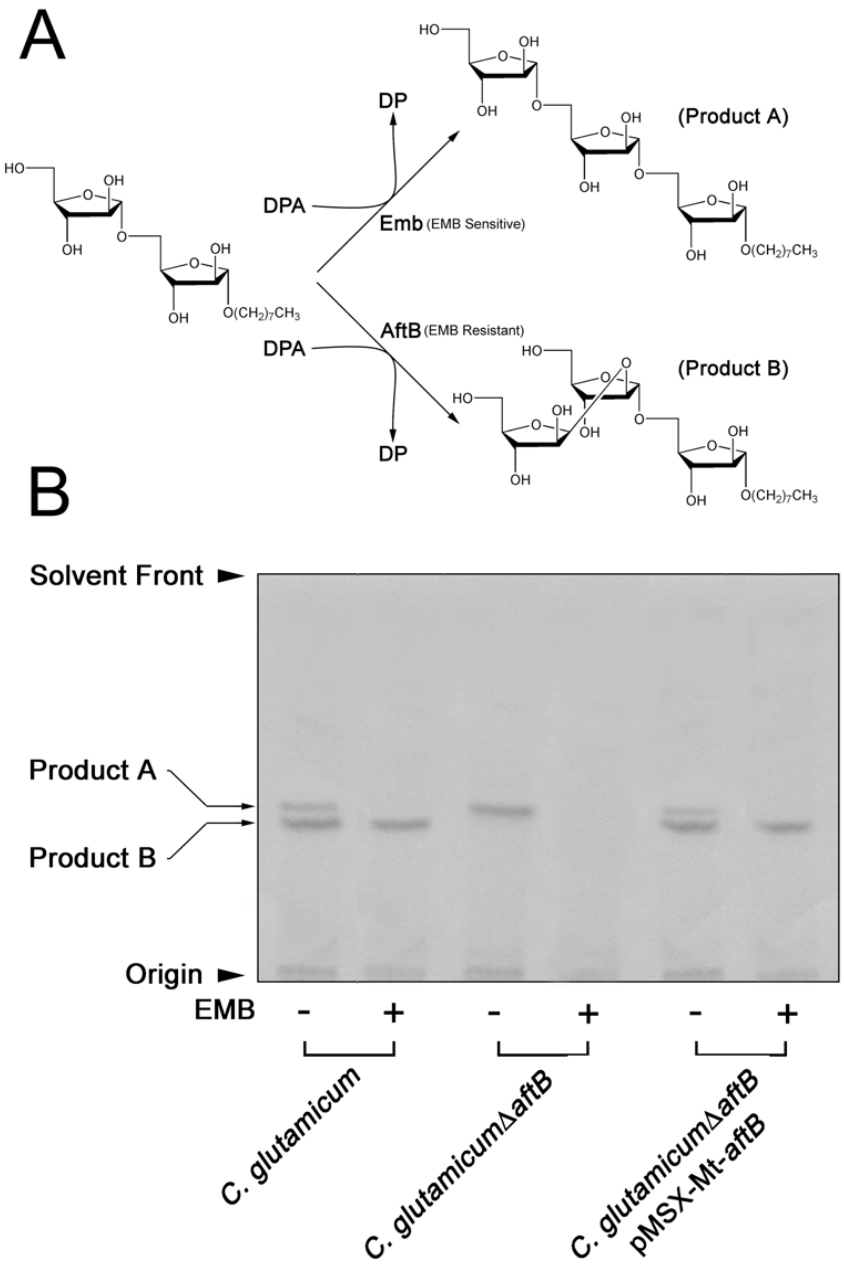

Fig. 7. Arabinofuranosyltransferase activity in membranes prepared from *C. glutamicum*, *C. glutamicun*Δ*aftB* and *C. glutamicum*Δ*aftB* pMSX-Mt-*aftB*. *A*, Biosynthetic reaction scheme of products formed in arabinofuranosyltransferase assays using α-D-Ara*f*-(1→5)-α-D-Araf-*O*C_8. *B*, Arabinofuranosyltransferase activity was determined using the synthetic α-D-Ara*f*- (1→5)-α-D-Araf-*O*-C_8 acceptor in a cell-free assay as described previously (24). The products of the assay were resuspended prior to scintillation counting and subjected to TLC using silica gel plates (5735 silica gel 60F_{254}, Merck) in $CHCl_3$:CH_3OH:H_2O:NH_4OH (65/25/3.6/0.5, v/v/v/v) with the reaction products visualized by autoradiography.

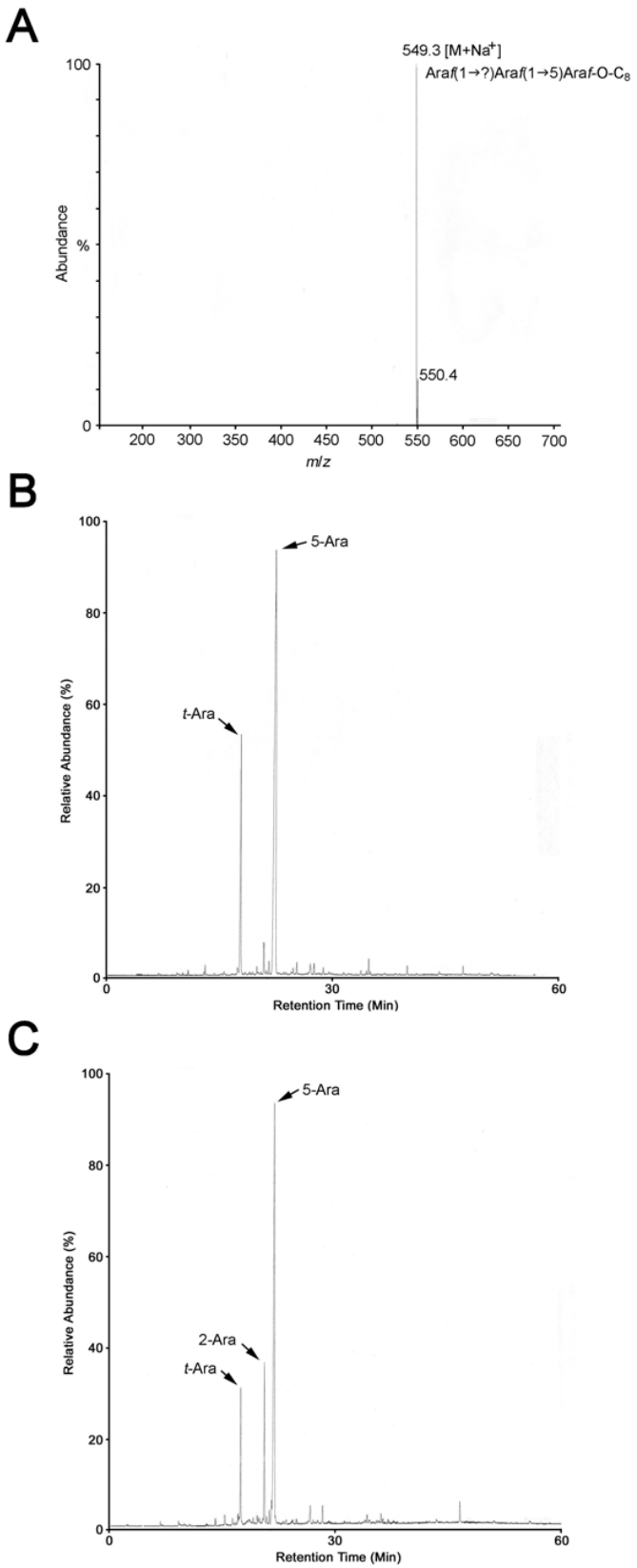

Fig. 8. ES-MS and GC/MS characterization of products A and B. *A*, ES-MS analysis of products from assays containing membranes prepared from *C. glutamicum* treated with EMB and *C. glutamicum*Δ*aftB* (data not shown). *B*, GC/MS analysis of the partially per-*O*methylated, per-*O*-acetylated alditol acetate derivative of product A obtained from assays containing membranes prepared from *C. glutamicum*Δ*aftB*. *C*, GC/MS analysis of the partially per-*O*-methylated, per-*O*-acetylated alditol acetate derivative of product B obtained from assays containing membranes and EMB prepared from *C. glutamicum*.

DISCUSSION

The biosynthesis of AG in *M. tuberculosis* has been the subject of intense research over the past decade (5,9,12,19,21,37,38). Since cell wall biosynthesis is the target for several anti-tubercular agents, such as EMB, the requirement for a complete understanding of the enzymes involved is imperative. We recently identified a unique DPA dependent α-D-arabinofuranosyltransferase (AftA), which is responsible for the deposition of the first Ara*f* residue onto the galactan moiety of AG, thus "priming" the polysaccharide for further extension by the Emb proteins (19). However, our current understanding of further downstream arabinan biosynthesis of AG is limited to that of the Emb proteins and is poorly defined (9,39). *M. tuberculosis* possesses three Emb proteins encoded within the *embCAB* operon, of which EmbA and EmbB have been implicated in cell wall arabinan biosynthesis (39), whereas EmbC is involved in LAM biosynthesis (31,40,41). The catalytic mechanism of how these enzymes are able to synthesize the array of arabinan glycosidic linkages, α(1→5), α(1→3) and β(1→2), present in both *M. tuberculosis* and *C. glutamicum* remains to be elucidated. This catalytic conundrum is further questioned by the fact that members belonging to the *Corynebacteria*, such as *C. glutamicum* and *C. diphtheriae,* contain only a single *emb* gene (18). Therefore, one might assume that other arabinofuranosyltransferases could be involved in concert with the Emb proteins to build the arabinan domain of AG.

In this study, we have identified Rv3805c, which we have termed AftB, as a novel retaining arabinofuranosyltransferase, and is likely to form a new family which is distinct from the inverting arabinofuranosyltransferase enzymes (EmbA, B, C, and AftA) in GT-83/85 families (42). More precisely, AftB adds to the non-reducing end of the arabinan domain of AG β(1→2) Ara*f* residues as shown through both *in vivo* and *in vitro* experiments. For instance, incubation of membranes prepared from *C. glutamicum* with DP[^{14}C]A and the disaccharide neoglycolipid acceptor resulted in the appearance of two trisaccharide products (A and B), which equate to the transfer of both α(1→5) and β(1→2)Ara*f* residues, respectively. Through further chemical characterization of the products by TLC, ES-MS, and glycosyl linkage analyzes an α(1→5) linked trisaccharide product could only be identified in assays conducted with membranes prepared from *C. glutamicum*Δ*aftB*. This clear loss of β(1→2)Ara*f* activity corroborates the cell wall analysis of the *C. glutamicum*Δ*aftB* mutant, where the loss of β(1→2) linked Ara*f* residues could also be observed. We also attempted to inhibit AftB activity by incubation of the assay components in the presence of high concentrations of EMB (up to 1 mg/ml), a known inhibitor of the Emb proteins in *M. tuberculosis* and *C. glutamicum*. In doing so, analysis of the corresponding products

synthesized from *C. glutamicum* membranes following EMB treatment clearly show evidence of an EMB resistant β(1→2) arabinofuranosyltransferase activity and an EMB sensitive α(1→5) arabinofuranosyltransferase activity. In addition, since we have previously established that the EMB-resistant AftA introduces the priming Ara*f* residue at the 8th, 10th and 12th Gal*f* residue of the galactan backbone, it can be concluded that the bulk α(1→5)Ara*f* stems of AG represent the primary target of EMB. It is interesting to note that EMB resistance is simply not due to AftB being a retaining arabinofuranosyltransferase in contrast to the inverting arabinofuranosyltransferase Mt-EmbA and Mt-EmbB, since AftA, which is also an inverting arabinofuranosyltransferase, is also EMB resistant (19).

A modified scheme for terminal cell wall arabinan biosynthesis in *Corynebacterianeae* is presented in Figure 9. It is possible that the AftB protein is responsible for the successive addition of two β(1→2) Ara*f* residues at a 3,5-Ara*f* branched residue. Although, this may be a reasonable inference from the *in vivo* structural work with the *aftB* deletion strain, it has not been completely verified by our *in vitro* assay. Therefore, it is formally possible that the AftB-dependent addition of one β(1→2) Ara*f* residue is required, before a second GT-C related arabinofuranosyltransferase adds the second terminal β(1→2) Ara*f* residue as shown in Figure 9.

The arabinofuranosyltransferases of the Emb family (EmbC, EmbA and EmbB) (12,13,31,39), and AftA (19), and AftB, possess some sequence similarity. This relates to a modified Glycosyltransferase motif, which is defined in the GT-C glycosyltransferase superfamily as either DXD, EXD, DDX, or DEX (29). The most distant is probably AftA with only one negatively charged D residue however possessing an adjacent polar Q residue (19). In AftB there are two adjacent D residues (Fig. 1*B*), which due to our mutational study are likely to be directly involved in glycosyl hydrolysis and transfer. Also, the high number of charged amino acyl residues of the strongly conserved loop region following the first TM helix might contribute to the proper orientation of substrates at the catalytic centre. The glycosyltransferase motif of arabinofuranosyltransferases so far identified is always located in a periplasmic loop region, which connects TM III-IV in EmbC, TM III-IV in AftA, and TM I-II in AftB (Fig. 1*B*). A further feature common of the Emb, AftA and AftB proteins is that they consist of an Nterminal region, which has a number of hydrophobic segments spanning the TM, and a large C-terminal domain, which in Emb has been demonstrated to be located towards the periplasmic side (30). The number of TMs is different amongst these proteins, but the involvement of these TMs could be considered as being important for the translocation of DPA, the lipid linked substrate of these glycosyltransferases. The weak structural identities of

the membrane embedded part of the arabinofuranosyltransferases, indicates that transport and presentation of DPA to the catalytic site might be different for these enzymes. A "Pro-motif" as identified in the Emb proteins (31) is not present in AftB and AftA.

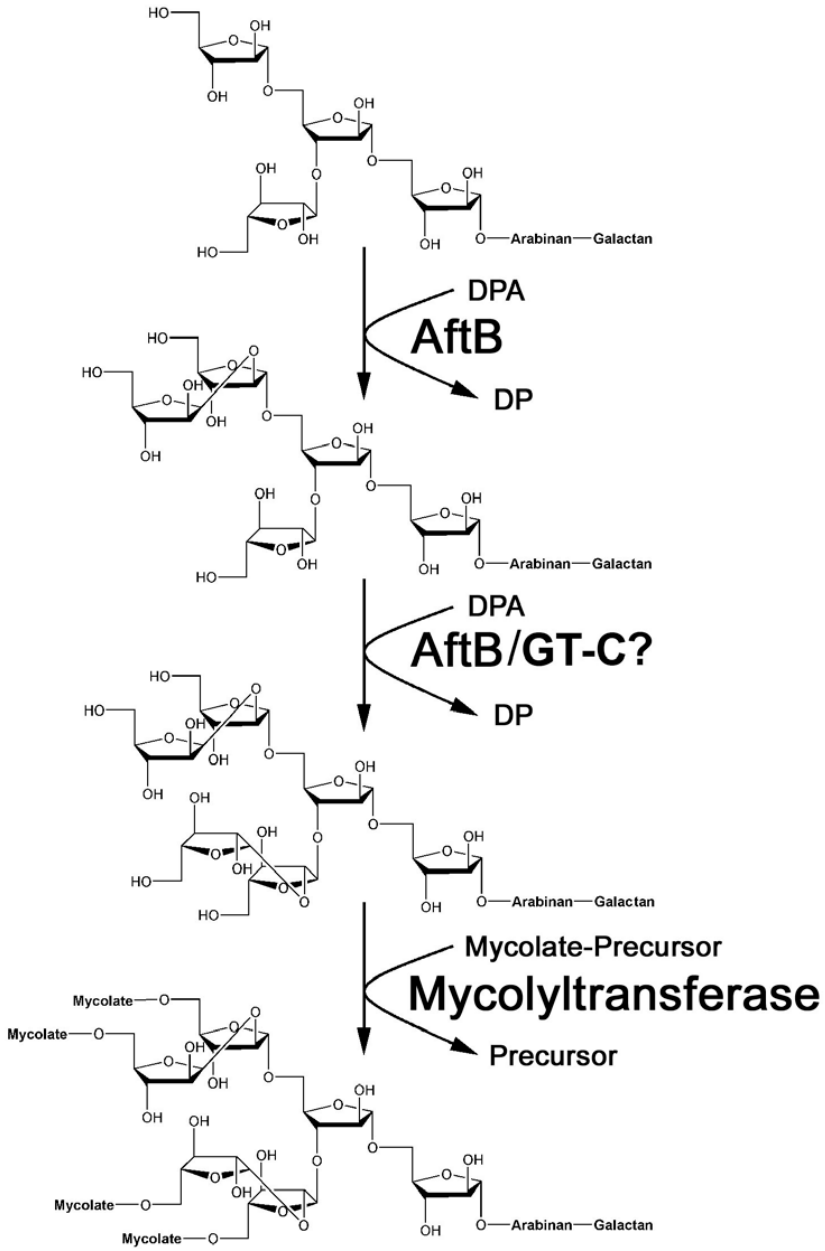

Fig. 9. Proposed biosynthetic pathway leading to arabinan formation in *M. tuberculosis* AG. For reasons of simplicity it is shown that one of the β(1→2) linked Ara*f* residues is added by AftB, whilst the second β(1→2) linked Ara*f* residue may be catalyzed by AftB or *via* an unknown GT-C arabinofuranosyltransferase, presumably closely related to AftB. Mycolylation is shown to occur after the final step of introducing both terminal β(1→2) linked Ara*f* residues of AG. However, mycolylation at the α(1→5) linked Araf residue may occur prior to completion or simultaneously during establishment of the unique Ara6 motif of AG in *M. tuberculosis*. In addition, mycolylation of the penultimate Ara*f* residue may also occur before the β(1→2) linked Araf residue is attached.

This motif is typical for polysaccharide co-polymerases and is assumed to control the chain length in polysaccharide biosynthesis. Its absence in AftA and AftB seems plausible, since these enzymes add only singular Ara*f* residues, but the Emb proteins presumably add a number of α(1→5) linked Ara*f* residues to form the inner chain of the AG domain.

It is noteworthy that deletion of *aftB* in *C. glutamicum* results in only a weak phenotype (Fig. 2*B*). In *M. tuberculosis* mycolic acids are attached to the terminal β(1→2)Ara*f* and penultimate α(1→5)Ara*f*residue of the Ara_6 motif of AG (6). This appears to be similar in *C. glutamicum*, since in the absence of terminal β(1→2) Ara*f* residues mycolic acids are still bound to AG, thus emphasizing in this respect the cell wall similarity of these bacteria. However, in *C. glutamicum* a maximal 5% of the mycolic acids are covalently attached to AG (43), whereas this value is about 10% in *M. tuberculosis* (6). The fact that the *aftB* deletion mutant of *C. glutamicum* possesses less AG bound mycolic acids, also results in an increased abundance of TMCM. This situation can be entirely different in *M. tuberculosis* due to the essentiality of *aftB* in *M. tuberculosis* (44) and requires further investigation.

We conclude that AftB represents a novel arabinofuranosyltransferase in *Corynebacterianeae*, such as *M. tuberculosis*, which is responsible for the addition of the terminal β(1→2) linked Ara*f* residues. In doing so, we now propose a contemporary revision of cell wall arabinan biosynthesis (Fig. 9) which may aid in a more detailed understanding of the pathogenicity and persistence of *M. tuberculosis.*

REFERENCES

1. Gupta, R., Kim, J. Y., Espinal, M. A., Caudron, J. M., Pecoul, B., Farmer, P. E., and Raviglione, M. C. (2001) *Science* **293**(5532), 1049-1051
2. Zignol, M., Hosseini, M. S., Wright, A., Weezenbeek, C. L., Nunn, P., Watt, C. J., Williams, B. G., and Dye, C. (2006) *J Infect Dis* **194**(4), 479-485
3. Singh, J. A., Upshur, R., and Padayatchi, N. (2007) *PLoS Med* **4**(1), e504. McNeil, M., Daffe, M., and Brennan, P. J. (1990) *J Biol Chem* **265**(30), 18200-18206
5. Besra, G. S., Khoo, K. H., McNeil, M. R., Dell, A., Morris, H. R., and Brennan, P. J. (1995) *Biochemistry* **34**(13), 4257-4266
6. McNeil, M., Daffe, M., and Brennan, P. J. (1991) *J Biol Chem* **266**(20), 13217-13223
7. Chatterjee, D., Bozic, C. M., McNeil, M., and Brennan, P. J. (1991) *J Biol Chem* **266**(15), 9652-9660
8. Daffe, M., Brennan, P. J., and McNeil, M. (1990) *J Biol Chem* **265**(12), 6734-6743
9. Alderwick, L. J., Radmacher, E., Seidel, M., Gande, R., Hitchen, P. G., Morris, H. R., Dell, A., Sahm, H., Eggeling, L., and Besra, G. S. (2005) *J Biol Chem* **280**(37), 32362-32371
10. Minnikin, D. E., Kremer, L., Dover, L. G., and Besra, G. S. (2002) *Chem Biol* **9**(5), 545-553
11. Takayama, K., and Kilburn, J. O. (1989) *Antimicrob Agents Chemother* **33**(9), 1493-1499
12. Belanger, A. E., Besra, G. S., Ford, M. E., Mikusova, K., Belisle, J. T., Brennan, P. J., and Inamine, J. M. (1996) *Proc Natl Acad Sci U S A* **93**(21), 11919-11924
13. Telenti, A., Philipp, W. J., Sreevatsan, S., Bernasconi, C., Stockbauer, K. E., Wieles, B., Musser, J. M., and Jacobs, W. R., Jr. (1997) *Nat Med* **3**(5), 567-570
14. Winder, F. G., and Collins, P. B. (1970) *J Gen Microbiol* **63**(1), 41-48
15. Banerjee, A., Dubnau, E., Quemard, A., Balasubramanian, V., Um, K. S., Wilson, T., Collins, D., de Lisle, G., and Jacobs, W. R., Jr. (1994) *Science* **263**(5144), 227-230

16. Gande, R., Gibson, K. J., Brown, A. K., Krumbach, K., Dover, L. G., Sahm, H., Shioyama, S., Oikawa, T., Besra, G. S., and Eggeling, L. (2004) *J Biol Chem* **279**(43), 44847-44857
17. Portevin, D., De Sousa-D'Auria, C., Houssin, C., Grimaldi, C., Chami, M., Daffe, M., and Guilhot, C. (2004) *Proc Natl Acad Sci U S A* **101**(1), 314-319
18. Kalinowski, J., Bathe, B., Bartels, D., Bischoff, N., Bott, M., Burkovski, A., Dusch, N., Eggeling, L., Eikmanns, B. J., Gaigalat, L., Goesmann, A., Hartmann, M., Huthmacher, K., Kramer, R., Linke, B., McHardy, A. C., Meyer, F., Mockel, B., Pfefferle, W., Puhler, A., Rey, D. A., Ruckert, C., Rupp, O., Sahm, H., Wendisch, V. F., Wiegrabe, I., and Tauch, A. (2003) *J Biotechnol* **104**(1-3), 5-25
19. Alderwick, L. J., Seidel, M., Sahm, H., Besra, G. S., and Eggeling, L. (2006) *J Biol Chem* **281**(23), 15653-15661
20. Mikusova, K., Yagi, T., Stern, R., McNeil, M. R., Besra, G. S., Crick, D. C., and Brennan, P. J. (2000) *J Biol Chem* **275**(43), 33890-33897
21. Kremer, L., Dover, L. G., Morehouse, C., Hitchin, P., Everett, M., Morris, H. R., Dell, A., Brennan, P. J., McNeil, M. R., Flaherty, C., Duncan, K., and Besra, G. S. (2001) *J Biol Chem* **276**(28), 26430-26440
22. Radmacher, E., Stansen, K. C., Besra, G. S., Alderwick, L. J., Maughan, W. N., Hollweg, G., Sahm, H., Wendisch, V. F., and Eggeling, L. (2005) *Microbiology* **151**(Pt 5), 1359-1368
23. Wolucka, B. A., McNeil, M. R., de Hoffmann, E., Chojnacki, T., and Brennan, P. J. (1994) *J Biol Chem* **269**(37), 23328-2333524. Lee, R. E., Brennan, P. J., and Besra, G. S. (1997) *Glycobiology* **7**(8), 1121-1128
25. Lee, R. E., Mikusova, K., Brennan, P. J., and Besra, G. S. (1995) *J. Am. Chem. Soc* **117**(48), 11829-11832
26. Alderwick, L. J., Dover, L. G., Seidel, M., Gande, R., Sahm, H., Eggeling, L., and Besra, G. S. (2006) *Glycobiology* **16**(11), 1073-1081
27. Huang, H., Scherman, M. S., D'Haeze, W., Vereecke, D., Holsters, M., Crick, D. C., and McNeil, M. R. (2005) *J Biol Chem* **280**(26), 24539-24543
28. Mikusova, K., Huang, H., Yagi, T., Holsters, M., Vereecke, D., D'Haeze, W., Scherman, M. S., Brennan, P. J., McNeil, M. R., and Crick, D. C. (2005) *J Bacteriol* **187**(23), 8020-8025
29. Liu, J., and Mushegian, A. (2003) *Protein Sci* **12**(7), 1418-1431
30. Seidel, M., Alderwick, L. J., Sahm, H., Besra, G. S., and Eggeling, L. (2007) *Glycobiology* **17**(2), 210-219
31. Berg, S., Starbuck, J., Torrelles, J. B., Vissa, V. D., Crick, D. C., Chatterjee, D., and Brennan, P. J. (2005) *J Biol Chem* **280**(7), 5651-5663
32. Eggeling, L., and Bott, M. (2005) *Handbook of Corynebacterium glutamicum.*, CRC Press, Taylor Francis Group
33. Eikmanns, B. J., Kleinertz, E., Liebl, W., and Sahm, H. (1991) *Gene* **102**(1), 93-98
34. Schafer, A., Tauch, A., Jager, W., Kalinowski, J., Thierbach, G., and Puhler, A. (1994) *Gene* **145**(1), 69-73
35. Lee, R. E., Brennan, P. J., and Besra, G. S. (1998) *Bioorg Med Chem Lett* **8**(8), 951-954
36. Belisle, J. T., Vissa, V. D., Sievert, T., Takayama, K., Brennan, P. J., and Besra, G. S. (1997) *Science* **276**(5317), 1420-1422
37. Daffe, M., McNeil, M., and Brennan, P. J. (1993) *Carbohydr Res* **249**(2), 383-398
38. Berg, S., Kaur, D., Jackson, M., and Brennan, P. J. (2007) *Glycobiology*, Advanced Access, Jan 29, 2007
39. Escuyer, V. E., Lety, M. A., Torrelles, J. B., Khoo, K. H., Tang, J. B., Rithner, C. D., Frehel, C., McNeil, M. R., Brennan, P. J., and Chatterjee, D. (2001) *J Biol Chem* **276**(52), 48854-48862
40. Zhang, N., Torrelles, J. B., McNeil, M. R., Escuyer, V. E., Khoo, K. H., Brennan, P. J., and Chatterjee, D. (2003) *Mol Microbiol* **50**(1), 69-76
41. Shi, L., Berg, S., Lee, A., Spencer, J. S., Zhang, J., Vissa, V., McNeil, M. R., Khoo, K. H., and Chatterjee, D. (2006) *J Biol Chem* **281**(28), 19512-19526
42. Coutinho, P. M., and Henrissat, B. (1999) Carbohydrate-active enzymes: an integrated database approach. In: Gilbert, H. J., Davies, G., Henrissat, B., and Svensson, B. (eds). *Recent Advances in Carbohydrate Bioengineering*, The Royal Society of Chemistry, Cambridge
43. Puech, V., Chami, M., Lemassu, A., Laneelle, M. A., Schiffler, B., Gounon, P.,Bayan, N., Benz, R., and Daffe, M. (2001) *Microbiology* **147**(Pt 5), 1365-1382
44. Sassetti, C. M., Boyd, D. H., and Rubin, E. J. (2003) *Mol Microbiol* **48**(1), 77-84
45. Pan, F., Jackson, M., Ma, Y., and McNeil, M. (2001) *J Bacteriol* **183**(13), 3991-3998
46. Cserzo, M., Wallin, E., Simon, I., von Heijne, G., and Elofsson, A. (1997) *Protein Eng* **10**(6), 673-676

FOOTNOTES

[#]MS and LJA contributed equally to this work. LJA is a Biotechnology and Biological Sciences Research Council Quota Student. GSB acknowledges support in the form of a Personal Research Chair from Mr. James Bardrick, as a former Lister Institute-Jenner Research Fellow, the Medical Research Council (UK), the Wellcome Trust, and HS support from the Fonds der Chemischen Industrie for support. *M. tuberculosis* H37Rv DNA was obtained from the Tuberculosis Research Materials Contract (NIH) at Colorado State University. We thank Graham Burns for technical assistance.

[1]The abbreviations used are: AG, arabinogalactan; Ara, arabinose; CMAME, corynomycolic acid methyl ester; DPA, decaprenol phosphoarabinose; DPPR, decaprenylphosphoryl-5-phospho-ribose; EMB, ethambutol; Gal, galactose; GC, gas chromatography; GC/MS, gas chromatography/mass spectrometry; mAGP, mycolyl-arabinogalactan-peptidoglycan; pRpp, 5-phospho-ribofuranose-pyrophosphate; Rha, rhamnose; TBAH, tetrabutyl ammoniumhydroxide; TLC, thin layer chromatography.

[2]GSB (unpublished results)

D Zusammenfassung

Innerhalb der *Actinomycetales* fasst die Unterordnung der *Corynebacterianeae* eine Gruppe von Bakterien zusammen, zu denen neben dem industriell bedeutsamen Bakterium *Corynebacterium glutamicum* auch das pathogene Bakterium *Mycobacterium tuberculosis* gehört, welches der Verursacher der Tuberkulose ist. Die Besonderheit der *Corynebacterianeae* liegt in ihrem einzigartigen Zellwandaufbau. Dabei ist das Peptidoglykan mit einem Heteropolysaccharid aus Arabinose und Galaktose, dem Arabinogalaktan, verbunden. Dieses Heteropolysaccharid ist in *M. tuberculosis* essentiell und zur Struktur und Synthese liegen nur sehr begrenzte Kenntnisse vor.

In dieser Arbeit konnte eine bislang unbekannte Arabinofuranosyltransferase (AftA) aus *C. glutamicum* und *M. tuberculosis* identifiziert werden. Es wurde eine Deletionsmutante hergestellt, deren chemische Analyse zusammen mit Enzymtests ergab, dass das AftA-Protein am Galaktan den ersten Arabinoserest einführt. Weitere Arabinosereste werden unter Beteiligung der Arabinofuranosyltransferase Emb eingeführt, wie die chemische Analyse einer für diesen Zweck hergestellten *emb* Deletionsmutante zeigte. Darüberhinaus konnte noch eine zusätzliche, bislang unbekannte Arabinofuranosyltransferase identifiziert werden (AftB), die einen Arabinoserest mit dem Ende der Arabinandomäne verknüpft.

Die untersuchten Arabinosyltransferasen sind membranintegrierte Proteine. Es wurde die Topologie des Emb-Proteins untersucht. Dabei zeigte sich, dass die C-terminalen Aminosäurereste 753 bis 1146 als globuläre Domäne im Periplasma lokalisiert sind, wogegen die vergleichbar große N-terminale Domäne mit 15 hydrophoben Bereichen in der Cytoplasmamembran lokalisiert ist.

Durch ortsgerichtete Mutagenese in dem Emb-Protein aus *C. glutamicum* und dem AftB-Protein aus *M. tuberculosis* wurden essentielle Aminosäurereste identifiziert, die an der Glykosyltransferaseaktivität beteiligt sind.

Summary

Within the *Actinomycetales* the subspecies of *Corynebacterinaeae* includes species like the industrial relevant *Corynebacterium glutamicum* and pathogen bacteria like the causative of tuberculosis disease *Mycobacterium tuberculosis*. The *Corynebacterianea* are unique to their complex building of the cell wall. Their cell wall consists of peptidoglycan that is connected to a special heteropolysaccharide. This is made of the monomers arabinose and galactose and is known as arabinogalactan. This heteropolysaccharide is essential for *M. tuberculosis* but little is known about the synthesis and structure.

As a part of this work the Arabinofuranosyltranserferase A (AftA) was identified as a new protein in *C. glutamicum* and *M. tuberculosis*. Deletion mutants of the *aftA* gene have been constructed. By use of chemical analysis as well as enzyme assays the AftA protein has been identified to catalyze the binding of the first arabinose to the galactan. Further elongation of the first arabinose is catalyzed by the Emb protein which was verified by chemical analysis of a *C. glutamicum emb* deletion mutant. Moreover, another Arabinofuranosyltransferase (AftB) has been identified to be responsible for connecting arabinose with the terminal part of the arabinan domain.

All Arabinosyltransferases explored in this work are integrated membrane proteins. Investigation on topology of the Emb protein was carried out. It has been shown that the C-terminal aminoacid residues 753 to 1146 are forming a globular domain which is located at the periplasm. However, the N-terminal domain with 15 hydrophobic regions is located inside the cytoplasmic membrane.

Due to site directed mutagenesis of the proteins Emb of *C. glutamicum* Emb as well as AftB of *M. tuberulosis* essential amino acid residues for glycolsyltransferase activity of both proteins could be determined.

E Literatur

Alderwick, L. J., Radmacher, E., Seidel, M., Gande, R., Hitchen, P. G., Morris, H. R., Dell, A., Sahm, H., Eggeling, L., Besra, G. S. (2005) Deletion of Cg-*emb* in Corynebacterianeae Leads to a Novel Truncated Cell Wall Arabinogalactan, whereas Inactivation of Cg-*ubiA* Results in an Arabinan-deficient Mutant with a Cell Wall Galactan Core. *J Biol Chem* **280:** 32362-32371

Alderwick, L. J., Seidel, M., Sahm, H., Besra, G. S., Eggeling, L. (2006) Identification of a Novel Arabinofuranosyltransferase (AftA) Involved in Cell Wall Arabinan Biosynthesis in *Mycobacterium tuberculosis*. *J Biol Chem* **281:** 15653-15661

Becker, A. & Pühler, A. (1998) Specific amino acid substitutions in the proline-rich motif of the Rhizobium meliloti ExoP protein result in enhanced production of low-molecular-weight succinoglycan at the expense of high-molecular-weight succinoglycan. *J Bacteriol* **180:** 395-399

Belanger, A. E., Besra, G. S., Ford, M. E., Mikusova, K., Belisle, J. T., Brennan, P. J., Inamine, J. M. (1996) The embAB genes of Mycobacterium avium encode an arabinosyl transferase involved in cell wall arabinan biosynthesis that is the target for the antimycobacterial drug ethambutol. *Proc Natl Acad Sci U S A* **93:** 11919-11924

Berg, S., Starbuck, J., Torrelles, J. B., Vissa, V. D., Crick, D. C., Chatterjee, D., Brennan, P. J. (2005) Roles of conserved proline and glycosyltransferase motifs of EmbC in biosynthesis of lipoarabinomannan. *J Biol Chem* **280:** 5651-5663

Besra, G. S., Khoo, K. H., McNeil, M. R., Dell, A., Morris, H. R., Brennan, P. J. (1995) A new interpretation of the structure of the mycolyl-arabinogalactan complex of Mycobacterium tuberculosis as revealed through characterization of oligoglycosylalditol fragments by fast-atom bombardment mass spectrometry and 1H nuclear magnetic resonance spectroscopy. *Biochemistry* **34:** 4257-4266

Besra, G. S., Morehouse, C. B., Rittner, C. M., Waechter, C. J., Brennan, P. J. (1997) Biosynthesis of mycobacterial lipoarabinomannan. *J Biol Chem* **272:** 18460-18466

Brennan, P. J. & Nikaido, H. (1995) The envelope od mycobacteria. *Annu Rev Biochem* **64:** 29-63

Breton, C., Heissigerova, H., Jeanneau, C., Moravcova, J., Imberty, A. (2002) Comparative aspects of glycosyltransferases. *Biochem Soc Symp* **69:** 23-32

Breton, C., Snajdrova, L., Jeanneau, C., Koca, J., Imberty, A. (2006) Structures and mechanisms of glycosyltransferases. *Glycobiology* **16:** 29 - 37

Chatterjee, D., Bozic, C. M., McNeil, M., Brennan, P. J. (1991) Structural features of the arabinan component of the lipoarabinomannan of Mycobacterium tuberculosis. *J Biol Chem* **266:** 9652-9660

Cole, S. T., Brosch, R., Parkhill, J., Garnier, T., Churcher, C., Harris, D., Gordon, S. V., Eiglmeier, K., Gas, S., Barry, C. E., 3rd, Tekaia, F., Badcock, K., Basham, D., Brown, D., Chillingworth, T., Connor, R., Davies, R., Devlin, K., Feltwell, T., Gentles, S., Hamlin, N., Holroyd, S., Hornsby, T., Jagels, K., Barrell, B. G. & et al. (1998) Deciphering the biology of Mycobacterium tuberculosis from the complete genome sequence. *Nature* **393:** 537-544

Coutinho, P. M., Deleury, E., Davies, G. J., Henrissat, B. (2003) An evolving hierarchical family classification for glycosyltransferases. *J Mol Biol* **328:** 307-317

Cren, S., Gurcha, S. S., Blake, A. J., Besra, G. S., Thomas, N. R. (2004) Synthesis and biological evaluation of new inhibitors of UDP-Galf transferase--a key enzyme in M. tuberculosis cell wall biosynthesis. *Org Biomol Chem* **2:** 2418-2420

Dabour, N. & LaPointe, G. (2005) Identification and molecular characterization of the chromosomal exopolysaccharide biosynthesis gene cluster from Lactococcus lactis subsp. cremoris SMQ-461. *Appl Environ Microbiol* **71:** 7414-7425

Daffe, M., Brennan, P. J., McNeil, M. (1990) Predominant structural features of the cell wall arabinogalactan of Mycobacterium tuberculosis as revealed through characterization of oligoglycosyl alditol fragments by gas chromatography/mass spectrometry and by 1H and 13C NMR analyses. *J Biol Chem* **265:** 6734-6743

Daniels, C. & Morona, R. (1999) Analysis of Shigella flexneri wzz (Rol) function by mutagenesis and cross-linking: wzz is able to oligomerize. *Mol Microbiol* **34:** 181-94

Daniels, C., **Griffiths, C**., **Cowles, B**., **Lam, J. S**. (**2002)** Pseudomonas aeruginosa O-antigen chain length is determined before ligation to lipid A core. *Environ Microbiol* **4:** 883-897

Dover, L. G., Cerdeno-Tarraga, A. M., Pallen, M. J., Parkhill, J., Besra, G. S. (2004) Comparative cell wall core biosynthesis in the mycolated pathogens, Mycobacterium tuberculosis and Corynebacterium diphtheriae. *FEMS Microbiol Rev* **28:** 225-250

Eggeling, L., Krumbach, K., Sahm, H. (2001) L-glutamate efflux with Corynebacterium glutamicum: why is penicillin treatment or Tween addition doing the same? *J Mol Microbiol Biotechnol* **3:** 67-68

Escuyer, V. E., Lety, M. A., Torrelles, J. B., Khoo, K. H., Tang, J. B., Rithner, C. D., Frehel, C., McNeil, M. R., Brennan, P. J., Chatterjee, D. (2001) The role of the embA and embB gene products in the biosynthesis of the terminal hexaarabinofuranosyl motif of Mycobacterium smegmatis arabinogalactan. *J Biol Chem* **276:** 48854-48862

Gande, R., Gibson, K. J., Brown, A. K., Krumbach, K., Dover, L. G., Sahm, H., Shioyama, S., Oikawa, T., Besra, G. S., Eggeling, L. (2004) Acyl-CoA carboxylases (accD2 and accD3), together with a unique polyketide synthase (Cg-pks), are key to mycolic acid biosynthesis in Corynebacterianeae such as Corynebacterium glutamicum and Mycobacterium tuberculosis. *J Biol Chem* **279:** 44847-44857

Gastinel, L. N., Cambillau, C., Bourne, Y. (1999). Crystal structures of the bovine β4galactosyltransferase catalytic domain and its complex with uridine diphosphogalactose. *EMBO J* **18:** 3546–3557

Gibson, K. J., Eggeling, L., Maughan, W. N., Krumbach, K., Gurcha, S. S., Nigou, J., Puzo, G., Sahm, H., Besra, G. S. (2003) Disruption of Cg-Ppm1, a polyprenyl monophosphomannose synthase, and the generation of lipoglycan-less mutants in Corynebacterium glutamicum. *J Biol Chem* **278:** 40842-40850

Hancock, I. C., Carman, S., Besra, G. S., Brennan, P. J., Waite, E. (2002) Ligation of arabinogalactan to peptidoglycan in the cell wall of Mycobacterium smegmatis requires concomitant synthesis of the two wall polymers. *Microbiology* **148:** 3059-3067

Hitchcock, A. L., Auld, K., Gygi, S. P., Silver, P. A. (2003) A subset of membrane-associated proteins is ubiquitinated in response to mutations in the endoplasmic reticulum degradation machinery. Proc Natl Acad Sci USA **100:** 12735-12740

Huang, H., Scherman, M. S., D'Haeze, W., Vereecke, D., Holsters, M., Crick, D. C., McNeil, M. R. (2005) Identification and active expression of the M. tuberculosis gene encoding, 5-phospho-alpha -D-ribose-1-diphosphate: decaprenyl-phosphate 5-phosphoribosyltransferase, the first enzyme committed to decaprenylphosphoryl-D-arabinose synthesis. *J Biol Chem* **280:** 24539-24543

Hu, Y. & Walker, S. (2002) Remarkable structural similarities between diverse glycosyltransferases. *Chem Biol* **9:** 1287-1296

Imbach, T., Burda, P., Kuhnert, P., Wevers, R.A., Aebi, M. (1999) A mutation in the human ortholog of the Saccharomyces cerevisiae ALG6 gene causes carbohydrate-deficient glycoprotein syndrome type-Ic. Proc Natl Acad Sci USA **96:** 6982-6987

Kapitonov, D. & Yu, R. K. (1999) Conserved domains of glycosyltransferases. *Glycobiology* **9:** 961-978

Khasnobis, S., Zhang, J., Angala, S. K., Amin, A. G., McNeil, M. R., Crick, D. C., Chatterjee, D. (2006) Characterization of a specific arabinosyltransferase activity involved in mycobacterial arabinan biosynthesis. *Chem Biol* **13:** 787-795

Kinoshita, S., Udaka, S., Shimono, M. (1957) Studies on the amino acid fermentation. Production of L-glutamate by various microorganisms. *J Gen Appl Microbiol* **3:** 193-205

Kojima, Y., Fukumoto, S., Furukawa, K., Okajima, T., Wiels J., Yokoyama K., Suzuki, Y., Urano, T., Ohta, M., Furukawa, K. (2000) Molecular cloning of globotriaosylceramide/CD77 synthase, a glycosyltransferase that initiates the synthesis of globo series glycosphingolipids. *J Biol Chem* **275:** 15152-15156

Kol, M. A., de Kruijff , B., de Kroon, A. I. (2002) Phospholipid flip-flop in biogenic membranes: what is needed to connect opposite sides. *Semin Cell Dev Biol* **13:** 163-170

Körner, C., Knauer, R., Stephani, U., Marquardt, T., Lehle, L., vonFigura, K. (1999) Carbohydrate deficient glycoprotein syndrome type IV: deficiency of dolichyl-P-an:Man(5)GlcNAc(2)-PP-dolichyl mannosyltransferase. *EMBO J* **18:** 6816-6822

Kremer, L., Dover, L. G., Morehouse, C., Hitchin, P., Everett, M., Morris, H. R., Dell, A., Brennan, P. J., McNeil, M. R., Flaherty, C., Duncan, K., Besra, G. S. (2001) Galactan

biosynthesis in Mycobacterium tuberculosis. Identification of a bifunctional UDP-galactofuranosyltransferase. *J Biol Chem* **276:** 26430-26440

Lairson, L. L., Chiu, C. P., Ly, H. D., He, S., Wakarchuk, W. W., Strynadka, N. C., Withers, S. G. (2004) Intermediate trapping on a mutant retaining alpha-galactosyltransferase identifies an unexpected aspartate residue. *J Biol Chem* **279:** 28339-28344

Liu, J. & Mushegian, A. (2003) Three monophyletic superfamilies account for the majority of the known glycosyltransferases. *Protein Sci* **12:** 1418-1431

Luca, S., **Heise, H**., **Baldus, M**. (**2003**) High-resolution solid-state NMR applied to polypeptides and membrane proteins. *Acc Chem Res* **36:** 858-865

Luzhetskyy, A., Taguchi, T., Fedoryshyn, M., Durr, C., Wohlert, S. E., Novikov, V., Bechthold, A. (2005) LanGT2 Catalyzes the First Glycosylation Step during landomycin A biosynthesis. *Chembiochem* **6:** 1406-1410

Maeda, Y., Watanabe, R., Harris, C. L., Hong, Y., Ohishi, K., Kinoshita, K., Kinoshita, T. (2001). PIG-M transfers the first mannose to glycosylphosphatidylinositol on the lumenal side of the ER. *EMBO J* **20:** 250-261

McNeil, M., Daffe, M., Brennan, P. J. (1990) Evidence for the nature of the link between the arabinogalactan and peptidoglycan of mycobacterial cell walls. *J Biol Chem* **265:** 18200-18206

McNeil, M., Daffe, M., Brennan, P. J. (1991) Location of the mycolyl ester substituents in the cell walls of mycobacteria. *J Biol Chem* **266:** 13217-13223

McNeil, M. R., Robuck, K. G., Harter, M., Brennan, P. J. (1994) Enzymatic evidence for the presence of a critical terminal hexa-arabinoside in the cell walls of Mycobacterium tuberculosis. *Glycobiology* **4:** 165-173

Mikusova, K., Mikus, M., Besra, G. S., Hancock, I., Brennan, P. J. (1996) Biosynthesis of the linkage region of the mycobacterial cell wall. *J Biol Chem* **271:** 7820-7828

Mikusova, K., Yagi, T., Stern, R., McNeil, M. R., Besra, G. S., Crick, D. C., Brennan, P. J. (2000) Biosynthesis of the galactan component of the mycobacterial cell wall. *J Biol Chem* **275:** 33890-33897

Mikusova, K., Huang, H., Yagi, T., Holsters, M., Vereecke, D., D'Haeze, W., Scherman, M. S., Brennan, P. J., McNeil, M. R., Crick, D. C. (2005) Decaprenylphosphoryl arabinofuranose, the donor of the D-arabinofuranosyl residues of mycobacterial arabinan, is formed via a two-step epimerization of decaprenylphosphoryl ribose. *J Bacteriol* **187:** 8020-8025

Mikusova, K., Belanova, M., Kordulakova, J., Honda, K., McNeil, M. R., Mahapatra, S., Crick, D. C., Brennan, P. J. (2006) Identification of a novel galactosyl transferase involved in biosynthesis of the mycobacterial cell wall. *J Bacteriol* **188:** 6592-6598

Mills, J. A., Motichka, K., Jucker, M., Wu, H. P., Uhlik, B. C., Stern, R. J., Scherman, M. S., Vissa, V. D., Pan, F., Kundu, M., Ma, Y. F., McNeil, M. (2004) Inactivation of the mycobacterial rhamnosyltransferase, which is needed for the formation of the arabinogalactan-peptidoglycan linker, leads to irreversible loss of viability. *J Biol Chem* **279:** 43540-43546

Minnikin, D. E. & Goodfellow, M. (1980) Lipid composition in the classification and identification of acid-fast bacteria. *Soc Appl Bacteriol Symp Ser* **8:** 189-256

Morona, R., van den Bosch, L., Daniels, C. (2000) Evaluation of Wzz/MPA1/MPA2 proteins based on the presence of coiled-coil regions. *Microbiology* **146**: 1–4

Murray, G. L., Attridge, S. R., Morona, R. (2003) Regulation of Salmonella typhimurium lipopolysaccharide O antigen chain length is required for virulence; identification of FepE as a second Wzz. *Mol Microbiol* **47:** 1395-1406

Nakamura, Y., Nishio, Y., Ikeo, K., Gojobori, T. (2003) The genome stability in *Corynebacterium* species due to lack of the recombinational repair system. *Gene* **317:** 149-155

Niederweis, M. (2003) Mycobacterial porins--new channel proteins in unique outer membranes. *Mol Microbiol* **49:** 1167-1177

Pan, F., Jackson, M., Ma, Y., McNeil, M. (2001) Cell wall core galactofuran synthesis is essential for growth of mycobacteria. *J Bacteriol* **183:** 3991-3998

Puech, V., Chami, M., Lemassu, A., Laneelle, M. A., Schiffler, B., Gounon, P., Bayan, N., Benz, R., Daffe, M. (2001) Structure of the cell envelope of corynebacteria: importance of the non-covalently bound lipids in the formation of the cell wall permeability barrier and fracture plane. *Microbiology* **147:** 1365-1382

Radmacher, E., Stansen, K. C., Besra, G.S., Alderwick, L. J., Maughan, W. N., Hollweg, G., Sahm, H., Wendisch, V. F., Eggeling, L. (2005) Ethambutol, a cell wall inhibitor of *Mycobacterium tuberculosis*, elicits L-glutamate efflux of *Corynebacterium glutamicum*. *Microbiology* **151:** 1359-1368

Ramaswamy, S. V., Amin, A. G., Goksel, S., Stager, C. E., Dou, S. J., El Sahly, H., Moghazeh, S. L., Kreiswirth, B. N., Musser, J. M. (2000) Molecular genetic analysis of nucleotide polymorphisms associated with ethambutol resistance in human isolates of Mycobacterium tuberculosis. *Antimicrob Agents Chemother* **44:** 326-336

Ramaswamy, S. V., Dou, S. J., Rendon, A., Yang, Z., Cave, M. D., Graviss, E. A. (2004) Genotypic analysis of multidrug-resistant Mycobacterium tuberculosis isolates from Monterrey, Mexico. *J Med Microbiol* **53:** 107-113

Rose, N. L., Completo, G. C., Lin, S. J., McNeil, M., Palcic, M. M., Lowary, T. L. (2006) Expression, purification, and characterization of a galactofuranosyltransferase involved in Mycobacterium tuberculosis arabinogalactan Biosynthesis. *J Am Chem Soc* **128:** 6721-6729

Sahm, H., Eggeling, L., de Graaf, A. A. (2000) Pathway analysis and metabolic engineering in Corynebacterium glutamicum. *Biol Chem* **381:** 899-910

Scherman, M., Weston, A., Duncan, K., Whittington, A., Upton, R., Deng, L., Comber, R., Friedrich, J. D., McNeil, M. (1995) Biosynthetic origin of mycobacterial cell wall arabinosyl residues. *J Bacteriol* **177:** 7125-7130

Schirmer, T. (1998) General and specific porins from bacterial outer membranes. *J Struct Biol* **121:** 101-109

Schleifer, K. H. & Kandler, O. (1972) Peptidoglycan types of bacterial cell walls and their taxonomic implications. *Bacteriol Rev* **36:** 407-477

Seidel, M., Alderwick, L. J., Sahm, H., Besra, G. S., Eggeling, L. (2007a) Topology and mutational analysis of the single Emb arabinofuranosyltransferase of *Corynebacterium glutamicum* as a model of Emb proteins of *Mycobacterium tuberculosis*. *Gycobiology* **17:** 210-219

Seidel, M., Alderwick, L. J., Birch, H. L., Sahm, H., Eggeling, L., Besra, G. S. (2007b) Identification of a novel arabinofuranosyl-transferase AftB involved in a terminal step of cell wall arabinan biosynthesis in C*orynebacterianeae*, such as *Corynebacterium glutamicum* and *Mycobacterium tuberculosis*. *J Biol Chem in press*, March 26

Sreevatsan, S., Stockbauer, K. E., Pan, X., Kreiswirth, B. N., Moghazeh, S. L., Jacobs, W. R., Jr., Telenti, A., Musser, J. M. (1997) Ethambutol resistance in Mycobacterium tuberculosis: critical role of embB mutations. *Antimicrob Agents Chemother* **41:** 1677-1681

Stackebrandt, E., Rainey, F. A., Ward-Rainey, N. L. (1997) Proposal for a new hierarchic classification system, *Actinobacteria* classis nov. *Int J Syst Bacteriol* **47:** 479-491

Subramanian, A. R., Weyer-Menkhoff, J., Kaufmann, M., Morgenstern, B. (2005) DIALIGN-T: an improved algorithm for segment-based multiple sequence alignment BMC. *Bioinformatics* **6:** 66

Tatituri, R. V., Illarionov, P. A., Dover, L. G., Nigou, J., Gilleron, M., Hitchen, P., Krumbach, K., Morris, H. R., Spencer, N., Dell, A., Eggeling, L., Besra, G. S. (2007) Inactivation of Corynebacterium glutamicum NCgl0452 and the role of MgtA in the biosynthesis of a novel mannosylated glycolipid involved in lipomannan biosynthesis. J Biol Chem. **282:** 4561-4572

Telenti, A., Philipp, W. J., Sreevatsan, S., Bernasconi, C., Stockbauer, K. E., Wieles, B., Musser, J. M., Jacobs, W. R., Jr. (1997) The emb operon, a gene cluster of Mycobacterium tuberculosis involved in resistance to ethambutol. *Nat Med* **3:** 567-570

Thorson, J. S., Hosted, Jr., T. J., Jiang, J., Biggins, J. B. & Ahlert, J. (2001) Nature's carbohydrate chemists: The enzymatic glycosylation of bioactive bacterial metabolites. *Current Organic Chemistry* **5:** 139-167.

Videira, P. A., Garcia, A. P., Sa-Correia, I. (2005) Functional and topological analysis of the Burkholderia cenocepacia priming glucosyltransferase BceB, involved in the biosynthesis of the cepacian exopolysaccharide. *J Bacteriol* **187:** 5013-5018

Wang, L. Y., Li, S. T., Li, Y. (2003) Identification and characterization of a new exopolysaccharide biosynthesis gene cluster from Streptomyces. *FEMS Microbiol Lett* **220:** 21-27

Wiggins, C. A. & Munro, S. (1998). Activity of the yeast MNN1 α-1,3-mannosyltransferase requires a motif conserved in many other families of glycosyltransferases. *Proc Natl Acad Sci USA* **95:** 7945–7950

World Health Organisation (2006) Global Tuberculosis Control: Surveillance, Planning, Financing. WHO Report 2006.

Yagi, T., Mahapatra, S., Mikusova, K., Crick, D. C., Brennan, P. J. (2003) Polymerization of mycobacterial arabinogalactan and ligation to peptidoglycan. *J Biol Chem* **278:** 26497-26504

Yernool, D., Boudker, O., Jin, Y., Gouaux, E. (2004) Structure of a glutamate transporter homologue from Pyrococcus horikoshii. *Nature* **431:** 811-818

Zhang, N., Torrelles, J. B., McNeil, M. R., Escuyer, V. E., Khoo, K. H., Brennan, P. J., Chatterjee, D. (2003) The Emb proteins of mycobacteria direct arabinosylation of lipoarabinomannan and arabinogalactan via an N-terminal recognition region and a C-terminal synthetic region. *Mol Microbiol* **50:** 69-76

Danksagungen

Herrn Prof. Dr. H. Sahm danke ich für die Überlassung des interessanten Themas und die freundlichen Diskussionen im Rahmen meiner Promotion.

Herrn Prof. Dr. Karl-Erich Jäger möchte ich für die freundliche Übernahme des Korefferates danken.

Für die sehr gute Betreuung der gesamten Arbeiten, die zur Erstellung dieser Dissertation stattfanden und dafür, dass er es mir ermöglichte, mehrmals die originale britische Luft zu schnuppern, gilt mein Dank insbesondere Herrn Dr. Lothar Eggeling. Ferner möchte ich mich für das stetige Interesse am Fortgang meiner Arbeit, sowie die regen und fruchtbaren Diskussionen in den letzten Jahren bedanken.

Herrn Prof. Dr. Gurdyal Besra und Herrn Luke Alderwick möchte ich für die anregenden und interessanten Diskussionen über den *global killer* und das Birmingham *Ale* danken.

Frau Karin Krumbach danke ich für die Unterstützung bei der Durchführung einiger Experimente und der Hilfe bei der Ausformulierung des Themas dieser Arbeit.

Für die entspannte und fröhliche Atmosphäre im und außerhalb des Büros 119 danke ich Ramon, Laure, Jens und Melanie.

Meiner Familie und meinen Freunden möchte ich für die Unterstützung in den letzten Jahren und vor allem im Laufe meiner Promotion (Abwesenheit) besonders danken.

Mein herzlichster Dank gilt Andrea, die jederzeit für mich da war, mich liebevoll unterstützt hat und mir stets Halt gegeben hat.

Die hier vorgelegte Dissertation habe ich eigenständig und ohne unerlaubte Hilfe angefertigt. Die Dissertation wurde in der vorgelegten oder in ähnlicher Form noch bei keiner anderen Institution eingereicht. Ich habe bisher keine erfolglosen Promotionsversuche unternommen.

Düsseldorf,